

Aus dem Institut für Virologie  
der Medizinischen Fakultät Charité – Universitätsmedizin Berlin

DISSERTATION

Antiviral Responses against Chikungunya Virus Infection in a Novel  
Primary Cell Model

Antivirale Antworten gegen das Chikungunyavirus in einem  
neuartigen Primärzellmodell

zur Erlangung des akademischen Grades  
Doctor of Philosophy (PhD)

vorgelegt der Medizinischen Fakultät  
Charité – Universitätsmedizin Berlin

von

Fabian Pott  
aus Paderborn

Datum der Promotion: 03.03.2023

# Table of Contents

List of Abbreviations .....	1
Abstract.....	3
Zusammenfassung .....	4
<b>1 Introduction .....</b>	<b>5</b>
<b>1.1 Chikungunya Virus – a Re-Emerging Threat.....</b>	<b>5</b>
1.1.1 Epidemiology and Clinical Features of Chikungunya and Other Alphaviruses .....	5
1.1.2 Molecular Biology of Chikungunya Virus.....	6
1.1.3 Innate Immune Responses Induced and Antagonized by Chikungunya Virus .....	9
1.1.4 Immune Cell-Mediated and Adaptive Immune Responses.....	11
1.1.5 Intervention and Vaccine Strategies against Chikungunya Virus .....	12
<b>1.2 Fibroblasts in Health and Disease .....</b>	<b>13</b>
1.2.1 Synovial Fibroblasts in Rheumatoid Arthritis.....	13
1.2.2 Fibroblasts as Drivers of Arthralgia in Chikungunya Virus Infections.....	14
<b>1.3 Current State of the Research in the Field and Importance of this Study .....</b>	<b>15</b>
1.3.1 State of the Art.....	15
1.3.2 Importance.....	15
<b>2 Methods.....</b>	<b>17</b>
<b>2.1 Cell Culture, <i>In Vitro</i> Stimulations and Virus Infections .....</b>	<b>17</b>
2.1.1 Culture of Primary Human Fibroblasts and Immortalized Cell Lines.....	17
2.1.2 Virus Infections and Impact of Treatments.....	17
<b>2.2 Analysis of Cellular Protein and mRNA Expression .....</b>	<b>18</b>
2.2.1 Quantitative RT-PCR.....	18
2.2.2 Flow Cytometry, Microscopy, and Immunoblotting .....	18
<b>2.3 Transcriptomic Analysis of CHIKV-Infected Fibroblasts.....</b>	<b>19</b>
2.3.1 Bulk RNA-Seq Analysis .....	19
2.3.2 Single-Cell RNA-Seq Analysis .....	19
<b>3 Results and Interpretation .....</b>	<b>21</b>
<b>3.1 Human Synovial Fibroblasts are Suitable for <i>Ex Vivo</i> Infection Studies with CHIKV and MAYV .....</b>	<b>21</b>
3.1.1 Primary Human Synovial Fibroblasts Support the Replication Cycle of Alphaviruses .....	21
3.1.2 Cytokines Produced Upon Infection and Induced Innate Immune Responses Impact Infection .....	22
<b>3.2 Transcriptomic Analysis of CHIKV-Infected Fibroblasts Reveals Active Viral Replication Despite a Strongly Induced Innate Immune Response .....</b>	<b>23</b>

3.2.1 Cell-Intrinsic Immunity in Fibroblasts is Strongly Induced Upon Infection with CHIKV.....	23
3.2.2 The CHIKV Genome is Actively Replicated in Infected Synovial Fibroblasts.....	24
<b>3.3 Exogenously Added IFN Strongly Reduces the Infection Efficiency in Synovial Fibroblasts and Immortalized Cell Lines.....</b>	<b>24</b>
<b>3.4 Single-Cell Transcriptomics Defines a Threshold of Viral RNA for Repression of Cell-Intrinsic Immunity.....</b>	<b>25</b>
3.4.1 Viral Protein and RNA Expression is Invertly Connected to Innate Immune Responses.....	25
3.4.2 Quantification of Viral RNA Expression per Cell Identifies a Subset of Cells Supporting Strong Viral Replication.....	26
3.4.3 Cells with Low or Undetectable Amounts of Viral RNA Highly Express Antiviral Genes.....	26
3.4.4 Repressed Transcription Factor Activity is Associated with Strong Viral Gene Expression.....	27
<b>4 Discussion and Importance.....</b>	<b>29</b>
<b>4.1 Scientific Context and Further Interpretation of the Results.....</b>	<b>29</b>
<b>4.2 Clinical and Scientific Importance.....</b>	<b>30</b>
<b>4.3 Limitations of the Study.....</b>	<b>31</b>
<b>4.4 Open Questions and Outlook.....</b>	<b>32</b>
<b>References.....</b>	<b>34</b>
<b>Eidesstaatliche Versicherung.....</b>	<b>47</b>
<b>Declaration of Own Contribution.....</b>	<b>48</b>
<b>Excerpt from the Journal Summary List.....</b>	<b>49</b>
<b>Publication.....</b>	<b>50</b>
<b>Curriculum Vitae.....</b>	<b>79</b>
<b>List of Publications.....</b>	<b>80</b>
<b>Acknowledgements.....</b>	<b>82</b>

## List of Abbreviations

BHK-21	Baby Hamster Kidney Cells
C	Capsid Protein
CD	Cluster of Differentiation
cGAS	Cyclic GMP-AMP Synthase
CHIKV	Chikungunya Virus
DMARD	Disease-Modifying Anti-Rheumatic Drug
DNA	Deoxyribonucleic Acid
dsRNA	double-stranded RNA
E	Envelope Protein
EGFP	Enhanced Green Fluorescent Protein
ELISA	Enzyme Linked Immunosorbent Assay
<i>FHL1</i>	Four and a Half LIM Domain Protein 1 Gene
<i>GAPDH</i>	Glyceraldehyde 3-phosphate Dehydrogenase Gene
GM-CSF	Granulocyte-Macrophage Colony Stimulating Factor
HEK293T	Human Embryonic Kidney Cells Expressing the SV40 T Antigen
HFF-1	Human Foreskin Fibroblast Cells
HSF	Healthy Donor Synovial Fibroblasts
<i>IFI16</i>	Interferon Gamma-Inducible Protein 16 Gene
<i>IFIT1</i>	Interferon Induced Protein With Tetratricopeptide Repeats 1 Gene
IFITM	Interferon Induced Transmembrane Protein
IFN	Interferon
IFNAR	Interferon Alpha/Beta Receptor
IKK $\epsilon$	Inhibitor of NF $\kappa$ B Subunit Epsilon
IL	Interleukin
IMS	Interferon Module Score
IRF	Interferon Regulatory Factor
ISG	Interferon-Stimulated Gene
ISRE	Interferon-Stimulated Response Element
JAK	Janus Kinase
MXRA8	Matrix Remodeling Associated 8 Protein
m <sup>7</sup> GMP	7-Methyl-Guanosine-5'-Monophosphate
MAVS	Mitochondrial Antiviral Signaling Protein

MAYV	Mayaro Virus
MCP-1	Monocyte Chemoattractant Protein 1
MDA5	Melanoma Differentiation-Associated Protein 5
MMP	Matrix-Metalloprotease
MOI	Multiplicity of Infection
mRNA	Messenger RNA
<i>MX2</i>	MX Dynamin Like GTPase 2 Gene
MYD88	Myeloid Differentiation Primary Response Protein 88
NFκB	Nuclear Factor Kappa-B Kinase
NK Cell	Natural Killer Cell
nsP	Non-Structural Protein
OASF	Osteoarthritic Donor Synovial Fibroblasts
ORF	Open Reading Frame
PAMP	Pathogen-Associated Molecular Pattern
PCA	Principal Component Analysis
PRR	Pattern Recognition Receptor
RA	Rheumatoid Arthritis
RAG	Recombination Activating Gene
<i>RANKL</i>	Receptor Activator of NFκB ligand Gene
<i>RANTES</i>	Regulated on Activation, Normal T cell Expressed and Secreted Gene
RASF	Rheumatoid Arthritis Synovial Fibroblasts
RIG-I	Retinoic Acid Inducible Gene I
RNA	Ribonucleic Acid
SARS-CoV-2	Severe Acute Respiratory Syndrome Coronavirus 2
SDS	Sodium Dodecyl Sulphate
STAT	Signal Transducers and Activators of Transcription
TBK1	TANK-Binding Kinase 1
TF	Transframe Protein
TLR	Toll-Like Receptor
TNF	Tumor Necrosis Factor
TYK2	Tyrosine Kinase 2
U2OS	Human Osteosarcoma Cells
UMAP	Uniform Manifold Approximation and Projection
UTR	Untranslated Region

## Abstract

Arthritogenic alphaviruses such as Chikungunya virus (CHIKV) and Mayaro virus (MAYV) are mosquito-transmitted, positive-strand RNA viruses, which have caused outbreaks with millions of patients involved and are increasingly emerging in non-endemic regions as climate change fosters the expansion of vector ranges. The infection causes an acute febrile illness and a devastating polyarthralgia, which can progress into a chronic disease. The symptoms are thought to be caused by a deregulated immune response, which has characteristics similar to rheumatoid arthritis (RA), but remains mostly uncharacterized. Here, we established a comprehensive profile of *ex vivo* CHIKV-infected primary synovial fibroblasts prepared from knee tissue biopsies of healthy and osteoarthritic human donors. This cell type is a prime target for CHIKV *in vivo* and contributes to the pathogenesis of RA. The cells were found to be susceptible and permissive for an infection with CHIKV and MAYV, which in turn induced the expression of antiviral genes and proteins restricting the infection in JAK/STAT pathway-dependent manner. Bulk RNA-seq data showed an exceptionally high induction of innate immunity and proinflammatory response genes, surpassing the response induced in immortalized cell lines. Analyzing the expression of the viral genome in infected cells, an excess of subgenomic RNA over full-length genomic RNA was observed. Type I interferons were secreted upon infection and provided protection against infection when added exogenously. After the highest expression of antiviral proteins was detected in cells in which virus-encoded reporter protein was absent, we performed single-cell RNA-seq to determine differential responses in cells bearing low and high amounts of viral RNA. In line with previous results, immune responses were most pronounced in cells with low-to-intermediate quantities of viral RNA and in RNA-negative bystander cells. A correlational analysis of host gene expression with viral RNA quantity argued for an active antagonistic mechanism, which is only functional when viral proteins are expressed in sufficient quantities. In summary, *ex vivo*-infected fibroblasts are a suitable model to study the immunopathophysiology of CHIKV infections and may enhance our understanding of the interplay between resident joint cells and immune cells. Furthermore, the in-depth analysis of immune responses in combination with the intracellular viral RNA level provides a novel view on the relationship between the progression of the viral replication, cell-intrinsic immune responses, and viral antagonism. This might help us to understand the determinants and the underlying mechanisms of chronic disease.

## Zusammenfassung

Arthritogene Alphaviren wie das Chikungunya-Virus (CHIKV) und das Mayaro-Virus (MAYV) sind von Stechmücken übertragene Positivstrang-RNA-Viren, die Ausbrüche mit Millionen von Patienten verursacht haben und zunehmend in nicht endemischen Regionen auftreten, da der Klimawandel die Ausbreitung der Überträger begünstigt. Die Infektion verursacht eine akute, fiebrige Erkrankung und eine schmerzhafte Polyarthralgie, die im Verlauf chronisch werden kann. Es wird angenommen, dass die Symptome durch eine deregulierte Immunreaktion verursacht werden, die Ähnlichkeit zur rheumatoiden Arthritis (RA) aufweist. In dieser Studie haben wir *ex vivo* CHIKV-infizierte primäre synoviale Fibroblasten, die aus den Knien gesunder und an Osteoarthritis leidender menschlicher Spender gewonnen wurden, charakterisiert. Synoviale Fibroblasten werden von CHIKV *in vivo* infiziert und tragen bekanntermaßen zur Pathogenese von RA bei. Die extrahierten Zellen waren suszeptibel und permissiv für eine Infektion mit CHIKV und MAYV. Die Infektion induzierte die Expression von antiviralen Genen und Proteinen, welche vor allem JAK/STAT-vermittelt die weitere Verbreitung der Infektion einschränkten. Durch RNA-Sequenzierung konnte eine außergewöhnlich ausgeprägte Immunantwort nachgewiesen werden, welche die in immortalisierten Zelllinien induzierte Reaktion übertraf. Bei Infektion wurden Typ I Interferone sekretiert, welche auch nach exogener Zugabe die Infektion auch funktional inhibieren konnte. Bei der Untersuchung antiviraler Proteine konnten wir die höchste Expression in Zellen ohne virales Reporterprotein festgestellt. Daher wurde eine Einzelzell-RNA-Sequenzierung durchgeführt, um unterschiedliche Reaktionen in Zellen mit geringen und hohen Mengen viraler RNA zu bestimmen. Die Immunreaktion war in Zellen mit geringen bis mittleren Mengen an viraler RNA und in RNA-negativen Bystander-Zellen am stärksten ausgeprägt. Durch Korrelation der humanen Genexpression mit der Menge viraler RNA pro Zelle wurden Hinweise auf einen aktiver antagonistischen Mechanismus gefunden, der nur bei ausreichender viraler Proteinexpression erfolgreich ist. Zusammenfassend zeigt sich, dass *ex vivo* infizierte Fibroblasten ein geeignetes Modell sind, um die Immunpathophysiologie von CHIKV-Infektionen zu untersuchen, und dass sie unser Verständnis des Zusammenspiels zwischen residenten Zellen und Immunzellen im Gelenk verbessern können. Darüber hinaus bietet die eingehende Analyse der Immunreaktionen in Kombination mit der intrazellulären viralen RNA einen neuen Blick auf die Beziehung zwischen dem Fortschreiten der viralen Replikation, zelleigenen Immunreaktionen und dem viralen Antagonismus. Dies könnte uns helfen, die zugrunde liegenden Mechanismen der chronischen Krankheit zu verstehen.

# 1 Introduction

## 1.1 Chikungunya Virus – a Re-Emerging Threat

### 1.1.1 Epidemiology and Clinical Features of Chikungunya and Other Alphaviruses

While only few diseases are restricted to the human population, most pathogens frequently circulate between human and animal hosts. In addition, certain pathogens can readily cross the species barrier and can newly emerge in the human population, as recently demonstrated by the SARS-CoV-2 pandemic. Arthropod-borne viruses, or arboviruses, are transmitted through the bites of insects such as mosquitos and ticks and circulate between humans, insects, and animal reservoirs. Recently, arboviruses gain increasing attention due to the worldwide spread of their insect vectors. This spread is driven by increasing travel and trade connections worldwide, and accelerated by climate change, which allows mosquitos to breed in more temperate regions [1].

A prime example for a re-emerging, formerly tropical virus is Chikungunya virus (CHIKV), which has initially been isolated in present-day Tanzania [2], but can today be found in sub-Saharan Africa, central and south America, and southeast Asia, with additional outbreaks reported in North America and Europe [3-5]. CHIKV, an arthritogenic alphavirus of the family *Togaviridae*, has been majorly transmitted by the mosquito *Aedes aegypti*. A single mutation in one of the CHIKV glycoproteins (E1 A226V) during a 2006 outbreak on the island La Reunión allowed CHIKV to be transmitted successfully by the related mosquito species *Ae. albopictus* [6]. In comparison to *Ae. aegypti*, *Ae. albopictus* has the potential to establish colonies in colder regions such as North America and southern parts of Europe, which raises the risk of a typically tropical disease to become endemic in non-tropical regions [7, 8]. In addition to CHIKV, *Aedes* mosquitos can transmit other alphaviruses such as Mayaro virus (MAYV) [9] and flaviviruses such as Dengue and Yellow Fever virus [10]. MAYV is closely related to CHIKV and can lead to similar symptoms upon infection, but differences in the cytokine response have been observed between patients infected with CHIKV and MAYV [11]. However, antibodies generated from the infection with one of the viruses can often cross-neutralize the other virus due to the high similarity of their structural proteins [12]. To date, neither specific treatment options nor protective vaccines are available for CHIKV and MAYV.

Upon infection, CHIKV patients usually present with a short phase of febrile illness, rash, myalgia, and a strong polyarthralgia in multiple peripheral joints, which is mostly self-limiting and resolves within five to seven days [13, 14]. CHIKV infections display an estimated case fatality rate of 0.1 % [15]. However, a substantial fraction of patients experiences a long-term



continuation and/or periodic relapses of arthralgia and other rheumatic symptoms, with over 20 % of patients failing to fully recover after twelve months [16]. The chronic symptoms are associated with cytokine signatures usually detected in patients suffering from rheumatoid arthritis (RA), with strong expression levels of the cytokines IL-6, IL-1 $\beta$ , RANTES, and GM-CSF [17, 18]. Profound evidence for a persistent productive infection is missing, but animal studies and human biopsies indicate that the chronic inflammatory state in CHIKV patients may be driven by cells (such as macrophages and fibroblasts) harboring viral RNA up to 16 weeks post infection [19-21]. The tropism of CHIKV includes the epithelial and endothelial cells of many organs, including the skin, muscles, liver, and spleen, as well as lymphoid tissue and macrophages [13]. Additionally, in animal models and patients with a fatal outcome of the disease the central nervous system and the brain have been found to be infected [20, 22], although this complication seems to be rare [23, 24].

Taken together, the threatening expansion of the range of CHIKV vectors and the troubling long-term consequences of the infection make a better understanding of the immunopathophysiology of CHIKV an essential basis to combat the disease.

### *1.1.2 Molecular Biology of Chikungunya Virus*

CHIKV, a positive-sense, single-stranded RNA virus, forms enveloped virions of spherical form with a diameter of approximately 70 nm. The virions consist of the capsid protein (C) with the envelope (E) glycoproteins E1 and E2 embedded into the lipid envelope. In total, 240 heterodimers of E1 and E2 form 80 homotrimeric spikes on the virion's surface, which are important for attachment and entry. The 11.5-12 kb CHIKV genome encodes a total of nine proteins in two open reading frames (ORFs) and differs in length due to differences in variable domains in the first ORF and in the untranslated regions. The first ORF contains the nonstructural proteins nsP1 to nsP-4, while the second ORF, preceded by a subgenomic promoter, encodes for the structural proteins C, E1 and E2, and for the associated proteins E3, 6K, and TF [25]. Additionally, the genome contains untranslated regions (UTRs) at both the 5' and the 3' ends, which serve as promoter regions and contribute to masking the viral RNA from the innate immune system [26].

CHIKV enters the cell via receptor-mediated endocytosis. Several cellular candidates were found to enhance attachment and entry of particles, with the most important example being MXRA8 [27], but none proved to be essential for the infection. The broad cellular and tissue tropism and the possibility that multiple attachment factors and receptors can potentially mediate

entry in a synergistic fashion have impeded the search for a distinct alphavirus entry receptor [28, 29]. Upon entry, the viral membrane fuses with the endosomal membrane, mediated by the low endosomal pH and a resulting conformational change in the E1 protein. The viral genome is then released into the cytosol from the disassembling capsid core [30]. Afterwards, the first ORF, coding for the nonstructural proteins, is translated into a polyprotein and cleaved through the proteolytic function of nsP2. During processing, a partly cleaved polyprotein has an important role in the RNA replication process. A complex of noncleaved nsP123 and nsP4 has been shown to be majorly responsible for the synthesis of the minus-strand RNA, while a complex of the fully cleaved nonstructural proteins is responsible for the reproduction of the full-length genome and the 26S RNA coding for the structural part of the genome [31]. nsP4 functions as the RNA-dependent RNA polymerase to produce all three species of viral RNA – genomic, subgenomic, and minus-strand RNA – present in infected cells. The subgenomic RNA is the most abundant RNA in productively infected cells and ensures the efficient mass production of viral structural proteins. It is not packaged into the mature virions, as the packaging signal responsible for the interaction with the capsid protein is located in the nsP2-coding region of the genome [32]. In addition to their joint function in the viral RNA replication machinery, nsP1-3 serve multiple other functions. nsP1 anchors the replication complex to host membranes and catalyzes the formation of the m<sup>7</sup>GMP cap to the 5' end of the viral RNA. nsP2 consists of an N-terminal helicase domain, which supports the capping reaction and acts as a nucleoside triphosphatase, and a C-terminal protease domain, which cleaves the viral nonstructural polyprotein after translation. The immune-antagonistic functions of nsP2 are described in the next chapter. nsP3 consists of three domains, whose functions are less well described and partly unclear. The N-terminal macrodomain is able to release the posttranslational modification mono- and poly-ADP-ribose from cellular proteins, probably manipulating their abundance and function. The alphavirus-unique domain is essential for viral RNA replication, but its function remains to be determined. The C-terminal hypervariable domain is, as the name implies, poorly conserved between different members of the alphavirus family, and can be manipulated and used to insert reporter proteins without loss of replication capacity. The hypervariable domain is highly phosphorylated and can potentially bind to multiple host factors, including the host protein FHL1, which is essential for replication [33]. The functions of nsP1-4 are reviewed in detail in [31, 34].

The translation of the structural polyprotein from the second ORF starts with the capsid protein, which is autocatalytically cleaved from the polyprotein and associates with the viral genomic RNA to form the nucleocapsid core. The remaining polyprotein including E3, E2, 6K,

and E1 is translocated to the ER by a signal peptide in the E3 part, and processed into the single proteins during the maturation in the endoplasmic reticulum and the Golgi apparatus by cellular proteases such as Furin and other signal peptidases. Processed E1 and E2 are subject to post-

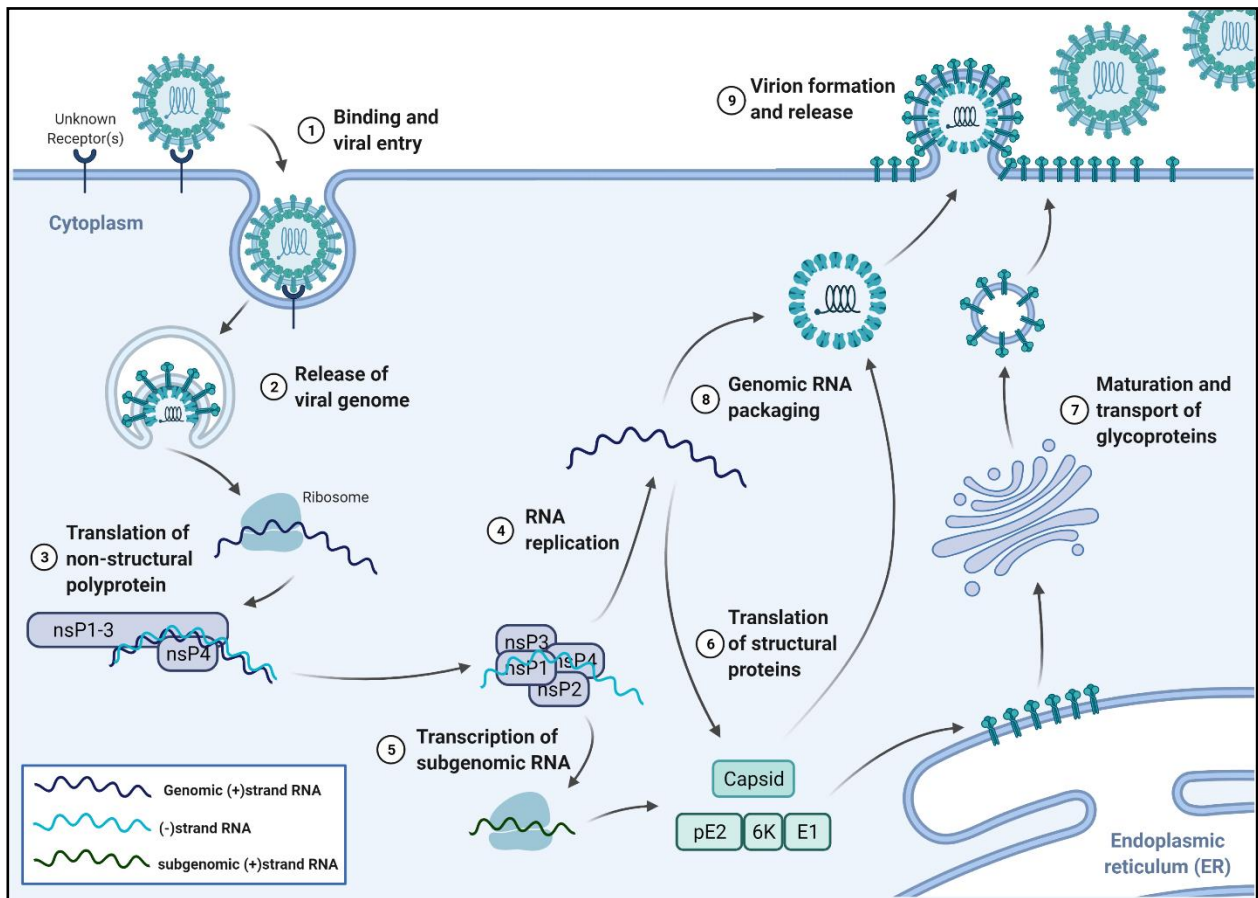


**Fig. 1: Replication cycle of Chikungunya virus in the host cell.** Upon entry through receptor-mediated endocytosis (1), the viral membrane fuses with the endosomal membrane in a pH-dependent manner (2). The nonstructural proteins (nsPs) are being translated by the host and the partly cleaved complex nsP123+4 synthesizes negative-stranded RNA (3), which serves as a template for the replication of full-length positive-stranded genomic RNA (4) and subgenomic RNA encoding for the structural proteins (5). The positive-stranded RNA is produced by a complex of fully cleaved nsPs. Structural proteins are then translated from the genomic and subgenomic RNA (6). The glycoproteins migrate through the endoplasmic reticulum and the Golgi apparatus, where they undergo final processing and posttranslational modifications (7). The capsid and the genomic RNA form the nucleocapsid and migrate to the cell surface (8), where the virion formation and budding to release new particles takes place (9). Adapted from [13]. Created with BioRender.com.

translational modification and are transported to the cell surface via the secretory pathway [35]. Additionally, a transframe (TF) version of the 6K protein can be produced through a frameshift translation, which is also incorporated into the mature virion [36]. 6K and TF act as viroporins and attach to host membranes through palmitoylated sites. Additionally, they support the budding process of virus particles at the cell membrane, but only TF is frequently incorporated

into the virion [33]. E3 shields the acid-sensitive region of the E2 protein and protects E2 during the transport through the cell [35]. Finally, the nucleocapsid core buds from the infected cell and acquires its lipid envelope with the glycoprotein spikes during this process, forming the mature, infectious virion [36]. An overview of the replication cycle is given in figure 1.

### *1.1.3 Innate Immune Responses Induced and Antagonized by Chikungunya Virus*

Similar to other RNA viruses, CHIKV-derived pathogen-associated molecular patterns (PAMPs) are recognized by cellular sensors of the innate immune system throughout its replication cycle and induces antiviral responses. Upon endosomal entry into the cells, single-stranded RNA is sensed through toll-like receptor (TLR)-7 and -8, leading to MYD88-mediated early immune responses [37, 38]. The role of the double-stranded RNA sensor TLR-3 in recognition of CHIKV infection, however, is debated in the literature. On the one hand, loss of Tlr-3 function in a mouse model led to increased CHIKV replication and more severe pathology due to a reduced neutralization capacity of the produced antibodies [39]. On the other hand, a different study failed to detect differences in viral RNA burden in the serum and different organ tissues of *Tlr3*<sup>-/-</sup> mice as compared to wild-type mice [40]. The sensing of CHIKV through cytosolic pattern recognition receptors (PRRs) has been studied in greater detail. Two proteins, RIG-I and MDA5, are mainly responsible for the cellular sensing of double-stranded viral RNA (dsRNA), a replication intermediate of positive-stranded RNA viruses. RIG-I has been shown to recognize 5'-phosphorylated dsRNA, but not the non-phosphorylated dsRNA mimic poly(I:C) [41]. Additionally, a panhandle structure at the 5' end of the viral genome is an important recognition structure in the context of RIG-I-dependent sensing of an authentic viral infection [42]. While a stronger response is induced through sensing by RIG-I than through MDA5 [43], both PRRs are able to sense CHIKV RNA in a concentration-dependent manner [44]. In addition to successfully produced genomic and subgenomic RNAs, defective viral genomes arise during the infection due to the low fidelity of the viral polymerase. Defective viral genomes are potent inducers of innate immune signaling [45]. Upon binding to viral RNA, RIG-I and MDA5 expose a CARD-like domain, allowing them to interact with mitochondria-bound MAVS proteins. MAVS in turn activates a signaling cascade via TBK1 and IKK $\epsilon$  to phosphorylate and thereby activate NF $\kappa$ B, IRF3, and IRF7, which translocate into the nucleus and induce transcription of antiviral genes along with type I interferon (IFN) genes [46].

Type I IFN is well characterized in its ability to inhibit alphavirus infection and replication. Patients and animal models infected with CHIKV display high serum levels of IFN- $\alpha$

during the acute phase of the infection [20, 40]. Importantly, in *Ifnar*<sup>-/-</sup> or *Stat1*<sup>-/-</sup> C57BL/6 and 129 mice, both deficient in type I IFN signaling, a CHIKV infection is lethal, while wild-type

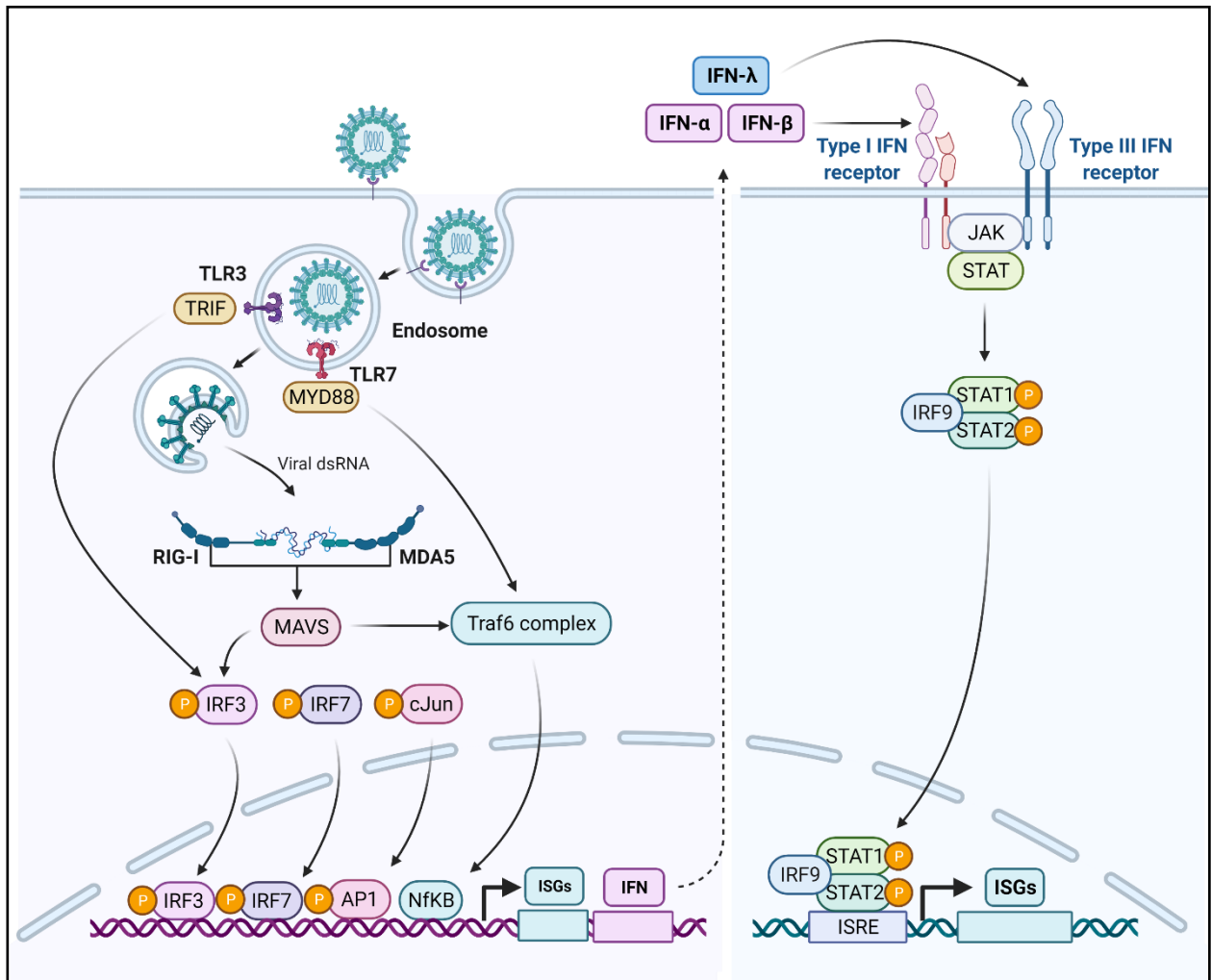


**Fig. 2: Innate immunity signaling pathways.** Upon entry, the genome of CHIKV and other alphaviruses can be sensed in the endosomes via Toll-like receptor (TLR)-3 and -7/8 or in the cytosol via RIG-I and MDA5. This leads to a downstream induction of antiviral proteins and interferons (IFNs) via IRFs and NFκB. The secreted IFNs further act in an auto- and paracrine way to induce the transcription of IFN-stimulated genes (ISGs) via the JAK/STAT pathway. Adapted from [46, 47]. Created with BioRender.com.

mice recover from an infection [22, 48]. This can be explained by the induction of IFN-stimulated genes (ISGs) through the action of IFN to its receptor. The IFN- $\alpha/\beta$  receptor consists of two subunits, IFNAR1 and -2, which heterodimerize by the binding of IFN. The dimerization activates the kinases TYK2 and JAK1, which phosphorylate STAT1 and -2 heterodimers. The dimers, in complex with IRF9, translocate to the nucleus and activate IFN-stimulated response elements (ISREs), leading to the expression of downstream ISGs. The signal transduction is similar for type III IFNs, although it signals through a distinct receptor consisting of the IFNLR

and the IL10R $\beta$  subunits [47]. An overview over the innate immune signaling pathways involved in CHIKV sensing is given in figure 2.

In the context of infection by CHIKV and other alphaviruses, several ISGs have been characterized in their ability to impact viral replication and spread. A large-scale study overexpressing 380 ISGs individually in *STAT1*<sup>-/-</sup> fibroblasts showed broad inhibitory functions of several genes such as *IRF1*, *RIG-I*, and *IFITM3* for multiple viruses including CHIKV [49]. Interestingly, the DNA sensor cGAS was identified as broadly antiviral and was later described to maintain a basal level of immunity in the cell by constant signaling, which supports cells in their defense against RNA viruses [50]. IFITM3 interferes with CHIKV entry and to reduce virion infectivity, and is susceptible to antagonism by CHIKV [51, 52]. The related proteins IFITM1 and -2 can also exert antiviral function against CHIKV and other alphaviruses during the entry step [51, 53]. During later steps, IFIT1 can inhibit translation and replication of alphaviral RNA by acting on the 5'UTR of the viral genome [54]. Other ISGs such as *IFI16* and *ISG15* also impair CHIKV infection, although the mechanism is not fully established [55, 56].

CHIKV is clearly a target of the PRR- and IFN-mediated innate immune response, as shown multiple times in *in vitro* and *in vivo* studies. However, the virus has also developed sophisticated ways to counteract the host's immune response, allowing for successful replication even in fully immunocompetent hosts. A key role for the immune evasion strategies is taken by the viral protein nsP2, which interferes with JAK/STAT signaling [57]. This was later shown to be achieved by actively exporting STAT1 from the nucleus [58]. Additionally, a shutdown of the host transcriptional machinery by degradation of a subunit of the RNA polymerase II has been observed [59, 60]. Lastly, the above-mentioned basal antiviral state in the host cell through cGAS-mediated signaling is antagonized by CHIKV through degradation of cGAS [61]. Taken together, a strong innate immune response is a hallmark of a CHIKV infection. The response is initiated through recognition of the viral RNA, then amplified and extended through IFN, which induces ISG expression through JAK/STAT signaling. CHIKV has, in turn, developed several mechanisms to counteract the host's immune response.

#### *1.1.4 Immune Cell-Mediated and Adaptive Immune Responses*

Apart from cell-intrinsic and IFN-mediated innate immune responses, a cell-mediated innate and adaptive immune response is critical for the clearance of CHIKV *in vivo*. Macrophage depletion in mouse models typically leads to an increased viremia, and monocytes and macrophages are targets of a CHIKV infection themselves [20, 62]. Macrophages may also be key players in the

arthralgia-inducing immune response in the joints [63, 64]. The role of natural killer (NK) cells is less well studied, however, they tend to accumulate in musculoskeletal tissue during the acute phase of the infection and display a potentially damaging phenotype during the course of the disease [65, 66]. Dendritic cells contribute to the sensing of CHIKV-infected cells, and induce IFN-dependent antiviral responses to control the infection in mice [67].

In terms of adaptive immunity, there is a clear need for a neutralizing antibody response for the clearance of CHIKV. In B cell-depleted mice, CHIKV viremia can persist for over a year, indicating the critical role for antibodies in controlling the infection. Anti-CHIKV antibodies often act via binding of the E2 protein and thereby inhibiting viral binding and entry [68-70]. Antibodies induced upon CHIKV infection are often cross-reactive against other alphaviruses [12, 71, 72]. In addition to inhibiting viral entry, neutralizing antibodies can also interfere with the budding and release of newly formed viral particles from the host cell by coalescing the viral glycoproteins on the cell surface [68, 71, 73]. Cell surface-bound antibodies can also activate immune cells to kill the infected cell [73]. The role of T-cells seems to be less important for the immunity against CHIKV. CD4<sup>+</sup> T-cells may even be responsible for the joint pathology without contributing to clear the infection [74]. Granzyme A, a protein secreted by T and NK cells, has been identified to contribute to the arthralgia symptoms experienced by CHIKV patients [75]. CD8<sup>+</sup> T-cells do not seem to play a role in the clearance of CHIKV and contribute minimally the inflammation in the joints [74] due to a potential active evasion strategy against CD8<sup>+</sup> T-cell responses [76]. Taken together, the main correlate of protection against disease are neutralizing antibodies, as demonstrated by multiple pre-clinical and clinical vaccine studies [77-81] and a passive immunization study in mice, which protected against a lethal challenge [82]. This has implications for the design of novel vaccines and the clinical approval thereof.

#### *1.1.5 Intervention and Vaccine Strategies against Chikungunya Virus*

So far, an acute CHIKV infection cannot be specifically treated. As the infection in immunocompetent people is usually self-limiting, a symptomatic treatment to reduce pain and fever is usually the only measure taken. Although novel and established antivirals such as ribavirin and favipiravir inhibit CHIKV *in vitro*, direct-acting antivirals have not been approved for therapy of CHIKV-infected patients so far [83]. For the treatment of chronic sequelae, specifically post-CHIKV arthralgia, the clinically approved, immunomodulatory drug methotrexate has been applied, although the drug has severe adverse effects and a possible

benefit has not been finally evaluated through randomized, prospective, placebo-controlled trials [84, 85].

In addition to an urgently required treatment strategy for acutely and chronic CHIKV patients, a protective vaccine would greatly reduce the burden of disease in affected countries. Multiple attempts have been made to produce a CHIKV vaccine, but none has been finally successful so far. One of the first candidates was the live-attenuated virus strain 181/25, whose attenuation was achieved through serial passaging, leading to mutations in the E2 glycoprotein. Clinical trials with the 181/25 vaccine candidate were stopped after 8 % of vaccinees developed arthralgia, highlighting the difficulties in developing an effective vaccine with traditional methods [86]. Prominently, an engineered live-attenuated vaccine candidate with a partial deletion of the nsP3 gene has entered a phase III trial in the United States, and has produced promising results with 98.5 % of participants developing neutralizing antibody titers [87]. Another vaccine based on a recombinant measles vector was successful in a phase I trial with 100 % seroconversion in the candidate vaccine group [88]. Overall, a vaccine against CHIKV currently presents the best option to combat the disease and to protect travelers, but it may be challenging to provide a broad distribution in affected regions. Therefore, an effective treatment for the long-term sequelae in combination with improved prevention against mosquito-borne diseases, for example through vector control measures, would greatly reduce the burden in endemic countries.

## **1.2 Fibroblasts in Health and Disease**

### *1.2.1 Synovial Fibroblasts in Rheumatoid Arthritis*

Synovial fibroblasts in joints of healthy individuals provide the extracellular matrix and thereby maintain the cartilage integrity and lubrication, but change their role during the genetically predisposed condition of RA [89, 90], which affects about 0.5 % of all adult people worldwide [91]. RA is a chronic inflammatory disease characterized by the destruction of cartilage in the joints with associated pain and loss of function in the affected joints of patients. Early on, autoreactive B- and T-cells are responsible for the production of autoantibodies and the invasion into the tissue as aggressive effector cells, respectively [92]. The progression from an acute to a chronic phenotype is additionally accompanied by the dedifferentiation of synoviocytes and their massive expansion, leading to a thickened layer of the synovial membrane with increased migration of proinflammatory cells [93]. The fibroblasts contribute to the cartilage destruction by



the overproduction of matrix-metalloproteases (MMPs) and immune cell-stimulatory cytokines such as IL-6, IL-8, RANKL, and different chemokines [94, 95]. Through crosstalk with B-cells, synovial fibroblasts can extend their life span and activate them to produce autoantibodies [96, 97]. Synovial fibroblasts in RA can also crosstalk with T-cells, monocytes and macrophages, and endothelial cells, leading to enhanced inflammation and immune cell recruitment [98]. Additionally, the metabolism of the fibroblasts changes, leading to the production of bioactive lipids and increased metabolic exchange between cells [99]. Interestingly, the fibroblasts of the synovium are not a homogenous group, but are organized into subgroups expressing different surface markers with localization to specific regions within the synovium. During RA, the proportion of these subgroups changes, and they may exert different functions during the course of disease [100]. Synovial fibroblasts have been suggested as a target in the treatment of RA by modulation of their metabolism, their surface marker expression or their signal transduction cascades. Additionally, the imprinted epigenetic landscape constitutes a promising target for the reversal of RA and treatment with different histone-modifying drugs has shown some efficacy in pre-clinical and early stage clinical trials [98]. Overall, synovial fibroblasts are clearly majorly involved in the induction and progression of RA and need to be considered in strategies to combat the disease.

### *1.2.2 Fibroblasts as Drivers of Arthralgia in Chikungunya Virus Infections*

An infection with CHIKV often leads to a chronic polyarthralgia reminiscent of RA. Several studies have emphasized the similarities between CHIKV infection-induced and genetically predisposed RA [75, 101, 102]. As described in the previous chapter, synovial fibroblasts contribute to the induction of RA by producing cartilage-destroying matrix-metalloproteases and secretion of pro-inflammatory and immune cell-attracting cytokines. During a CHIKV infection, synovial fibroblasts serve as an active site of replication [22, 103-105]. Importantly, the secretion of IL-6, IL-8, RANKL, and MCP-1 by infected fibroblasts has been reported, which attracts and stimulates phagocytes such as monocytes and macrophages [63]. The migration of immune cells to the joints potentially increases the inflammatory milieu in this region. Subsequently, the expression and secretion of MMPs by synovial fibroblasts may then be induced through external stimuli with IL-1 and TNF- $\alpha$  [94]. In summary, the role of synovial fibroblasts is well established in RA, but remains unclear in the context of arthritogenic alphavirus infections. Although these cells can be infected, their interplay with other cell types, either in the joint-resident or infiltrating, is largely uncharacterized *in vivo*, but may hold key information to treat acute and chronic sequelae.

## **1.3 Current State of the Research in the Field and Importance of this Study**

### *1.3.1 State of the Art*

To this day, CHIKV is considered a neglected tropical disease and recognized by the World Health Organization as a major threat to endemic countries. The development of prevention and intervention strategies are of major importance for an increasing number of countries, and a basic understanding of the viral replication cycle, subsequent immune responses, and of the reasons for the chronic course of the disease will be vital for such strategies. However, clinically relevant model systems are often limited to immunodeficient mice, while human model systems such as organoids or primary cells are underrepresented in CHIKV research. Research in less physiologically relevant models such as immortalized cell lines is valuable, but often fails to produce clinically relevant results. Even though fibroblasts are known to be drivers of arthralgic responses as well as prime targets for a CHIKV infection *in vivo*, research on them has been infrequent [63, 104, 106] without a comprehensive immune response profiling. One study has explored the connection of infected synovial fibroblasts to monocytes in the induction of arthralgia [63], which is a topic to be addressed in the model system presented here.

Additionally, virus infections in single cells have only been marginally investigated by transcriptomic studies so far, with a recent major focus on SARS-CoV-2. In-depth kinetic analysis of alphavirus infections via single-cell RNA-seq has not been conducted. Similar experiments have for example been performed with West Nile virus [107], Influenza A virus [108], and Herpes Simplex virus 1 [109], but these studies were directed at different aims than this study, such as the analysis of the viral genome or the identification of specific host factors. Taken together, this study provides novel insights into the kinetics of cell-intrinsic immune responses in the early and later stages of an acute alphavirus infection.

### *1.3.2 Importance*

CHIKV affects thousands to millions of people worldwide every year, with a peak of an estimated two million infections in 2006. Furthermore, expanding vector mosquito ranges due to climate change and increased travel and trade expose formerly unaffected countries to CHIKV and other alphaviruses. The infection usually results in a short acute phase febrile illness together with rashes, myalgia, and polyarthralgia. Importantly, the polyarthralgia is known to progress into a chronic disease in a subgroup of patients, with varying percentages depending on the virus strain, the outbreak, and host determinants. Through the ongoing development of one or several

vaccines against CHIKV, a solution for the expanding reach of CHIKV seems to be in sight. However, distribution and administration of a CHIKV vaccine into endemic, often developing countries remains a challenge and it is likely that outbreaks in this regions will not be prevented by a vaccine. Therefore, ongoing research is essential to improve our understanding of the disease and of possible treatment options.

In this study, we combined well-established methods such as Western Blot, qRT-PCR, flow cytometry, and fluorescence microscopy with bulk and single-cell RNA sequencing to provide a comprehensive insight into the cell-intrinsic immune reactions exerted by primary human synovial fibroblasts upon *ex vivo* infection with CHIKV. The virus-inclusive single-cell sequencing approach is so far unique for any member of the alphavirus genus. For other viruses, the interplay between viral replication and the host response has rarely been mapped in detail over time and over multiple infection conditions. The resulting findings contribute to the knowledge about the role of synovial fibroblasts in CHIKV-induced arthralgia. They also offer a possible explanation to the question whether the virus is able to antagonize innate immune responses, a process that has been mostly addressed using overexpression of single CHIKV proteins or replicon systems [57, 58, 60]. To properly address the CHIKV-induced immune response, we used full-length, replication-competent virus in this study, leading to the strong induction of ISGs and proinflammatory cytokines in infected cell cultures. While no evidence for viral antagonism was detectable via bulk RNA sequencing, the single-cell approach disclosed that cells the immune response was antagonized in highly infected cells only. This may explain the seemingly controversial observations between studies describing viral antagonism through the actions of the viral protein nsP2 and studies failing to observe an active antagonism. Taken together, this study provides a valuable contribution to the knowledge about early events in viral infections and the non-linear association between viral replication and cell-intrinsic responses.

## 2 Methods

A comprehensive description of the methods and technical details for the reagents can be found in the original publication this dissertation is based on [110]. Here, I present key methods and elaborate on details which were not included in the publication due to space constraints. All experiments and analysis were performed by me, if not noted otherwise.

### 2.1 Cell Culture, *In Vitro* Stimulations and Virus Infections

#### 2.1.1 Culture of Primary Human Fibroblasts and Immortalized Cell Lines

Fibroblasts from healthy individuals (healthy synovial fibroblasts, HSF) and from individuals suffering from osteoarthritis (osteoarthritic synovial fibroblasts, OASF) were extracted in the Kerckhoff Clinics in Bad Nauheim by E. Neumann during routine surgeries. All patients gave informed written consent and the study was approved under the ethical votes IDs 66-08 and 74-05 by the ethic committee of the Justus-Liebig-University Gießen. OASF and HSF were taken into culture after purification and shipped frozen after two to four passages as described before [111]. Afterwards, the cells were further cultured as adherent cultures and used for experiments up to passage eight due to observed gene expression patterns over longer passages [111]. Other cells used for infection experiments included the human osteosarcoma cells line U2OS, the human embryonic kidney cell line HEK293T, and the human foreskin fibroblast cell line HFF-1. Additional cell lines used for the detection of type I IFN and for virus production were human HL116 and hamster BHK-21 cells, respectively. All cells were cultured as described in the original publication [110].

#### 2.1.2 Virus Infections and Impact of Treatments

To analyze different aspects of infection in primary cells and cell lines, cell cultures were inoculated with CHIKV and MAYV by mixing virus stocks with cell culture medium and incubating them for one hour on the cells. Afterwards, the inoculum was removed and replaced by fresh cell culture medium or, in case of the transcriptomic analysis, by pre-conditioned medium. Virus stocks were produced by electroporation of *in vitro*-transcribed viral RNA into BHK-21 cells and subsequent filtration of the supernatant after four days of incubation. The viral molecular clones used in this study, 5'EGFP-CHIKV and 5'EGFP-MAYV have been described previously [112, 113] and encode an enhanced green fluorescent protein (EGFP) reporter gene

under the control of a second subgenomic promotor, which is identical to the promotor for the structural gene cassette, between the structural and the nonstructural part of the genome. Virus titers were determined by incubation of HEK293T cells with virus-containing supernatant in serial dilutions, and subsequent analysis of the cells for EGFP expression 24 hours post infection using flow cytometry. Positivity values in a linear range were used to calculate the amount of infectious units per ml.

The infection efficiency of target cells was determined similarly using flow cytometric readout of EGFP expression, indicative of a productive infection. To modulate infection, type I or III interferon (IFN) were added prior to or after infection, or the JAK/STAT-inhibitor Ruxolitinib was used to interrupt IFN signaling. IL-1 $\beta$  was used to induce secretion of IL-6. The production of type I IFN by OASF was quantified by incubating the reporter cell line HL116, which carries a firefly luciferase gene under the control of an IFN-sensitive promotor, with cell culture supernatant for six hours and subsequent measuring of luciferase activity [114]. IL-6 secretion into the supernatant was measured by ELISA. Immunostimulatory nucleic acids in form of plasmid DNA and modified RNA (5'-triphosphate RNA) were introduced into OASF by transfection using Lipofectamine 2000. Virus particles were neutralized by the viral glycoprotein-blocking antibody C9 and recombinant MXRA-Fc proteins.

## **2.2 Analysis of Cellular Protein and mRNA Expression**

### *2.2.1 Quantitative RT-PCR*

For the analysis of cellular gene expression, a Taqman-based system using primers and probes specific for the gene of interest and a housekeeping gene (*RNASEP* or *GAPDH*) were used. After manual, spin-column based or automated RNA extraction, equal quantities of RNA were used to produce cDNA by reverse transcription. Afterwards, quantitative RT-PCRs were performed on the Applied Biosystems ABI 7500 Fast or the Roche LightCycler 480 and the relative change of the gene of interest was determined using the  $\Delta\Delta C_t$  method.

### *2.2.2 Flow Cytometry, Microscopy, and Immunoblotting*

The rate of EGFP-positive cells as well as the expression levels of various proteins of interest was determined by flow cytometry. For protein analysis, cells were permeabilized with 0.1 % Triton-X and stained with primary antibodies in combination with AlexaFluor-labelled secondary antibodies and subsequent measurement employing suitable controls on the BD

FACSCalibur or FACSLyric. Microscopy was performed with the Zeiss LSM800 Airyscan Confocal Microscope. Immunostaining on PFA-fixed cells was performed as described for flow cytometry immunostaining, and live-cell imaging was performed under regular cell culture conditions in a CO<sub>2</sub>- and temperature-controlled atmosphere with the Zeiss LSM800 Airyscan Confocal Microscope. Cellular proteins were analyzed by SDS-polyacrylamide gel electrophoresis and subsequent immunoblotting using specific antibodies. Secondary fluorophore-coupled antibodies were detected with the LI-COR Odyssey Fc system.

## **2.3 Transcriptomic Analysis of CHIKV-Infected Fibroblasts**

### *2.3.1 Bulk RNA-Seq Analysis*

OASF and HSF were infected with CHIKV at an MOI of 10 and RNA was extracted from infected and mock-infected cells at 24 hours post infection. After next generation sequencing library preparation, Illumina HiSeq4000 or NovaSeq6000 sequencing with 50 bp paired-end reads aiming for 30 to 65 mio reads per sample was performed. The resulting reads were mapped onto the human hg19 reference genome and the CHIKV LR2006-OPY genome and statistically analyzed using the CLC Genomics Workbench software. Overrepresentation of biological processes was determined using the Gene Ontology enrichment analysis tool [115]. The raw and processed sequencing data can be accessed at the NCBI GEO database under the accession number GSE152782.

### *2.3.2 Single-Cell RNA-Seq Analysis*

For single-cell RNA-seq analysis, OASF were infected at a range of MOIs (0.01, 0.1, 1, and 10) and analyzed at six and 24 h post infection. To obtain a single-cell suspension, cells were trypsinized and filtered before diluting them to a proper concentration, aiming for a recovery of 10000 cells per sample. Using the 10X Genomics Chromium Controller with the appropriate reagents from the 3'GEM, library & Gel bead kit v3.1, cells were separated together with gel beads into an oil-in-water emulsion and incubated for reverse transcription within the emulsion. Afterwards, resulting cDNA was bulk amplified and prepared for library sequencing. The libraries were sequenced on an Illumina HiSeq4000 with 100 bp paired-end sequencing aiming for 175 mio reads per library, and the resulting reads were mapped to the human and CHIKV genomes as described above using CellRanger v5.0. Afterwards, the data was analyzed using the R packages Seurat v4.0 [116] and DoRothEA v3.12 [117]. Briefly, the data underwent quality

control with filtering of cells with high amounts (>20 %) of reads mapping to mitochondrial genes to exclude dead cells. Afterwards, the data was normalized with Seurat's SCTransform function including cell cycle regression, and principal component analysis (PCA) and Uniform Manifold Approximation and Projection (UMAP) were used for dimensional reduction and visualization. All samples from one time point were integrated using Seurat's IntegrateData function. All generated code can be accessed at [https://github.com/GoffinetLab/CHIKV\\_scRNAseq-fibroblast](https://github.com/GoffinetLab/CHIKV_scRNAseq-fibroblast), the raw and processed data can be downloaded from the NCBI GEO database under the accession number GSE176361.

## 3 Results and Interpretation

The results described here are a summary of the key points of the original publication this manuscript is based on [110], together with further explanations and interpretations not included in the publication. Figures referenced in this section refer to the figures in the original publication.

### 3.1 Human Synovial Fibroblasts are Suitable for *Ex Vivo* Infection Studies with CHIKV and MAYV

#### 3.1.1 Primary Human Synovial Fibroblasts Support the Replication Cycle of Alphaviruses

Synovial fibroblasts have been identified to be primary target cells for CHIKV infection *in vivo* [104, 118] and may be a crucial component in the induction and chronification of CHIKV-mediated arthralgia [63]. To determine whether synovial fibroblasts are susceptible and permissive to CHIKV and MAYV infection *ex vivo*, fibroblasts from healthy donors (healthy synovial fibroblasts, HSF) and from patients suffering from osteoarthritis (osteoarthritic synovial fibroblasts, OASF) were extracted and taken into culture. The rationale behind using cells from two different sources was the limited availability of cells from healthy donors, while OASF were readily accessible through routine surgery procedures. Therefore, we performed a qualitative assessment of infection dynamics, cofactor expression, and transcriptomic responses following infection to potentially identify differences between cells from both donor types. As determined by infection with EGFP-expressing reporter viruses and subsequent supernatant titration on HEK293T cells, both OASF and HSF were susceptible and permissive to infection with CHIKV and MAYV. CHIKV infection resulted in lower percentages of EGFP-positive cells, but in higher virus titers than MAYV infection in both cell systems at 24 and 48 hours post infection. Interestingly, HSF cultures displayed similar infection rates as OASF cultures, but produced lower amounts of infectious units in almost all conditions (Fig. 1A, B). The viral attachment-enhancing cell-surface protein MXRA8 [27] as well as the essential viral replication cofactor FHL1 [33] were expressed in cells from both sources (Fig. 1C). Additionally, we demonstrated the importance of MXRA8 by blocking the binding site on the virus particles with a recombinant soluble MXRA8-Fc protein, which resulted in a reduction of the infection efficiency (Fig. 1D). In summary, we characterized synovial fibroblasts from both healthy and osteoarthritic donors to be suitable for infection studies with CHIKV and MAYV, as they support the full viral replication cycle and express critical cofactors for viral entry and replication.



### 3.1.2 Cytokines Produced Upon Infection and Induced Innate Immune Responses Impact Infection

Cytokines such as IL-1 $\beta$  and IL-6 as well as IFNs are produced by synovial fibroblasts and other cell types during an infection with CHIKV and are a predictive marker for the severity of the disease [18, 119]. Therefore, we treated fibroblasts with IL-1 $\beta$ , which activates fibroblasts during RA [120], and quantified the resulting production of IL-6, and RA-driving cytokine, in the presence and absence of CHIKV infection. IL-1 $\beta$ , but also CHIKV infection, induced IL-6 secretion, while the treatment did not affect the infection efficiency (Fig. 1E, S1A). Together, this suggests that synovial fibroblasts can, either through the infection itself or by stimulation with cytokines produced by infiltrating lymphocytes, contribute to the pro-inflammatory and arthralgia-mediating milieu present in the joints of affected patients.

We analyzed the impact of cell-intrinsic and IFN-triggered immunity on the spread of CHIKV and MAYV infection by infecting OASF in presence of Ruxolitinib, an inhibitor of the JAK/STAT pathway, a major signal transduction cascade for IFN-triggered responses. After six hours of pretreatment and subsequent infection for 24 or 48 hours, the infection rate under the treatment with Ruxolitinib was enhanced 1.3-4.7 and 1.3-7.7-fold, respectively, as compared to mock-treated, infected OASF (Fig. 1F). The immune response following infection as measured by *IFIT1* and *MX2* mRNA induction was diminished in Ruxolitinib-treated cells, in particular the strictly IFN-dependent induction of *MX2* gene expression was completely abrogated (Fig. 1G). Overall, MAYV infection as compared to CHIKV infection was less enhanced by Ruxolitinib treatment, which may be due to a higher base-line infection rate in mock-treated cells as determined by flow cytometry (Fig. S1C). Additionally, MAYV infection triggered a lower induction of *IFIT1* mRNA at 48 hours post infection in mock-treated cells, which was not reduced after Ruxolitinib treatment, suggesting a less important role of IFN in MAYV infection (Fig. 1G). Supporting this, the secretion of type I IFN as measured by a reporter cell system was most pronounced after infection with CHIKV at an MOI of 10, while MAYV infection resulted in lower, often undetectable levels of type I IFN in the supernatant (Fig. S1B). Live-cell imaging showed that treatment with Ruxolitinib resulted in a faster spread of CHIKV infection and a higher percentage of EGFP-positive cells at the peak of infection between 30 and 36 hours post infection (Fig. 1H, S1D). Taken together, synovial fibroblasts are not only susceptible for infection with CHIKV and MAYV, but also support viral replication and the release of new infectious virions into the supernatant. Infection provokes the production of proinflammatory

cytokines and the induction of antiviral gene expression. In turn, fibroblasts are able to limit viral spread in culture via JAK/STAT-mediated innate immune responses.

### **3.2 Transcriptomic Analysis of CHIKV-Infected Fibroblasts Reveals Active Viral Replication Despite a Strongly Induced Innate Immune Response**

#### *3.2.1 Cell-Intrinsic Immunity in Fibroblasts is Strongly Induced Upon Infection with CHIKV*

To gain insights into CHIKV infection-induced changes, we established a comprehensive transcriptomic profile of infected OASF and HSF by RNA-sequencing on low-passage fibroblasts infected at an MOI of ten. As a control, we used a neutralizing antibody-treated virus separately as inoculum to determine possible effects of free viral RNA and/or weak virus binding without establishment of an active infection. While the non-neutralized virus infection led to ~5-25 % EGFP-positive cells at 24 hours post infection, the neutralized virus resulted in <1 % EGFP positive cells, as expected (Fig. 2A). As expected, the infection led to a strong and significant upregulation of hundreds of genes, which in major parts belonged to antiviral, proinflammatory cellular pathways (Fig. 2C, F, Suppl. Fig. 2D). Additionally, some genes known to be expressed during RA, such as *TNF*, *IL6*, and *RANTES*, but no genes coding for RA effector proteins such as matrix metalloproteases were upregulated. Interestingly, no IFN- $\alpha$  transcripts were induced or even detectable, but IFN- $\beta$  and - $\lambda$ 1, - $\lambda$ 2, and - $\lambda$ 3 were strongly upregulated upon infection (Fig. 2F). The infection with neutralized virus did not result in a proinflammatory response and caused upregulation of expression of an only small number of genes in some cultures. This was corroborated by the absence of viral and cellular antiviral proteins in these cultures, while regularly infected cultures exhibited enhanced expression of IFITM3, MX2, and IFIT1 along with CHIKV capsid and E1/E2 proteins (Fig. 2B).

Concerning the similarity between OASF and HSF, a substantial part of the upregulated genes overlapped between OASF and HSF, while in HSF more genes were significantly downregulated upon infection (Fig. 2E). Overall, the correlation of gene expression between uninfected OASF and HSF was high with  $R^2 > 0.9$  and significant changes occurred only in genes not related to inflammatory processes (Suppl. Fig. 2A-C). A correlation of selected genes involved in antiviral and RA-mediating processes revealed a similar transcriptomic profile in CHIKV-infected OASF and HSF (Fig. 2D). Overall, this shows the similarity of OASF and HSF and the exceptionally strong transcriptomic response with a major focus on ISGs in infected fibroblasts. Additionally, the induction of a subgroup of RA-mediating genes suggests the

potential of synovial fibroblasts to contribute to the CHIKV-induced arthralgia. However, the response external stimulation with IL-1 $\beta$  indicates that paracrine stimulation, possibly through infiltrating immune cells, is necessary to drive arthralgia *in vivo*, while a direct infection of synovial fibroblasts is not sufficient to induce RA-like symptoms.

### 3.2.2 The CHIKV Genome is Actively Replicated in Infected Synovial Fibroblasts

In addition to mapping reads to the human genome, we aligned the non-human reads to the CHIKV genome. In infected samples, we detected reads covering the entire CHIKV genome, with a ~5-fold higher abundance of reads mapping to the structural protein-coding part of the genome (Fig. 3A, B). Since this part of the genome is, in addition to the full-length genome, replicated as a subgenomic RNA, a higher relative abundance was expected [121, 122], though the actual ratio had not been determined before. As the packaging signal for the alphaviral genome is located in the nsP2 region, an accidental packaging of the genome into the virions and, thereby, higher abundance of the subgenomic RNA upon initial entry into the cell is unlikely [32]. A higher relative abundance of the structural protein-coding part was also detectable in cells infected with neutralized virus, consistent with a productive infection in a small number of cells in these cultures. In some cultures, over 50 % of the total reads were attributed to the viral genome, demonstrating the ability of CHIKV to replicate to high levels even in IFN-competent cells. In summary, the presence of subgenomic RNA suggests active viral RNA replication reaching high levels despite the induced antiviral responses.

### 3.3 Exogenously Added IFN Strongly Reduces the Infection Efficiency in Synovial Fibroblasts and Immortalized Cell Lines

Type I and III IFNs are produced by a number of different cells in the human body and act antivirally in an autocrine and paracrine way [119]. We determined the impact of exogenously added IFN on CHIKV infection of OASF and, for comparison, of commonly used immortalized cell lines, by stimulation of the cells with IFN prior to infection. This pre-incubation allowed for the expression of antiviral genes, of which *IFIT1* and *MX2* expression was representatively quantified, in a dose-dependent manner. OASF as well as the osteosarcoma cell line U2OS were responsive to IFN- $\alpha$ , while the fibroblast cell line HFF-1 only showed low expression of *IFIT1* and *MX2* after stimulation. Only U2OS cells were highly responsive to IFN- $\lambda$  treatment, contrasting low responses in OASF and HFF-1 cells (Suppl. Fig. 3B). This was mostly reflected

in the suppression of infection when measured at 24 and 48 hours post infection by flow cytometry, as IFN- $\alpha$  treatment caused an almost complete suppression of infection in all cell types, while IFN- $\lambda$  treatment was most effective in U2OS cells. Surprisingly, IFN- $\lambda$  also led to lower percentages of EGFP-positive OASF at 48 hours post infection, despite the common notion that fibroblasts are not responsive to IFN- $\lambda$  [123] (Fig. 4C).

When given in a therapy-like setting at four hours post infection, IFN- $\alpha$  proved to be most effective in suppressing CHIKV infection in OASF as compared to immortalized cell lines. In all cell types, the expression of *IFIT1* and *MX2* over increasing amounts of IFN was higher in cells additionally infected with CHIKV than in cells only treated with IFN (Suppl. Fig. 3C). However, the infection efficiency was only slightly decreased by IFN treatment in U2OS and HFF-1 cells, while even low amounts of IFN could suppress the infection in OASF efficiently (Fig. 4D). In summary, IFN treatment provokes stronger immune responses in primary fibroblasts than in the two cell lines tested and is in turn more efficient in suppressing viral infection through IFN-mediated processes. This indicates a fast response in primary fibroblasts, which, *in vivo*, could be beneficial for a rapid clearance of the infection, but also potentially harmful by inducing an overreactive, RA-mediating milieu in the joints.

### **3.4 Single-Cell Transcriptomics Defines a Threshold of Viral RNA for Repression of Cell-Intrinsic Immunity**

#### *3.4.1 Viral Protein and RNA Expression is Invertly Connected to Innate Immune Responses*

Upon CHIKV infection, a heterogeneous mixture of cells in different stages of is present in a culture after an initial incubation period. By flow cytometry, cells expressing viral (reporter) proteins can be separated from cells without detectable viral protein expression. Interestingly, immunostaining for IFITM3, IFIT1, and MX2 in combination with virally encoded EGFP expression revealed a high expression of these antiviral proteins in EGFP-negative cells, while the expression in EGFP-positive cells was similar to the expression in mock-infected cells (Fig. 5A). This initial finding suggests a more efficient immune response in cells not undergoing a productive infection. Cells in a stage of early infection and cells successfully suppressing viral proteins expression while still harboring viral RNA, however, cannot be detected using protein-based methods, but may still contribute to immune responses and disease.

To simultaneously determine the presence and amount of viral RNA independently of reporter protein expression in correlation with cellular gene expression, we performed single-cell

RNA-sequencing of infected OASF at different time points. At six and 24 hours post infection, OASF infected with CHIKV at MOIs of 0.01, 0.1, one, and ten were collected, and initially analyzed for reporter protein as well as *IFIT1* and *MX2* mRNA expression. As expected, *EGFP* expression was almost undetectable at six hours post infection, while at 24 hours post infection the reporter was expressed in an increasing number of cells reflecting the MOI. Analogously, immune responses were weak but detectable at six hours post infection, and stronger at 24 hours post infection, with increasing strength depending on the MOI (Fig. 5B). Subsequently, we subjected the cells from the infected and uninfected cultures to single-cell RNA-sequencing and, after preprocessing, integrated all data from one timepoint into a single matrix. While we identified no clearly separated clusters of cells in the UMAP projection, cells infected at high MOIs clustered together specifically (Fig. 5C). Plotting the expression of viral genes separately for each sample, the close clustering of CHIKV RNA-harboring cells became visible (Fig. 5D). Interestingly, a combined score of the expression of genes, which belong to the IFN signaling network (IFN module score (IMS), Table 1), was lowest in cells with high expression of viral genes, and more pronounced in cells with low CHIKV gene expression (Fig. 5D, Suppl. Fig. 4C). In summary, single-cell RNA-sequencing efficiently identified cells expressing viral RNA and allowed for clustering depending reads mapping to host and viral RNA.

#### *3.4.2 Quantification of Viral RNA Expression per Cell Identifies a Subset of Cells Supporting Strong Viral Replication*

As expected, most reads mapping to the CHIKV genome aligned to the 3' end of the genome due to the poly-A-tail based capturing method, but also reads for the 3' end of the EGFP subgenomic RNA were detected (Suppl. Fig. 4A). Digital sorting the cells by the expression of all genes expressed by CHIKV, a sharp increase in the percent of viral reads per cell effectively divided the cell population into cells with reads mostly mapping to cellular or viral RNA (Suppl. Fig. 4B).

#### *3.4.3 Cells with Low or Undetectable Amounts of Viral RNA Highly Express Antiviral Genes*

Following the separation of the population into cells with undetectable, low and high expression of CHIKV genes (“bystander”, “low”, and “high” groups), we determined the IMS for each groups, revealing an overall increase of the score with increasing MOI, but a decreasing score in the high group in all conditions (Fig. 6A, Suppl. Fig. 6A). Additionally, multiple antiviral genes

were expressed at significantly lower levels in the high group than in the low group, while both low and high groups expressed antiviral genes significantly higher than bystander cells (Suppl. Fig. 6B).

For greater detail, we digitally arranged the cells ascendingly according to the level of viral gene expression and the IMS was averaged over bins of 1000 cells. This method revealed a gradual increase of the IMS in the low group, and a gradual decrease in cells of the high group. Additionally, the expression of *EGFP* mRNA noticeably increased around the turning point of the IMS (Fig. 6B). It is reasonable to assume that the cells in the high group therefore correspond to the EGFP-positive cells measured by flow cytometry. Comparing the expression of single genes between bystander cells, the three bins with the highest IMS and the three bins with the highest CHIKV RNA expression, the trend observed by the IMS could be reinforced. While the expression of many ISGs was upregulated in the low group, the majority of genes were not significantly higher expressed in the high group than in bystander cells, and the expression of many genes was significantly downregulated between the low and high group. This was almost exclusively the case for antiviral, proinflammatory genes, and not for control genes (Fig. 6C). In summary, the observations made by flow cytometry were supported by the transcriptomic analysis, showing an inverse relationship between viral and host antiviral gene expression.

#### *3.4.4 Repressed Transcription Factor Activity is Associated with Strong Viral Gene Expression*

In addition to genes coding for direct-acting antiviral proteins, transcription factors of proinflammatory pathways such as IRFs and STATs were also affected. Since the expression and activity of transcription factors can provide a better insight into the development of the transcriptomic response than the “snapshot” gene expression profile of effector genes, we performed a detailed analysis for transcription factors of interest. By correlating the expression of viral RNA to the expression of all transcription factors included in the IMS, we found *STAT1*, *IRF7*, and *JAK1* to be of particular interest. *IRF7* and *STAT1* gene expression showed a positive correlation with viral RNA expression in the low group, which changed to a negative (*STAT1*) or an absent (*IRF7*) correlation in the high group. *JAK1* gene expression did not correlate with viral RNA expression in the low group, but was strongly negatively correlated in the high group (Fig. 6D). Additionally, the activity of these transcription factors, as measured by the expression of all genes that are belonging to the annotated regulon of the respective transcription factor, was calculated with the R package DoRothEA [117]. The activity of the transcription factors of interest, but also others, was strongly enhanced in the low and bystander group, and reduced to

basal levels in the high group again (Fig. 6E). Taken together, this dataset unravels a strong expression of viral RNA in a subset of cells, which most likely correspond to the cells that express measurable levels of EGFP. These cells seem to have passed a tipping point in the viral replication cycle, which leads to the active suppression of antiviral responses and the production of viral proteins; while cells with low levels of viral RNA expression are fighting the infection may still be able to suppress viral protein production.

## 4 Discussion and Importance

A comprehensive discussion of the results obtained in this study can be found in the original article [110]. Here, I discuss key scientific points of the study and comment on the clinical importance, limitations of the study, and remaining open questions.

### 4.1 Scientific Context and Further Interpretation of the Results

CHIKV infection and the often long-term sequelae are a severe burden for affected patients, and the RA-like symptoms are likely to involve SF-driven proinflammatory actions. Therefore, the response to CHIKV infection of SF was examined to create a comprehensive profile of cell-intrinsic changes over the course of infection. Of note, SF from two different sources, osteoarthritic and healthy donors, were used for the study. While OASF are readily available through routine knee replacement surgeries, their transcriptomic and secretory profile may differ from fibroblasts from healthy donors. Although some initial differences regarding the released amount of newly produced virions after infection were observed, the gene expression profile in uninfected OASF and HSF and CHIKV-infected OASF and HSF, respectively, was mostly similar. Thereby, OASF were considered suitable for further experiments.

CHIKV is known to induce immune responses through the cellular recognition of its viral RNA by the cytoplasmic pattern recognition receptor RIG-I, which in turn leads to IRF- and NF $\kappa$ B-mediated antiviral gene expression [43]. The following gene expression induces the production and secretion of IFNs, which can act in an auto- and paracrine manner to induce the JAK/STAT pathways, initiating further antiviral gene expression [119]. In this study, CHIKV infection provoked an immune response in SF exceeding the one of immortalized cell lines, suggesting that proposed viral antagonism mechanisms, including nuclear export of STAT1 from the nucleus or the suppression of the IFN- $\beta$  pathway by the viral protein nsP2, are not highly effective in SF [57, 58, 124]. Additionally, the stable expression of cellular housekeeping proteins and control genes argues against a transcriptional and/or translational shutdown in these cells. This powerful antagonism strategy by CHIKV has been described for multiple alphaviruses and involves the translocation of nsP2 into the nucleus and a degradation of the RNA polymerase II subunit RBP1 [59, 60, 125]. However, the presence of a strong and comprehensive innate immune response even in the overwhelming amounts of virus used here argued initially against a successful antagonism by viral proteins.



However, analysis methods such as bulk RNA-seq, which averages gene expression over a large number of cells, are likely to miss effects occurring in a subset of cells. Digitally splitting cells into groups depending on their expression of viral RNA, or aligning the amount of viral RNA to cellular gene expression for every single cell by single-cell RNA-seq, revealed a striking difference between cells in different stages of infection. A subgroup of cells containing particularly high amounts of viral RNA provided evidence for a selective and targeted inhibition of the transcription factor STAT1, with an associated loss of expression of genes whose expression is STAT1-dependent. Similar results of specific viral antagonism in highly infected cells have been obtained in studies with West Nile virus and Ebola virus, both *in vitro* and *in vivo* [107, 126]. The underlying difference in cells allowing for high viral replication is unknown, but may be impacted by the availability of cellular cofactors and the pre-existing expression of pattern recognition receptor and antiviral proteins. In contrast, cells with a low-to-intermediate expression of viral genes seem to be able to respond properly to the invading pathogen, and may either be at the beginning of a productive infection or in the process of clearing the virus. In either case, multiple factors may determine whether the cell reaches a tipping point, switching from a defensive to a permissive intracellular milieu. Combined protein and transcriptomic analysis indicate that surpassing this tipping point is associated with the enhanced presence of subgenomic RNA and viral proteins. In summary, experiments at single-cell resolution can successfully delineate the differential responses within an infected culture, and uncover viral antagonism effects not detectable in a cell population-based setting.

## **4.2 Clinical and Scientific Importance**

Synovial fibroblasts are, next to synovial macrophages, the major cell type lining the synovium, and are involved in the destruction of cartilage during RA [100, 127, 128]. Furthermore, SF are directly targeted by CHIKV *in vivo* and serve as sites for replication and long-term replication in animal models and humans [20-22]. So far, it remains unknown how a typically acute infection-inducing virus such as CHIKV can induce a long-term inflammatory disease, and if the virus is present and replicating over an extended period of time or if a dysregulated immune system in the absence of the pathogen is causing the chronic disease. SF themselves contribute to RA by destruction of cartilage and secretion of proinflammatory cytokines [93, 129], but also importantly stimulate monocyte migration and drive them towards an osteoclast-like phenotype [63]. This illustrates the direct, but also indirect and systemic importance of SF in CHIKV-induced arthralgia.

One method to investigate systemic responses upon CHIKV infection is the use of animal models. Mice are readily infectable with CHIKV, making them a valuable tool, although only for neonatal or IFNAR<sup>-/-</sup> mice the infection results in a lethal outcome, limiting the opportunity of survival studies in immunocompetent hosts [22]. However, immunocompetent mice can be used to study acute infections and to monitor the persistence of viral RNA and antigen over longer times [130, 131]. Studies on Rag<sup>-/-</sup> (lymphocyte deficient), Cd4<sup>-/-</sup> (CD4 T cell deficient), and  $\mu$ MT (B-cell deficient) mice missing the adaptive arm of the immune system have provided evidence for the essential role of adaptive immunity, in particular antibodies, for the early clearance of CHIKV in mice, without being necessary for survival [132, 133]. In addition to mice, non-human primate models have provided insights into acute disease and persistence [20], but these models are ethically disputed and expensive to maintain long-term. Therefore, models studying the infection and disease in highly relevant, non-animal models are urgently needed. Accessible biopsy material for *ex vivo* studies cannot capture the complexity of an *in vivo* environment, but may provide insight in parts of it.

In the context as a cellular reservoir for persistence and low-level replication of CHIKV RNA, dermal and muscle fibroblasts have been observed to survive a CHIKV infection and to harbor viral RNA for at least 16 weeks [19, 130]. While biopsies from human patients revealed a state of chronic infection in synovial macrophages in some patients [21], no experimental evidence has validated or excluded the involvement of SF in the long-lasting presence of viral RNA so far. Additionally, there are no approaches on how to resolve persisting viral RNA to end chronic inflammatory disease. An *ex vivo* model could therefore be suitable to induce a state of chronic infection and to test whether pharmacological interventions would lead to a complete clearance of infection. This could include treatment with the immunomodulatory drug methotrexate, as tested in patients before to relieve symptoms [84, 134], or antivirals with proven activity against CHIKV such as favipiravir [135] or ribavirin [136]. In conclusion, an *ex vivo* model of human cells as presented here can provide valuable comparisons to the data obtained in animal models and may be able to reproduce findings for cell type-specific mechanisms.

### **4.3 Limitations of the Study**

The presented study is based on *ex vivo* cultured, purified synovial fibroblasts. Even though the cells combine the function of target cells for the virus and effector cells for the subsequent morbidity, the milieu in which they usually are exposed to the virus is vastly different *in vivo*. The synovium is lined by a layer of fibroblasts and macrophages [127], which influence each

other through secretion of cytokines and IFNs. Furthermore, cells such as T-cells, neutrophils, monocytes, and NK cells infiltrate the synovium upon infection, causing further release of proinflammatory cytokines [14, 21]. The results in this study show that external stimulation with IL-1 $\beta$  can induce enhanced secretion of IL-6 by SF. *In vivo*, IL-1 $\beta$  is secreted by activated immune cells and can, in addition to IL-6, mediate the expression of cartilage-destructing matrix-metalloprotease, which expression is not induced by CHIKV infection alone [94].

In this study, the impact of a CHIKV infection on cells from healthy donors and cells from a diseased, but non-inflammatory background was determined. SF from patients suffering from inflammatory RA (RA synovial fibroblasts, RASF) may be an interesting additional control to compare CHIKV-induced and autoimmune arthritis and arthralgia. Similar induction of transcriptomic drivers of inflammation in RASF and CHIKV-infected SF could provide strategies to successfully treat and inhibit long-term consequences for CHIKV patients. Additionally, this study mostly focuses on the analysis of transcriptomic responses, which usually correspond to, but may not fully represent the changes in protein abundance and secretion. We complemented this study with the analysis of important ISG-encoded proteins and the secretion of IFN, which were in agreement with our transcriptomic findings. However, a multi-omics analysis would be needed to compare and correlate the expression levels of mRNA and proteins and to draw conclusions without this limitation.

#### **4.4 Open Questions and Outlook**

In this study, SF were described as target cells of CHIKV infection and important mediators of the main symptom, a polyarthralgia affecting multiple joints. However, in the complex synovial environment, resident as well as infiltrating cells are likely to influence the infection and the severity of symptoms. In an *ex vivo* setting, a co-culture of macrophages and SF, the two main cell types composing the synovial membrane, could potentially shed light on the mutual influence and on the susceptibility of macrophages. Macrophages have been described as susceptible in animal models and in human patients [20, 21], and can be infected in *in vitro* models [64, 137]. However, no study has been analyzing the combinations of both cell types or in complex tissue surrogates such as organoids.

In terms of clinical treatment of CHIKV infection, symptomatic treatment for acute disease involves the reduction of pain and inflammation with non-steroidal anti-inflammatory drugs [83]. For chronic sequelae, a continued treatment with anti-inflammatory drugs or disease-modifying anti-rheumatic drugs (DMARDs) such as methotrexate is the only option so far,

although DMARDs are often associated with severe side effects [138]. Therefore, the most promising strategy for a population-wide control of CHIKV is a functional vaccine. So far, multiple vaccine candidates have provided promising results in clinical phase I and II trials. These candidates include virus-like particles [79], a measles-based vaccine [88], and a live-attenuated vaccine [80], which was advanced from a phase I directly into a phase III trial [139]. Additionally, the recent progress in the production of mRNA-based vaccines has the potential for the rapid development of vaccines against emerging viruses, and the observed induction of a neutralizing antibody response in the case of SARS-CoV-2 indicates that this technology would be suitable for an anti-CHIKV vaccine [140]. Taken together, the development of a vaccine should be able to counteract upcoming outbreaks and serve as a measure to protect travelers in affected regions. However, the distribution of vaccines is still challenging in developing countries, and a population-wide immunity to CHIKV is unlikely to be achieved. Therefore, investigation into underlying mechanisms endeavors for the benefit of millions of people worldwide.

## References

1. Levi LI, Vignuzzi M. Arthritogenic Alphaviruses: A Worldwide Emerging Threat? *Microorganisms*. 2019; 7(5). DOI:10.3390/microorganisms7050133.
2. Ross RW. The Newala epidemic. III. The virus: isolation, pathogenic properties and relationship to the epidemic. *J Hyg (Lond)*. 1956; 54(2):177-91. DOI:10.1017/s0022172400044442.
3. Weaver SC, Lecuit M. Chikungunya virus and the global spread of a mosquito-borne disease. *The New England journal of medicine*. 2015; 372(13):1231-9. DOI:10.1056/NEJMra1406035.
4. Weaver SC, Forrester NL. Chikungunya: Evolutionary history and recent epidemic spread. *Antiviral Res*. 2015; 120:32-9. DOI:10.1016/j.antiviral.2015.04.016.
5. Amraoui F, Failloux AB. Chikungunya: an unexpected emergence in Europe. *Current opinion in virology*. 2016; 21:146-50. DOI:10.1016/j.coviro.2016.09.014.
6. Tsetsarkin KA, Vanlandingham DL, McGee CE, Higgs S. A single mutation in chikungunya virus affects vector specificity and epidemic potential. *PLoS pathogens*. 2007; 3(12):e201. DOI:10.1371/journal.ppat.0030201.
7. Kraemer MU, Sinka ME, Duda KA, Mylne AQ, Shearer FM, Barker CM, Moore CG, Carvalho RG, Coelho GE, Van Bortel W, Hendrickx G, Schaffner F, Elyazar IR, Teng HJ, Brady OJ, Messina JP, Pigott DM, Scott TW, Smith DL, Wint GR, Golding N, Hay SI. The global distribution of the arbovirus vectors *Aedes aegypti* and *Ae. albopictus*. *eLife*. 2015; 4:e08347. DOI:10.7554/eLife.08347.
8. Kamal M, Kenawy MA, Rady MH, Khaled AS, Samy AM. Mapping the global potential distributions of two arboviral vectors *Aedes aegypti* and *Ae. albopictus* under changing climate. *PloS one*. 2018; 13(12):e0210122. DOI:10.1371/journal.pone.0210122.
9. Diagne CT, Bengue M, Choumet V, Hamel R, Pompon J, Missé D. Mayaro Virus Pathogenesis and Transmission Mechanisms. *Pathogens*. 2020; 9(9):738. DOI:10.3390/pathogens9090738.
10. Kraemer MUG, Reiner RC, Jr., Brady OJ, Messina JP, Gilbert M, Pigott DM, Yi D, Johnson K, Earl L, Marczak LB, Shirude S, Davis Weaver N, Bisanzio D, Perkins TA, Lai S, Lu X, Jones P, Coelho GE, Carvalho RG, Van Bortel W, Marsboom C, Hendrickx G, Schaffner F, Moore CG, Nax HH, Bengtsson L, Wetter E, Tatem AJ, Brownstein JS, Smith DL, Lambrechts L, Cauchemez S, Linard C, Faria NR, Pybus OG, Scott TW, Liu Q, Yu H, Wint GRW, Hay SI, Golding N. Past and future spread of the arbovirus vectors *Aedes aegypti* and *Aedes albopictus*. *Nature microbiology*. 2019; 4(5):854-63. DOI:10.1038/s41564-019-0376-y.
11. Santiago FW, Halsey ES, Siles C, Vilcarrromero S, Guevara C, Silvas JA, Ramal C, Ampuero JS, Aguilar PV. Long-Term Arthralgia after Mayaro Virus Infection Correlates with Sustained Pro-inflammatory Cytokine Response. *PLoS neglected tropical diseases*. 2015; 9(10):e0004104. DOI:10.1371/journal.pntd.0004104.

12. Fumagalli MJ, Marciel de Souza W, de Castro-Jorge LA, de Carvalho RVH, Castro Í A, de Almeida LGN, Consonni SR, Zamboni DS, Figueiredo LTM. Chikungunya virus exposure partially cross-protects against Mayaro virus infection in mice. *Journal of virology*. 2021;Jvi0112221. DOI:10.1128/jvi.01122-21.
13. Schwartz O, Albert ML. Biology and pathogenesis of chikungunya virus. *Nature reviews Microbiology*. 2010; 8(7):491-500. DOI:10.1038/nrmicro2368.
14. Burt FJ, Chen W, Miner JJ, Lenschow DJ, Merits A, Schnettler E, Kohl A, Rudd PA, Taylor A, Herrero LJ, Zaid A, Ng LFP, Mahalingam S. Chikungunya virus: an update on the biology and pathogenesis of this emerging pathogen. *Lancet Infect Dis*. 2017; 17(4):e107-e17. DOI:10.1016/s1473-3099(16)30385-1.
15. Soares-Schanoski A, Baptista Cruz N, de Castro-Jorge LA, de Carvalho RVH, Santos CAD, Ros ND, Oliveira U, Costa DD, Santos C, Cunha MDP, Oliveira MLS, Alves JC, Ocea R, Ribeiro DR, Goncalves ANA, Gonzalez-Dias P, Suhrbier A, Zanotto PMA, Azevedo IJ, Zamboni DS, Almeida RP, Ho PL, Kalil J, Nishiyama MYJ, Nakaya HI. Systems analysis of subjects acutely infected with the Chikungunya virus. *PLoS pathogens*. 2019; 15(6):e1007880. DOI:10.1371/journal.ppat.1007880.
16. Paixao ES, Rodrigues LC, Costa M, Itaparica M, Barreto F, Gerardin P, Teixeira MG. Chikungunya chronic disease: a systematic review and meta-analysis. *Trans R Soc Trop Med Hyg*. 2018; 112(7):301-16. DOI:10.1093/trstmh/try063.
17. Chow A, Her Z, Ong EK, Chen JM, Dimatatac F, Kwek DJ, Barkham T, Yang H, Renia L, Leo YS, Ng LF. Persistent arthralgia induced by Chikungunya virus infection is associated with interleukin-6 and granulocyte macrophage colony-stimulating factor. *The Journal of infectious diseases*. 2011; 203(2):149-57. DOI:10.1093/infdis/jiq042.
18. Ng LF, Chow A, Sun YJ, Kwek DJ, Lim PL, Dimatatac F, Ng LC, Ooi EE, Choo KH, Her Z, Kourilsky P, Leo YS. IL-1beta, IL-6, and RANTES as biomarkers of Chikungunya severity. *PloS one*. 2009; 4(1):e4261. DOI:10.1371/journal.pone.0004261.
19. Young AR, Locke MC, Cook LE, Hiller BE, Zhang R, Hedberg ML, Monte KJ, Veis DJ, Diamond MS, Lenschow DJ. Dermal and muscle fibroblasts and skeletal myofibers survive chikungunya virus infection and harbor persistent RNA. *PLoS pathogens*. 2019; 15(8):e1007993. DOI:10.1371/journal.ppat.1007993.
20. Labadie K, Larcher T, Joubert C, Mannioui A, Delache B, Brochard P, Guigand L, Dubreil L, Lebon P, Verrier B, de Lamballerie X, Suhrbier A, Cherel Y, Le Grand R, Roques P. Chikungunya disease in nonhuman primates involves long-term viral persistence in macrophages. *J Clin Invest*. 2010; 120(3):894-906. DOI:10.1172/jci40104.
21. Hoarau JJ, Jaffar Bandjee MC, Krejbich Trotot P, Das T, Li-Pat-Yuen G, Dassa B, Denizot M, Guichard E, Ribera A, Henni T, Tallet F, Moiton MP, Gauzere BA, Bruniquet S, Jaffar Bandjee Z, Morbidelli P, Martigny G, Jolivet M, Gay F, Grandadam M, Tolou H, Vieillard V, Debre P, Autran B, Gasque P. Persistent chronic inflammation and infection by Chikungunya arthritogenic alphavirus in spite of a robust host immune response. *J Immunol*. 2010; 184(10):5914-27. DOI:10.4049/jimmunol.0900255.
22. Couderc T, Chrétien F, Schilte C, Disson O, Brigitte M, Guivel-Benhassine F, Touret Y, Barau G, Cayet N, Schuffenecker I, Desprès P, Arenzana-Seisdedos F, Michault A, Albert

- ML, Lecuit M. A mouse model for Chikungunya: young age and inefficient type-I interferon signaling are risk factors for severe disease. *PLoS pathogens*. 2008; 4(2):e29. DOI:10.1371/journal.ppat.0040029.
23. Lima STS, Souza WM, Cavalcante JW, da Silva Candido D, Fumagalli MJ, Carrera JP, Simões Mello LM, de Carvalho Araújo FM, Cavalcante Ramalho IL, de Almeida Barreto FK, de Melo Braga DN, Simião AR, Miranda da Silva MJ, Oliveira R, Lima CPS, Sousa Lins C, Barata RR, Melo MNP, de Souza MPC, Franco LM, Távora FRF, Queiroz Lemos DR, Alencar CHM, Jesus R, Souza Fonseca V, Dutra LH, Abreu AL, Araújo ELL, Ribas Freitas AR, Gonçalves Vianez Júnior J, Pybus OG, Moraes Figueiredo LT, Faria NR, Teixeira Nunes MR, Góes Cavalcanti LP, Miyajima F. Fatal outcome of chikungunya virus infection in Brazil. *Clin Infect Dis*. 2020. DOI:10.1093/cid/ciaa1038.
  24. Mehta R, Gerardin P, de Brito CAA, Soares CN, Ferreira MLB, Solomon T. The neurological complications of chikungunya virus: A systematic review. *Rev Med Virol*. 2018; 28(3):e1978. DOI:10.1002/rmv.1978.
  25. Lum FM, Ng LF. Cellular and molecular mechanisms of chikungunya pathogenesis. *Antiviral Res*. 2015; 120:165-74. DOI:10.1016/j.antiviral.2015.06.009.
  26. Hyde JL, Chen R, Trobaugh DW, Diamond MS, Weaver SC, Klimstra WB, Wilusz J. The 5' and 3' ends of alphavirus RNAs--Non-coding is not non-functional. *Virus research*. 2015; 206:99-107. DOI:10.1016/j.virusres.2015.01.016.
  27. Zhang R, Kim AS, Fox JM, Nair S, Basore K, Klimstra WB, Rimkunas R, Fong RH, Lin H, Poddar S, Crowe JE, Jr., Doranz BJ, Fremont DH, Diamond MS. Mxra8 is a receptor for multiple arthritogenic alphaviruses. *Nature*. 2018; 557(7706):570-4. DOI:10.1038/s41586-018-0121-3.
  28. Holmes AC, Basore K, Fremont DH, Diamond MS. A molecular understanding of alphavirus entry. *PLoS pathogens*. 2020; 16(10):e1008876. DOI:10.1371/journal.ppat.1008876.
  29. Schnierle BS. Cellular Attachment and Entry Factors for Chikungunya Virus. *Viruses*. 2019; 11(11):1078. DOI:10.3390/v11111078.
  30. Kielian M, Chanel-Vos C, Liao M. Alphavirus Entry and Membrane Fusion. *Viruses*. 2010; 2(4):796-825. DOI:10.3390/v2040796.
  31. Rupp JC, Sokoloski KJ, Gebhart NN, Hardy RW. Alphavirus RNA synthesis and non-structural protein functions. *J Gen Virol*. 2015; 96(9):2483-500. DOI:10.1099/jgv.0.000249.
  32. Kim DY, Firth AE, Atasheva S, Frolova EI, Frolov I. Conservation of a packaging signal and the viral genome RNA packaging mechanism in alphavirus evolution. *Journal of virology*. 2011; 85(16):8022-36. DOI:10.1128/jvi.00644-11.
  33. Meertens L, Hafirassou ML, Couderc T, Bonnet-Madin L, Kril V, Kummerer BM, Labeau A, Brugier A, Simon-Lorier E, Burlaud-Gaillard J, Doyen C, Pezzi L, Goupil T, Rafasse S, Vidalain PO, Bertrand-Legout A, Gueneau L, Juntas-Morales R, Ben Yaou R, Bonne G, de Lamballerie X, Benkirane M, Roingard P, Delaugerre C, Lecuit M, Amara A. FHL1 is a major host factor for chikungunya virus infection. *Nature*. 2019; 574(7777):259-63. DOI:10.1038/s41586-019-1578-4.

34. Ahola T, Merits A. Functions of Chikungunya Virus Nonstructural Proteins. *Chikungunya Virus: Advances in Biology, Pathogenesis, and Treatment*. 2016:75-98. DOI:10.1007/978-3-319-42958-8\_6.
35. Carrasco L, Sanz MA, González-Almela E. The Regulation of Translation in Alphavirus-Infected Cells. *Viruses*. 2018; 10(2):70. DOI:10.3390/v10020070.
36. Firth AE, Chung BY, Fleeton MN, Atkins JF. Discovery of frameshifting in Alphavirus 6K resolves a 20-year enigma. *Virology journal*. 2008; 5:108. DOI:10.1186/1743-422x-5-108.
37. Jensen S, Thomsen AR. Sensing of RNA viruses: a review of innate immune receptors involved in recognizing RNA virus invasion. *Journal of virology*. 2012; 86(6):2900-10. DOI:10.1128/jvi.05738-11.
38. Neighbours LM, Long K, Whitmore AC, Heise MT. Myd88-dependent toll-like receptor 7 signaling mediates protection from severe Ross River virus-induced disease in mice. *Journal of virology*. 2012; 86(19):10675-85. DOI:10.1128/jvi.00601-12.
39. Her Z, Teng TS, Tan JJ, Teo TH, Kam YW, Lum FM, Lee WW, Gabriel C, Melchiotti R, Andiappan AK, Lulla V, Lulla A, Win MK, Chow A, Biswas SK, Leo YS, Lecuit M, Merits A, Rénia L, Ng LF. Loss of TLR3 aggravates CHIKV replication and pathology due to an altered virus-specific neutralizing antibody response. *EMBO Mol Med*. 2015; 7(1):24-41. DOI:10.15252/emmm.201404459.
40. Schilte C, Couderc T, Chretien F, Sourisseau M, Gangneux N, Guivel-Benhassine F, Kraxner A, Tschopp J, Higgs S, Michault A, Arenzana-Seisdedos F, Colonna M, Peduto L, Schwartz O, Lecuit M, Albert ML. Type I IFN controls chikungunya virus via its action on nonhematopoietic cells. *J Exp Med*. 2010; 207(2):429-42. DOI:10.1084/jem.20090851.
41. Hornung V, Ellegast J, Kim S, Brzozka K, Jung A, Kato H, Poeck H, Akira S, Conzelmann KK, Schlee M, Endres S, Hartmann G. 5'-Triphosphate RNA is the ligand for RIG-I. *Science (New York, NY)*. 2006; 314(5801):994-7. DOI:10.1126/science.1132505.
42. Weber M, Gawanbacht A, Habjan M, Rang A, Borner C, Schmidt AM, Veitinger S, Jacob R, Devignot S, Kochs G, García-Sastre A, Weber F. Incoming RNA virus nucleocapsids containing a 5'-triphosphorylated genome activate RIG-I and antiviral signaling. *Cell host & microbe*. 2013; 13(3):336-46. DOI:10.1016/j.chom.2013.01.012.
43. Sanchez David RY, Combredet C, Sismeiro O, Dillies MA, Jagla B, Coppee JY, Mura M, Guerbois Galla M, Despres P, Tangy F, Komarova AV. Comparative analysis of viral RNA signatures on different RIG-I-like receptors. *eLife*. 2016; 5:e11275. DOI:10.7554/eLife.11275.
44. Akhrymuk I, Frolov I, Frolova EI. Both RIG-I and MDA5 detect alphavirus replication in concentration-dependent mode. *Virology*. 2016; 487:230-41. DOI:10.1016/j.virol.2015.09.023.
45. Levi LI, Rezelj VV, Henrion-Lacritick A, Erazo D, Boussier J, Vallet T, Bernhauerová V, Suzuki Y, Carrau L, Weger-Lucarelli J, Saleh MC, Vignuzzi M. Defective viral genomes from chikungunya virus are broad-spectrum antivirals and prevent virus dissemination in mosquitoes. *PLoS pathogens*. 2021; 17(2):e1009110. DOI:10.1371/journal.ppat.1009110.



46. Rehwinkel J, Gack MU. RIG-I-like receptors: their regulation and roles in RNA sensing. *Nat Rev Immunol.* 2020; 20(9):537-51. DOI:10.1038/s41577-020-0288-3.
47. Lazear HM, Schoggins JW, Diamond MS. Shared and Distinct Functions of Type I and Type III Interferons. *Immunity.* 2019; 50(4):907-23. DOI:10.1016/j.immuni.2019.03.025.
48. Gardner CL, Burke CW, Higgs ST, Klimstra WB, Ryman KD. Interferon-alpha/beta deficiency greatly exacerbates arthritogenic disease in mice infected with wild-type chikungunya virus but not with the cell culture-adapted live-attenuated 181/25 vaccine candidate. *Virology.* 2012; 425(2):103-12. DOI:10.1016/j.virol.2011.12.020.
49. Schoggins JW, Wilson SJ, Panis M, Murphy MY, Jones CT, Bieniasz P, Rice CM. A diverse range of gene products are effectors of the type I interferon antiviral response. *Nature.* 2011; 472(7344):481-5. DOI:10.1038/nature09907.
50. Schoggins JW, MacDuff DA, Imanaka N, Gainey MD, Shrestha B, Eitson JL, Mar KB, Richardson RB, Ratushny AV, Litvak V, Dabelic R, Manicassamy B, Aitchison JD, Aderem A, Elliott RM, Garcia-Sastre A, Racaniello V, Snijder EJ, Yokoyama WM, Diamond MS, Virgin HW, Rice CM. Pan-viral specificity of IFN-induced genes reveals new roles for cGAS in innate immunity. *Nature.* 2014; 505(7485):691-5. DOI:10.1038/nature12862.
51. Franz S, Pott F, Zillinger T, Schüler C, Dapa S, Fischer C, Passos V, Stenzel S, Chen F, Döhner K, Hartmann G, Sodeik B, Pessler F, Simmons G, Drexler JF, Goffinet C. Human IFITM3 restricts chikungunya virus and Mayaro virus infection and is susceptible to virus-mediated counteraction. *Life Sci Alliance.* 2021; 4(7). DOI:10.26508/lsa.202000909.
52. Poddar S, Hyde JL, Gorman MJ, Farzan M, Diamond MS. The Interferon-Stimulated Gene IFITM3 Restricts Infection and Pathogenesis of Arthritogenic and Encephalitic Alphaviruses. *Journal of virology.* 2016; 90(19):8780-94. DOI:10.1128/jvi.00655-16.
53. Weston S, Czieso S, White IJ, Smith SE, Wash RS, Diaz-Soria C, Kellam P, Marsh M. Alphavirus Restriction by IFITM Proteins. *Traffic.* 2016; 17(9):997-1013. DOI:10.1111/tra.12416.
54. Reynaud JM, Kim DY, Atasheva S, Rasaloukaya A, White JP, Diamond MS, Weaver SC, Frolova EI, Frolov I. IFIT1 Differentially Interferes with Translation and Replication of Alphavirus Genomes and Promotes Induction of Type I Interferon. *PLoS pathogens.* 2015; 11(4):e1004863. DOI:10.1371/journal.ppat.1004863.
55. Wichit S, Hamel R, Yainoy S, Gumpangseth N, Panich S, Phuadraksa T, Saetear P, Monteil A, Morales Vargas R, Misse D. Interferon-inducible protein (IFI) 16 regulates Chikungunya and Zika virus infection in human skin fibroblasts. *Excli j.* 2019; 18:467-76. DOI:10.17179/excli2019-1271.
56. Werneke SW, Schilte C, Rohatgi A, Monte KJ, Michault A, Arenzana-Seisdedos F, Vanlandingham DL, Higgs S, Fontanet A, Albert ML, Lenschow DJ. ISG15 is critical in the control of Chikungunya virus infection independent of UBE1L mediated conjugation. *PLoS pathogens.* 2011; 7(10):e1002322. DOI:10.1371/journal.ppat.1002322.

57. Fros JJ, Liu WJ, Prow NA, Geertsema C, Ligtenberg M, Vanlandingham DL, Schnettler E, Vlak JM, Suhrbier A, Khromykh AA, Pijlman GP. Chikungunya virus nonstructural protein 2 inhibits type I/II interferon-stimulated JAK-STAT signaling. *Journal of virology*. 2010; 84(20):10877-87. DOI:10.1128/jvi.00949-10.
58. Goertz GP, McNally KL, Robertson SJ, Best SM, Pijlman GP, Fros JJ. The Methyltransferase-Like Domain of Chikungunya Virus nsP2 Inhibits the Interferon Response by Promoting the Nuclear Export of STAT1. *Journal of virology*. 2018; 92(17). DOI:10.1128/jvi.01008-18.
59. Akhrymuk I, Kulemzin SV, Frolova EI. Evasion of the innate immune response: the Old World alphavirus nsP2 protein induces rapid degradation of Rpb1, a catalytic subunit of RNA polymerase II. *Journal of virology*. 2012; 86(13):7180-91. DOI:10.1128/jvi.00541-12.
60. Akhrymuk I, Lukash T, Frolov I, Frolova EI. Novel Mutations in nsP2 Abolish Chikungunya Virus-Induced Transcriptional Shutoff and Make the Virus Less Cytopathic without Affecting Its Replication Rates. *Journal of virology*. 2019; 93(4). DOI:10.1128/jvi.02062-18.
61. Webb LG, Veloz J, Pintado-Silva J, Zhu T, Rangel MV, Mutetwa T, Zhang L, Bernal-Rubio D, Figueroa D, Carrau L, Fenutria R, Potla U, Reid SP, Yount JS, Stapleford KA, Aguirre S, Fernandez-Sesma A. Chikungunya virus antagonizes cGAS-STING mediated type-I interferon responses by degrading cGAS. *PLoS pathogens*. 2020; 16(10):e1008999. DOI:10.1371/journal.ppat.1008999.
62. Gardner J, Anraku I, Le TT, Larcher T, Major L, Roques P, Schroder WA, Higgs S, Suhrbier A. Chikungunya virus arthritis in adult wild-type mice. *Journal of virology*. 2010; 84(16):8021-32. DOI:10.1128/jvi.02603-09.
63. Phuklia W, Kasisith J, Modhiran N, Rodpai E, Thannagith M, Thongsakulprasert T, Smith DR, Ubol S. Osteoclastogenesis induced by CHIKV-infected fibroblast-like synoviocytes: a possible interplay between synoviocytes and monocytes/macrophages in CHIKV-induced arthralgia/arthritis. *Virus research*. 2013; 177(2):179-88. DOI:10.1016/j.virusres.2013.08.011.
64. Felipe VLJ, Paula AV, Silvio UI. Chikungunya virus infection induces differential inflammatory and antiviral responses in human monocytes and monocyte-derived macrophages. *Acta tropica*. 2020; 211:105619. DOI:10.1016/j.actatropica.2020.105619.
65. Morrison TE, Oko L, Montgomery SA, Whitmore AC, Lotstein AR, Gunn BM, Elmore SA, Heise MT. A mouse model of chikungunya virus-induced musculoskeletal inflammatory disease: evidence of arthritis, tenosynovitis, myositis, and persistence. *Am J Pathol*. 2011; 178(1):32-40. DOI:10.1016/j.ajpath.2010.11.018.
66. Petitdemange C, Becquart P, Wauquier N, Béziat V, Debré P, Leroy EM, Vieillard V. Unconventional repertoire profile is imprinted during acute chikungunya infection for natural killer cells polarization toward cytotoxicity. *PLoS pathogens*. 2011; 7(9):e1002268. DOI:10.1371/journal.ppat.1002268.
67. Webster B, Werneke SW, Zafirova B, This S, Coleon S, Decembre E, Paidassi H, Bouvier I, Joubert PE, Duffy D, Walzer T, Albert ML, Dreux M. Plasmacytoid dendritic cells

- control dengue and Chikungunya virus infections via IRF7-regulated interferon responses. *eLife*. 2018; 7:e34273. DOI:10.7554/eLife.34273.
68. Jin J, Liss NM, Chen DH, Liao M, Fox JM, Shimak RM, Fong RH, Chafets D, Bakkour S, Keating S, Fomin ME, Muench MO, Sherman MB, Doranz BJ, Diamond MS, Simmons G. Neutralizing Monoclonal Antibodies Block Chikungunya Virus Entry and Release by Targeting an Epitope Critical to Viral Pathogenesis. *Cell Rep*. 2015; 13(11):2553-64. DOI:10.1016/j.celrep.2015.11.043.
  69. Zhou QF, Fox JM, Earnest JT, Ng TS, Kim AS, Fibriansah G, Kostyuchenko VA, Shi J, Shu B, Diamond MS, Lok SM. Structural basis of Chikungunya virus inhibition by monoclonal antibodies. *Proceedings of the National Academy of Sciences of the United States of America*. 2020; 117(44):27637-45. DOI:10.1073/pnas.2008051117.
  70. Kam YW, Lee WW, Simarmata D, Le Grand R, Tolou H, Merits A, Roques P, Ng LF. Unique epitopes recognized by antibodies induced in Chikungunya virus-infected non-human primates: implications for the study of immunopathology and vaccine development. *PLoS one*. 2014; 9(4):e95647. DOI:10.1371/journal.pone.0095647.
  71. Fox JM, Long F, Edeling MA, Lin H, van Duijl-Richter MKS, Fong RH, Kahle KM, Smit JM, Jin J, Simmons G, Doranz BJ, Crowe JE, Jr., Fremont DH, Rossmann MG, Diamond MS. Broadly Neutralizing Alphavirus Antibodies Bind an Epitope on E2 and Inhibit Entry and Egress. *Cell*. 2015; 163(5):1095-107. DOI:10.1016/j.cell.2015.10.050.
  72. Smith JL, Pugh CL, Cisney ED, Keasey SL, Guevara C, Ampuero JS, Comach G, Gomez D, Ochoa-Diaz M, Hontz RD, Ulrich RG. Human Antibody Responses to Emerging Mayaro Virus and Cocirculating Alphavirus Infections Examined by Using Structural Proteins from Nine New and Old World Lineages. *mSphere*. 2018; 3(2):e00003-18. DOI:10.1128/mSphere.00003-18.
  73. Jin J, Galaz-Montoya JG, Sherman MB, Sun SY, Goldsmith CS, O'Toole ET, Ackerman L, Carlson LA, Weaver SC, Chiu W, Simmons G. Neutralizing Antibodies Inhibit Chikungunya Virus Budding at the Plasma Membrane. *Cell host & microbe*. 2018; 24(3):417-28.e5. DOI:10.1016/j.chom.2018.07.018.
  74. Teo TH, Lum FM, Claser C, Lulla V, Lulla A, Merits A, Rénia L, Ng LF. A pathogenic role for CD4+ T cells during Chikungunya virus infection in mice. *J Immunol*. 2013; 190(1):259-69. DOI:10.4049/jimmunol.1202177.
  75. Wilson JA, Prow NA, Schroder WA, Ellis JJ, Cumming HE, Gearing LJ, Poo YS, Taylor A, Hertzog PJ, Di Giallonardo F, Hueston L, Le Grand R, Tang B, Le TT, Gardner J, Mahalingam S, Roques P, Bird PI, Suhrbier A. RNA-Seq analysis of chikungunya virus infection and identification of granzyme A as a major promoter of arthritic inflammation. *PLoS pathogens*. 2017; 13(2):e1006155. DOI:10.1371/journal.ppat.1006155.
  76. Davenport BJ, Bullock C, McCarthy MK, Hawman DW, Murphy KM, Kedl RM, Diamond MS, Morrison TE. Chikungunya Virus Evades Antiviral CD8(+) T Cell Responses To Establish Persistent Infection in Joint-Associated Tissues. *Journal of virology*. 2020; 94(9):e02036-19. DOI:10.1128/jvi.02036-19.
  77. Goo L, Dowd KA, Lin TY, Mascola JR, Graham BS, Ledgerwood JE, Pierson TC. A Virus-Like Particle Vaccine Elicits Broad Neutralizing Antibody Responses in Humans to All

- Chikungunya Virus Genotypes. *The Journal of infectious diseases*. 2016; 214(10):1487-91. DOI:10.1093/infdis/jiw431.
78. Zhang YN, Deng CL, Li JQ, Li N, Zhang QY, Ye HQ, Yuan ZM, Zhang B. Infectious Chikungunya Virus (CHIKV) with a Complete Capsid Deletion: a New Approach for a CHIKV Vaccine. *Journal of virology*. 2019; 93(15):e00504-19. DOI:10.1128/jvi.00504-19.
79. Chen GL, Coates EE, Plummer SH, Carter CA, Berkowitz N, Conan-Cibotti M, Cox JH, Beck A, O'Callahan M, Andrews C, Gordon IJ, Larkin B, Lampley R, Kaltovich F, Gall J, Carlton K, Mendy J, Haney D, May J, Bray A, Bailer RT, Dowd KA, Brockett B, Gordon D, Koup RA, Schwartz R, Mascola JR, Graham BS, Pierson TC, Donastorg Y, Rosario N, Pape JW, Hoen B, Cabie A, Diaz C, Ledgerwood JE. Effect of a Chikungunya Virus-Like Particle Vaccine on Safety and Tolerability Outcomes: A Randomized Clinical Trial. *Jama*. 2020; 323(14):1369-77. DOI:10.1001/jama.2020.2477.
80. Wressnigg N, Hochreiter R, Zoihsel O, Fritzer A, Bézay N, Klingler A, Lingnau K, Schneider M, Lundberg U, Meinke A, Larcher-Senn J, Čorbic-Ramljak I, Eder-Lingelbach S, Dubischar K, Bender W. Single-shot live-attenuated chikungunya vaccine in healthy adults: a phase 1, randomised controlled trial. *Lancet Infect Dis*. 2020; 20(10):1193-203. DOI:10.1016/s1473-3099(20)30238-3.
81. Folegatti PM, Harrison K, Preciado-Llanes L, Lopez FR, Bittaye M, Kim YC, Flaxman A, Bellamy D, Makinson R, Sheridan J, Azar SR, Campos RK, Tilley M, Tran N, Jenkin D, Poulton I, Lawrie A, Roberts R, Berrie E, Rossi SL, Hill A, Ewer KJ, Reyes-Sandoval A. A single dose of ChAdOx1 Chik vaccine induces neutralizing antibodies against four chikungunya virus lineages in a phase 1 clinical trial. *Nature communications*. 2021; 12(1):4636. DOI:10.1038/s41467-021-24906-y.
82. Akahata W, Yang ZY, Andersen H, Sun S, Holdaway HA, Kong WP, Lewis MG, Higgs S, Rossmann MG, Rao S, Nabel GJ. A virus-like particle vaccine for epidemic Chikungunya virus protects nonhuman primates against infection. *Nat Med*. 2010; 16(3):334-8. DOI:10.1038/nm.2105.
83. Tharmarajah K, Mahalingam S, Zaid A. Chikungunya: vaccines and therapeutics. *F1000Research*. 2017; 6:2114. DOI:10.12688/f1000research.12461.1.
84. Amaral JK, Sutaria R, Schoen RT. Treatment of Chronic Chikungunya Arthritis With Methotrexate: A Systematic Review. *Arthritis Care Res (Hoboken)*. 2018; 70(10):1501-8. DOI:10.1002/acr.23519.
85. Poon AN, Simon GL, Chang AY. Treatment of Chronic Chikungunya With Methotrexate. *J Clin Rheumatol*. 2019. DOI:10.1097/rhu.0000000000000998.
86. Gorchakov R, Wang E, Leal G, Forrester NL, Plante K, Rossi SL, Partidos CD, Adams AP, Seymour RL, Weger J, Borland EM, Sherman MB, Powers AM, Osorio JE, Weaver SC. Attenuation of Chikungunya virus vaccine strain 181/clone 25 is determined by two amino acid substitutions in the E2 envelope glycoprotein. *Journal of virology*. 2012; 86(11):6084-96. DOI:10.1128/jvi.06449-11.
87. Valneva. Valneva Announces Positive Phase 3 Pivotal Results for its Single-Shot Chikungunya Vaccine Candidate. Available from: <https://valneva.com/press->

release/valneva-announces-positive-phase-3-pivotal-results-for-its-single-shot-chikungunya-vaccine-candidate/ [Accessed on 23.07.2021].

88. Reisinger EC, Tschismarov R, Beubler E, Wiedermann U, Firbas C, Loebermann M, Pfeiffer A, Muellner M, Tauber E, Ramsauer K. Immunogenicity, safety, and tolerability of the measles-vectored chikungunya virus vaccine MV-CHIK: a double-blind, randomised, placebo-controlled and active-controlled phase 2 trial. *Lancet*. 2019; 392(10165):2718-27. DOI:10.1016/s0140-6736(18)32488-7.
89. Lefevre S, Meier FM, Neumann E, Muller-Ladner U. Role of synovial fibroblasts in rheumatoid arthritis. *Curr Pharm Des*. 2015; 21(2):130-41. DOI:10.2174/1381612820666140825122036.
90. Bartok B, Firestein GS. Fibroblast-like synoviocytes: key effector cells in rheumatoid arthritis. *Immunol Rev*. 2010; 233(1):233-55. DOI:10.1111/j.0105-2896.2009.00859.x.
91. Almutairi K, Nossent J, Preen D, Keen H, Inderjeeth C. The global prevalence of rheumatoid arthritis: a meta-analysis based on a systematic review. *Rheumatol Int*. 2021; 41(5):863-77. DOI:10.1007/s00296-020-04731-0.
92. Weyand CM, Goronzy JJ. The immunology of rheumatoid arthritis. *Nat Immunol*. 2020; 22(1):10-8. DOI:10.1038/s41590-020-00816-x.
93. Neumann E, Lefevre S, Zimmermann B, Gay S, Muller-Ladner U. Rheumatoid arthritis progression mediated by activated synovial fibroblasts. *Trends Mol Med*. 2010; 16(10):458-68. DOI:10.1016/j.molmed.2010.07.004.
94. Fuchs S, Skwara A, Bloch M, Dankbar B. Differential induction and regulation of matrix metalloproteinases in osteoarthritic tissue and fluid synovial fibroblasts. *Osteoarthritis Cartilage*. 2004; 12(5):409-18. DOI:10.1016/j.joca.2004.02.005.
95. Distler JH, Jünger A, Huber LC, Seemayer CA, Reich CF, 3rd, Gay RE, Michel BA, Fontana A, Gay S, Pisetsky DS, Distler O. The induction of matrix metalloproteinase and cytokine expression in synovial fibroblasts stimulated with immune cell microparticles. *Proceedings of the National Academy of Sciences of the United States of America*. 2005; 102(8):2892-7. DOI:10.1073/pnas.0409781102.
96. de Brito Rocha S, Baldo DC, Andrade LEC. Clinical and pathophysiologic relevance of autoantibodies in rheumatoid arthritis. *Adv Rheumatol*. 2019; 59(1):2. DOI:10.1186/s42358-018-0042-8.
97. Reparón-Schuijt CC, van Esch WJ, van Kooten C, Rozier BC, Levarht EW, Breedveld FC, Verweij CL. Regulation of synovial B cell survival in rheumatoid arthritis by vascular cell adhesion molecule 1 (CD106) expressed on fibroblast-like synoviocytes. *Arthritis Rheum*. 2000; 43(5):1115-21. DOI:10.1002/1529-0131.
98. Nygaard G, Firestein GS. Restoring synovial homeostasis in rheumatoid arthritis by targeting fibroblast-like synoviocytes. *Nat Rev Rheumatol*. 2020; 16(6):316-33. DOI:10.1038/s41584-020-0413-5.

99. Bustamante MF, Garcia-Carbonell R, Whisenant KD, Guma M. Fibroblast-like synoviocyte metabolism in the pathogenesis of rheumatoid arthritis. *Arthritis research & therapy*. 2017; 19(1):110. DOI:10.1186/s13075-017-1303-3.
100. Mizoguchi F, Slowikowski K, Wei K, Marshall JL, Rao DA, Chang SK, Nguyen HN, Noss EH, Turner JD, Earp BE, Blazar PE, Wright J, Simmons BP, Donlin LT, Kalliolias GD, Goodman SM, Bykerk VP, Ivashkiv LB, Lederer JA, Hacohen N, Nigrovic PA, Filer A, Buckley CD, Raychaudhuri S, Brenner MB. Functionally distinct disease-associated fibroblast subsets in rheumatoid arthritis. *Nature communications*. 2018; 9(1):789. DOI:10.1038/s41467-018-02892-y.
101. Amaral JK, Billsborrow JB, Schoen RT. Chronic Chikungunya Arthritis and Rheumatoid Arthritis: What They Have in Common. *Am J Med*. 2020; 133(3):e91-e7. DOI:10.1016/j.amjmed.2019.10.005.
102. Nakaya HI, Gardner J, Poo YS, Major L, Pulendran B, Suhrbier A. Gene profiling of Chikungunya virus arthritis in a mouse model reveals significant overlap with rheumatoid arthritis. *Arthritis Rheum*. 2012; 64(11):3553-63. DOI:10.1002/art.34631.
103. Selvamani SP, Mishra R, Singh SK. Chikungunya virus exploits miR-146a to regulate NF- $\kappa$ B pathway in human synovial fibroblasts. *PloS one*. 2014; 9(8):e103624. DOI:10.1371/journal.pone.0103624.
104. Agrawal M, Pandey N, Rastogi M, Dogra S, Singh SK. Chikungunya virus modulates the miRNA expression patterns in human synovial fibroblasts. *J Med Virol*. 2020; 92(2):139-48. DOI:10.1002/jmv.25588.
105. Sukkaew A, Thanagith M, Thongsakulprasert T, Mutso M, Mahalingam S, Smith DR, Ubol S. Heterogeneity of clinical isolates of chikungunya virus and its impact on the responses of primary human fibroblast-like synoviocytes. *J Gen Virol*. 2018; 99(4):525-35. DOI:10.1099/jgv.0.001039.
106. Thon-Hon VG, Denizot M, Li-Pat-Yuen G, Giry C, Jaffar-Bandjee MC, Gasque P. Deciphering the differential response of two human fibroblast cell lines following Chikungunya virus infection. *Virology journal*. 2012; 9:213. DOI:10.1186/1743-422x-9-213.
107. O'Neal JT, Upadhyay AA, Wolabaugh A, Patel NB, Bosinger SE, Suthar MS. West Nile Virus-Inclusive Single-Cell RNA Sequencing Reveals Heterogeneity in the Type I Interferon Response within Single Cells. *Journal of virology*. 2019; 93(6):e01778-18. DOI:10.1128/jvi.01778-18.
108. Ramos I, Smith G, Ruf-Zamojski F, Martínez-Romero C, Fribourg M, Carbajal EA, Hartmann BM, Nair VD, Marjanovic N, Monteagudo PL, DeJesus VA, Mutetwa T, Zamojski M, Tan GS, Jayaprakash C, Zaslavsky E, Albrecht RA, Sealfon SC, García-Sastre A, Fernandez-Sesma A. Innate Immune Response to Influenza Virus at Single-Cell Resolution in Human Epithelial Cells Revealed Paracrine Induction of Interferon Lambda 1. *Journal of virology*. 2019; 93(20):e00559-19. DOI:10.1128/jvi.00559-19.
109. Wyler E, Franke V, Menegatti J, Kocks C, Boltengagen A, Praktijnjo S, Walch-Rückheim B, Bosse J, Rajewsky N, Grässer F, Akalin A, Landthaler M. Single-cell RNA-sequencing

- of herpes simplex virus 1-infected cells connects NRF2 activation to an antiviral program. *Nature communications*. 2019; 10(1):4878. DOI:10.1038/s41467-019-12894-z.
110. Pott F, Postmus D, Brown RJP, Wyler E, Neumann E, Landthaler M, Goffinet C. Single-cell analysis of arthritogenic alphavirus-infected human synovial fibroblasts links low abundance of viral RNA to induction of innate immunity and arthralgia-associated gene expression. *Emerg Microbes Infect.* 2021; 10(1):2151-68. DOI:10.1080/22221751.2021.2000891.
  111. Neumann E, Riepl B, Knedla A, Lefevre S, Tarner IH, Grifka J, Steinmeyer J, Scholmerich J, Gay S, Muller-Ladner U. Cell culture and passaging alters gene expression pattern and proliferation rate in rheumatoid arthritis synovial fibroblasts. *Arthritis research & therapy*. 2010; 12(3):R83. DOI:10.1186/ar3010.
  112. Tsetsarkin K, Higgs S, McGee CE, De Lamballerie X, Charrel RN, Vanlandingham DL. Infectious clones of Chikungunya virus (La Reunion isolate) for vector competence studies. *Vector borne and zoonotic diseases (Larchmont, NY)*. 2006; 6(4):325-37. DOI:10.1089/vbz.2006.6.325.
  113. Li X, Zhang H, Zhang Y, Li J, Wang Z, Deng C, Jardim ACG, Terzian ACB, Nogueira ML, Zhang B. Development of a rapid antiviral screening assay based on eGFP reporter virus of Mayaro virus. *Antiviral Res.* 2019; 168:82-90. DOI:10.1016/j.antiviral.2019.05.013.
  114. Uzé G, Di Marco S, Mouchel-Vielh E, Monneron D, Bandu MT, Horisberger MA, Dorques A, Lutfalla G, Mogensen KE. Domains of interaction between alpha interferon and its receptor components. *J Mol Biol.* 1994; 243(2):245-57. DOI:10.1006/jmbi.1994.1651.
  115. Ashburner M, Ball CA, Blake JA, Botstein D, Butler H, Cherry JM, Davis AP, Dolinski K, Dwight SS, Eppig JT, Harris MA, Hill DP, Issel-Tarver L, Kasarskis A, Lewis S, Matese JC, Richardson JE, Ringwald M, Rubin GM, Sherlock G. Gene ontology: tool for the unification of biology. The Gene Ontology Consortium. *Nat Genet.* 2000; 25(1):25-9. DOI:10.1038/75556.
  116. Hao Y, Hao S, Andersen-Nissen E, Mauck WM, Zheng S, Butler A, Lee MJ, Wilk AJ, Darby C, Zagar M, Hoffman P, Stoeckius M, Papalexi E, Mimitou EP, Jain J, Srivastava A, Stuart T, Fleming LB, Yeung B, Rogers AJ, McElrath JM, Blish CA, Gottardo R, Smibert P, Satija R. Integrated analysis of multimodal single-cell data. *bioRxiv*. 2020:2020.10.12.335331. DOI:10.1101/2020.10.12.335331.
  117. Holland CH, Tanevski J, Perales-Patón J, Gleixner J, Kumar MP, Mereu E, Joughin BA, Stegle O, Lauffenburger DA, Heyn H, Szalai B, Saez-Rodriguez J. Robustness and applicability of transcription factor and pathway analysis tools on single-cell RNA-seq data. *Genome Biol.* 2020; 21(1):36. DOI:10.1186/s13059-020-1949-z.
  118. Sourisseau M, Schilte C, Casartelli N, Trouillet C, Guivel-Benhassine F, Rudnicka D, Sol-Foulon N, Le Roux K, Prevost MC, Fsihi H, Frenkiel MP, Blanchet F, Afonso PV, Ceccaldi PE, Ozden S, Gessain A, Schuffenecker I, Verhasselt B, Zamborlini A, Saib A, Rey FA, Arenzana-Seisdedos F, Despres P, Michault A, Albert ML, Schwartz O. Characterization of reemerging chikungunya virus. *PLoS pathogens*. 2007; 3(6):e89. DOI:10.1371/journal.ppat.0030089.

119. Mesev EV, LeDesma RA, Ploss A. Decoding type I and III interferon signalling during viral infection. *Nature microbiology*. 2019; 4(6):914-24. DOI:10.1038/s41564-019-0421-x.
120. Georganas C, Liu H, Perlman H, Hoffmann A, Thimmapaya B, Pope RM. Regulation of IL-6 and IL-8 expression in rheumatoid arthritis synovial fibroblasts: the dominant role for NF-kappa B but not C/EBP beta or c-Jun. *J Immunol*. 2000; 165(12):7199-206. DOI:10.4049/jimmunol.165.12.7199.
121. Lemm JA, Rümenapf T, Strauss EG, Strauss JH, Rice CM. Polypeptide requirements for assembly of functional Sindbis virus replication complexes: a model for the temporal regulation of minus- and plus-strand RNA synthesis. *Embo j*. 1994; 13(12):2925-34.
122. Shirako Y, Strauss JH. Regulation of Sindbis virus RNA replication: uncleaved P123 and nsP4 function in minus-strand RNA synthesis, whereas cleaved products from P123 are required for efficient plus-strand RNA synthesis. *Journal of virology*. 1994; 68(3):1874-85. DOI:10.1128/jvi.68.3.1874-1885.1994.
123. Sommereyns C, Paul S, Staeheli P, Michiels T. IFN-lambda (IFN-lambda) is expressed in a tissue-dependent fashion and primarily acts on epithelial cells in vivo. *PLoS pathogens*. 2008; 4(3):e1000017. DOI:10.1371/journal.ppat.1000017.
124. Bae S, Lee JY, Myoung J. Chikungunya Virus-Encoded nsP2, E2 and E1 Strongly Antagonize the Interferon-beta Signaling Pathway. *J Microbiol Biotechnol*. 2019; 29(11):1852-9. DOI:10.4014/jmb.1910.10014.
125. Fros JJ, Pijlman GP. Alphavirus Infection: Host Cell Shut-Off and Inhibition of Antiviral Responses. *Viruses*. 2016; 8(6). DOI:10.3390/v8060166.
126. Kotliar D, Lin AE, Logue J, Hughes TK, Khoury NM, Raju SS, Wadsworth MH, 2nd, Chen H, Kurtz JR, Digheo-Kemp B, Bjornson ZB, Mukherjee N, Sellers BA, Tran N, Bauer MR, Adams GC, Adams R, Rinn JL, Melé M, Schaffner SF, Nolan GP, Barnes KG, Hensley LE, McIlwain DR, Shalek AK, Sabeti PC, Bennett RS. Single-Cell Profiling of Ebola Virus Disease In Vivo Reveals Viral and Host Dynamics. *Cell*. 2020; 183(5):1383-401.e19. DOI:10.1016/j.cell.2020.10.002.
127. Müller-Ladner U, Ospelt C, Gay S, Distler O, Pap T. Cells of the synovium in rheumatoid arthritis. Synovial fibroblasts. *Arthritis research & therapy*. 2007; 9(6):223. DOI:10.1186/ar2337.
128. Heruth DP, Gibson M, Grigoryev DN, Zhang LQ, Ye SQ. RNA-seq analysis of synovial fibroblasts brings new insights into rheumatoid arthritis. *Cell & bioscience*. 2012; 2(1):43. DOI:10.1186/2045-3701-2-43.
129. Hillen J, Geyer C, Heitzmann M, Beckmann D, Krause A, Winkler I, Pavenstadt H, Bremer C, Pap T, Korb-Pap A. Structural cartilage damage attracts circulating rheumatoid arthritis synovial fibroblasts into affected joints. *Arthritis research & therapy*. 2017; 19(1):40. DOI:10.1186/s13075-017-1245-9.
130. Hawman DW, Stoermer KA, Montgomery SA, Pal P, Oko L, Diamond MS, Morrison TE. Chronic joint disease caused by persistent Chikungunya virus infection is controlled by



- the adaptive immune response. *Journal of virology*. 2013; 87(24):13878-88. DOI:10.1128/jvi.02666-13.
131. Poo YS, Rudd PA, Gardner J, Wilson JA, Larcher T, Colle MA, Le TT, Nakaya HI, Warrilow D, Allcock R, Bielefeldt-Ohmann H, Schroder WA, Khromykh AA, Lopez JA, Suhrbier A. Multiple immune factors are involved in controlling acute and chronic chikungunya virus infection. *PLoS neglected tropical diseases*. 2014; 8(12):e3354. DOI:10.1371/journal.pntd.0003354.
  132. Lum FM, Teo TH, Lee WW, Kam YW, Rénia L, Ng LF. An essential role of antibodies in the control of Chikungunya virus infection. *J Immunol*. 2013; 190(12):6295-302. DOI:10.4049/jimmunol.1300304.
  133. Seymour RL, Adams AP, Leal G, Alcorn MD, Weaver SC. A Rodent Model of Chikungunya Virus Infection in RAG1 <sup>-/-</sup> Mice, with Features of Persistence, for Vaccine Safety Evaluation. *PLoS neglected tropical diseases*. 2015; 9(6):e0003800. DOI:10.1371/journal.pntd.0003800.
  134. Bedoui Y, Giry C, Jaffar-Bandjee MC, Selambarom J, Guiraud P, Gasque P. Immunomodulatory drug methotrexate used to treat patients with chronic inflammatory rheumatism post-chikungunya does not impair the synovial antiviral and bone repair responses. *PLoS neglected tropical diseases*. 2018; 12(8):e0006634. DOI:10.1371/journal.pntd.0006634.
  135. Delang L, Segura Guerrero N, Tas A, Quérat G, Pastorino B, Froeyen M, Dallmeier K, Jochmans D, Herdewijn P, Bello F, Snijder EJ, de Lamballerie X, Martina B, Neyts J, van Hemert MJ, Leyssen P. Mutations in the chikungunya virus non-structural proteins cause resistance to favipiravir (T-705), a broad-spectrum antiviral. *J Antimicrob Chemother*. 2014; 69(10):2770-84. DOI:10.1093/jac/dku209.
  136. Briolant S, Garin D, Scaramozzino N, Jouan A, Crance JM. In vitro inhibition of Chikungunya and Semliki Forest viruses replication by antiviral compounds: synergistic effect of interferon-alpha and ribavirin combination. *Antiviral Res*. 2004; 61(2):111-7. DOI:10.1016/j.antiviral.2003.09.005.
  137. Guerrero-Arguero I, Høj TR, Tass ES, Berges BK, Robison RA. A comparison of Chikungunya virus infection, progression, and cytokine profiles in human PMA-differentiated U937 and murine RAW264.7 monocyte derived macrophages. *PloS one*. 2020; 15(3):e0230328. DOI:10.1371/journal.pone.0230328.
  138. Suhrbier A. Rheumatic manifestations of chikungunya: emerging concepts and interventions. *Nat Rev Rheumatol*. 2019; 15(10):597-611. DOI:10.1038/s41584-019-0276-9.
  139. Valneva. Valneva Initiates Phase 3 Clinical Study for its Chikungunya Vaccine Candidate VLA1553. Available from: <https://valneva.com/press-release/valneva-initiates-phase-3-clinical-study-for-its-chikungunya-vaccine-candidate-vla1553/> [Accessed on 23.07.2021].
  140. Chaudhary N, Weissman D, Whitehead KA. mRNA vaccines for infectious diseases: principles, delivery and clinical translation. *Nat Rev Drug Discov*. 2021; 20(11):817-38. DOI:10.1038/s41573-021-00283-5.

## **Eidesstaatliche Versicherung**

„Ich, Fabian Pott, versichere an Eides statt durch meine eigenhändige Unterschrift, dass ich die vorgelegte Dissertation mit dem Thema: „Antiviral Responses against Chikungunya Virus Infection in a Novel Primary Cell Model/Antivirale Antworten gegen das Chikungunyavirus in einem neuartigen Primärzellmodell“ selbstständig und ohne nicht offengelegte Hilfe Dritter verfasst und keine anderen als die angegebenen Quellen und Hilfsmittel genutzt habe.

Alle Stellen, die wörtlich oder dem Sinne nach auf Publikationen oder Vorträgen anderer Autoren/innen beruhen, sind als solche in korrekter Zitierung kenntlich gemacht. Die Abschnitte zu Methodik (insbesondere praktische Arbeiten, Laborbestimmungen, statistische Aufarbeitung) und Resultaten (insbesondere Abbildungen, Graphiken und Tabellen) werden von mir verantwortet.

Ich versichere ferner, dass ich die in Zusammenarbeit mit anderen Personen generierten Daten, Datenauswertungen und Schlussfolgerungen korrekt gekennzeichnet und meinen eigenen Beitrag sowie die Beiträge anderer Personen korrekt kenntlich gemacht habe (siehe Anteilserklärung). Texte oder Textteile, die gemeinsam mit anderen erstellt oder verwendet wurden, habe ich korrekt kenntlich gemacht.

Meine Anteile an etwaigen Publikationen zu dieser Dissertation entsprechen denen, die in der untenstehenden gemeinsamen Erklärung mit dem/der Erstbetreuer/in, angegeben sind. Für sämtliche im Rahmen der Dissertation entstandenen Publikationen wurden die Richtlinien des ICMJE (International Committee of Medical Journal Editors; [www.icmje.org](http://www.icmje.org)) zur Autorenschaft eingehalten. Ich erkläre ferner, dass ich mich zur Einhaltung der Satzung der Charité – Universitätsmedizin Berlin zur Sicherung Guter Wissenschaftlicher Praxis verpflichte.

Weiterhin versichere ich, dass ich diese Dissertation weder in gleicher noch in ähnlicher Form bereits an einer anderen Fakultät eingereicht habe.

Die Bedeutung dieser eidesstattlichen Versicherung und die strafrechtlichen Folgen einer unwahren eidesstattlichen Versicherung (§§156, 161 des Strafgesetzbuches) sind mir bekannt und bewusst.“

Datum

Unterschrift

## **Declaration of Own Contribution**

### **Ausführliche Anteilserklärung an der erfolgten Publikation als Top-Journal im Rahmen der Promotionsverfahren zum PhD bzw. MD/PhD**

Pott F, Postmus D, Brown RJP, Wyler E, Neumann E, Landthaler M, Goffinet C: "Single-cell analysis of arthritogenic alphavirus-infected human synovial fibroblasts links low abundance of viral RNA to induction of innate immunity and arthralgia-associated gene expression." *Emerging Microbes & Infections* (2021).

#### **Beitrag im Einzelnen:**

Die Studie wurde von F. Pott und C. Goffinet konzeptioniert. Alle experimentellen Teile dieser Publikation, inklusive der Kultivierung der Zellen, der Infektionsexperimente, und der molekularbiologischen Auswertungen, sind durch F. Pott entstanden. Aus den Ergebnissen der experimentellen Arbeit wurden die Abbildungen 1, 2A-B, 4A-D, und 5A-B von F. Pott erstellt. Die RNA-Sequenzierung wurde von der Sequencing Core Facility des Helmholtz-Zentrums für Infektionsforschung in Braunschweig und der Genomics Platform des Berlin Institute of Health (BIH) durchgeführt. Die statistische und bioinformatische Auswertung der daraus entstandenen Datensätze, dargestellt in den Abbildungen 2C-F und 3A-D, wurde von F. Pott unter Mithilfe von R. Brown durchgeführt. Die bioinformatische Analyse der Einzelzellsequenzierungs-Datensätze in Abbildung 5C-D und Abbildung 6A-E wurde von F. Pott unter Mithilfe von E. Wyler und D. Postmus durchgeführt. E. Neumann hat die initiale Extraktion der Fibroblasten durchgeführt und die Zellen zur weiteren Kultivierung an F. Pott übergeben. M. Landthaler und C. Goffinet haben die Durchführung der Studie überwacht. Die Auswertung und Aufbereitung der Daten wurde von F. Pott unter Anleitung und Diskussion von C. Goffinet durchgeführt. Das Manuskript wurde von F. Pott verfasst und durch C. Goffinet korrigiert und erweitert. Alle Ko-Autoren haben das Manuskript final korrigiert und der Veröffentlichung zugestimmt.

---

Unterschrift, Datum und Stempel des/der erstbetreuenden Hochschullehrers/in

---

Unterschrift des Doktoranden/der Doktorandin

## Excerpt from the Journal Summary List

Journal Data Filtered By: **Selected JCR Year: 2020** Selected Editions: SCIE,SSCI  
 Selected Categories: **"INFECTIOUS DISEASES"** Selected Category  
 Scheme: WoS

**Gesamtanzahl: 92 Journale**

Rank	Full Journal Title	Total Cites	Journal Impact Factor	Eigenfactor Score
1	LANCET INFECTIOUS DISEASES	42,483	25.071	0.070070
2	Lancet HIV	5,368	12.767	0.022020
3	CLINICAL INFECTIOUS DISEASES	89,276	9.079	0.113210
4	JOURNAL OF TRAVEL MEDICINE	5,260	8.490	0.004900
5	CLINICAL MICROBIOLOGY AND INFECTION	24,871	8.067	0.031710
6	Emerging Microbes & Infections	8,988	7.163	0.012560
7	EMERGING INFECTIOUS DISEASES	44,051	6.883	0.049780
8	Eurosurveillance	15,123	6.307	0.023830
9	Travel Medicine and Infectious Disease	5,034	6.211	0.003430
10	JOURNAL OF INFECTION	15,496	6.072	0.012570
11	INFECTIOUS DISEASE CLINICS OF NORTH AMERICA	4,090	5.982	0.006870
12	Virulence	5,784	5.882	0.007420
13	INTERNATIONAL JOURNAL OF HYGIENE AND ENVIRONMENTAL HEALTH	7,425	5.840	0.008110
14	JOURNAL OF ANTIMICROBIAL CHEMOTHERAPY	38,715	5.790	0.042490
15	Journal of the International AIDS Society	6,474	5.396	0.017390
16	Infectious Diseases and Therapy	1,331	5.322	0.003260
17	INTERNATIONAL JOURNAL OF ANTIMICROBIAL AGENTS	20,409	5.283	0.015470

## Single-cell analysis of arthritogenic alphavirus-infected human synovial fibroblasts links low abundance of viral RNA to induction of innate immunity and arthralgia-associated gene expression

Fabian Pott <sup>a,b</sup>, Dylan Postmus<sup>a,b</sup>, Richard J. P. Brown <sup>c</sup>, Emanuel Wyler<sup>d</sup>, Elena Neumann<sup>e</sup>, Markus Landthaler<sup>d,f</sup> and Christine Goffinet <sup>a,b</sup>

<sup>a</sup>Institute of Virology, Charité – Universitätsmedizin Berlin, corporate member of Freie Universität Berlin and Humboldt-Universität zu Berlin, Berlin, Germany; <sup>b</sup>Berlin Institute of Health at Charité, Universitätsmedizin Berlin, Berlin, Germany; <sup>c</sup>Division of Veterinary Medicine, Paul Ehrlich Institute, Langen, Germany; <sup>d</sup>Max-Delbrück-Center for Molecular Medicine in the Helmholtz Association (MDC), Berlin Institute for Medical Systems Biology (BIMSB), Berlin, Germany; <sup>e</sup>Internal Medicine and Rheumatology, Justus-Liebig-University Giessen, Bad Nauheim, Germany; <sup>f</sup>IRI Life Sciences, Institut für Biologie, Humboldt Universität zu Berlin, Berlin, Germany

### ABSTRACT

Infection by (re-)emerging RNA arboviruses including Chikungunya virus (CHIKV) and Mayaro virus primarily cause acute febrile disease and transient polyarthralgia. However, in a significant subset of infected individuals, debilitating arthralgia persists for weeks over months up to years. The underlying immunopathogenesis of chronification of arthralgia upon primary RNA-viral infection remains unclear. Here, we analysed cell-intrinsic responses to *ex vivo* arthritogenic alphaviral infection of primary human synovial fibroblasts isolated from knee joints, one of the most affected joint types during acute and chronic CHIKV disease. Synovial fibroblasts were susceptible and permissive to alphaviral infection. Base-line and exogenously added type I interferon (IFN) partially and potently restricted infection, respectively. RNA-seq revealed a CHIKV infection-induced transcriptional profile that comprised upregulation of expression of several hundred IFN-stimulated and arthralgia-mediating genes. Single-cell virus-inclusive RNA-seq uncovered a fine-tuned switch from induction to repression of cell-intrinsic immune responses depending on the abundance of viral RNA in an individual cell. Specifically, responses were most pronounced in cells displaying low-to-intermediate amounts of viral RNA and absence of virus-encoded, fluorescent reporter protein expression, arguing for efficient counteraction of innate immunity in cells expressing viral antagonists at sufficient quantities. In summary, cell-intrinsic sensing of viral RNA that potentially persists or replicates at low levels in synovial fibroblasts and other target cell types *in vivo* may contribute to the chronic arthralgia induced by alphaviral infections. Our findings might advance our understanding of the immunopathophysiology of long-term pathogenesis of RNA-viral infections.



**ARTICLE HISTORY** Received 9 July 2021; Revised 25 October 2021; Accepted 27 October 2021

**KEYWORDS** Chikungunya; fibroblasts; innate immunity; RNA-seq; transcriptomics

### Introduction

Chikungunya virus (CHIKV) and Mayaro virus (MAYV) are arthritogenic alphaviruses of the *Togaviridae* family, which are transmitted by *Aedes sp.* mosquitoes and circulate both in urban cycles between vectors and humans, and in sylvatic cycles [1,2]. Hallmarks of the typically relatively short acute disease are febrile illness, rashes, and excruciating pain in multiple joints. Relapsing-remitting arthralgia persists in a subgroup of patients for months to years [3]. The underlying immunopathophysiology of the chronic symptoms remains largely unclear, but appears to associate with circulating IL-6 [4] and IL-12 [5]. Interestingly, a much-discussed hypothesis suggests that it may involve persistence of viral RNA in synovial macrophages, muscle cells, and fibroblasts *in vivo* [5–7].

Multiple studies on alphaviruses in immortalized model cell lines and *in vivo* in immunodeficient mice have provided valuable information on key aspects of CHIKV and MAYV tropism and replication, including host factors for entry and replication [8,9], the impact of mutations in the viral glycoproteins on cell entry [10], and cellular restriction factors acting against CHIKV and other alphaviruses [11]. Additionally, studies investigating immune responses to infection have demonstrated that CHIKV nsP2 counteracts host immunity by blocking nuclear translocation of STAT1 [12] and inducing a host transcriptional shutdown [13]. Sensing of infection-induced DNA leakage, as described for RNA viruses before [14], is efficiently subverted by CHIKV through its nonstructural proteins [15]. However, the relevance and consequence

**CONTACT** Christine Goffinet  [christine.goffinet@charite.de](mailto:christine.goffinet@charite.de)  Institute for Virology, Charité – Universitätsmedizin Berlin, Charitéplatz 1, 10117, Berlin, Germany

 Supplemental data for this article can be accessed at <https://doi.org/10.1080/22221751.2021.2000891>

© 2021 The Author(s). Published by Informa UK Limited, trading as Taylor & Francis Group.

This is an Open Access article distributed under the terms of the Creative Commons Attribution-NonCommercial License (<http://creativecommons.org/licenses/by-nc/4.0/>), which permits unrestricted non-commercial use, distribution, and reproduction in any medium, provided the original work is properly cited.

of these and potentially additional immunity-subverting mechanisms in infected patients remain unclear. *In vivo* studies in mice, though recapitulating both innate and adaptive immune responses, require a type I interferon (IFN)-deficient background, neglecting the impact of type I IFN-mediated antiviral responses [16]. Type I IFN induced in and acting on nonhematopoietic cells appears to be essential for the control and early clearance of CHIKV *in vivo* [17]. Therefore, these models do not fully recapitulate the cellular environment of human primary cells and tissues that are targeted by CHIKV and MAYV *in vivo*. Primary human cells have been used sporadically for *ex vivo* infection [18,19], but their unique properties in terms of susceptibility to infection and cell-intrinsic responses remain poorly investigated. Synovial fibroblasts have been described to be a key driver for rheumatoid arthritis by facilitating proinflammatory processes and stimulating the degradation of cartilage [20], and it is plausible that they contribute to CHIKV spread and pathogenesis *in vivo*. Here, we perform an in depth-characterization of primary human synovial fibroblasts extracted from human knee joint biopsies as an *ex vivo* model of CHIKV and MAYV infection. We demonstrate that synovial fibroblasts are susceptible and permissive to infection by both arthritogenic alphaviruses. Using bulk and single-cell approaches, we identified cell-intrinsic immune responses that were most pronounced in non-productively infected cells, suggestive of effective viral antagonism of cellular responses in cells undergoing efficient virus replication.

## Material and methods

### Cells and viruses

Human osteosarcoma U2OS cells (a kind gift from T. Stradal, Hanover), human HEK293 T cells (a kind gift from J. Bohne, Hanover), human foreskin fibroblast HFF-1 cells (ATCC SCRC-1041), human HL116 cells (a kind gift from Sandra Pellegrini, Institut Pasteur, France [21]), and hamster BHK-21 cells (ATCC CCL-10) were grown in Dulbecco's modified Eagle's medium – high glucose (DMEM, Sigma-Aldrich D5671) supplemented with 10% heat-inactivated fetal bovine serum (FBS, Sigma-Aldrich F7524), 2 mM L-Glutamine (Gibco 25030081), and 100 units/ml penicillin–streptomycin (Gibco 11548876). HL116 cell received 1X HAT supplement (Gibco 21060017) in addition.

Primary human fibroblasts were obtained from synovial biopsies from knee joints from donors suffering from osteoarthritis (osteoarthritis synovial fibroblasts, OASF) or a non-arthritic background (healthy donor synovial fibroblasts, HSF), purified, and cultured as described before [22]. Mycoplasma testing was

routinely performed and negative in all primary human cell cultures. After 2–4 passages of initial cultivation, cells were expanded and used for experiments in high glucose DMEM supplemented with 20% FBS, 2 mM L-Glutamine, 100 units/ml penicillin–streptomycin, 1% non-essential amino acids (Gibco 11140050), and 1% sodium pyruvate (Gibco 11360070). The CHIKV LR2006-OPY 5'GFP and MAYV TRVL4675 5'GFP infectious clones expressing EGFP under the control of a subgenomic promoter (hereafter referred to as CHIKV and MAYV) have been described previously [23,24]. Virus was produced by *in vitro*-transcription of and subsequent electroporation of RNA into BHK-21 cells. Virus-containing supernatant was collected, passaged once on BHK-21 cells and viral titers were determined by titration on HEK293T cells.

### Infection, treatments, transfections

EGFP expression as surrogate for productive CHIKV or MAYV infection was quantified on a BD FACSCalibur, FACSLyric or Accuri C6. For neutralization assays, virus-containing supernatants were pre-incubated for one hour with anti-CHIKV E2 antibody C9 (Integral Molecular C9, Lot INT MAB-003) at 1 µg/ml or with recombinant MXRA8-Fc (a kind gift from M. Diamond) at 150 ng/ml. Recombinant IFN-α2a (Roferon L03AB04, Roche) and IFN-λ1 (Peprotech 300-02L) was used where indicated. Transfections were performed using Lipofectamine2000 (Thermo Fisher 11668019) for plasmid DNA (pcDNA6 empty vector) or 5' triphosphate dsRNA (InvivoGen ttrl-3prna).

### Bulk RNA-Seq analysis

RNA was extracted using the Promega Maxwell 16 with LEV simplyRNA Tissue Kits (Promega AS1270). RNA quality was assessed using the Agilent Bioanalyzer and appropriate samples were used for NGS library preparation with the NEBNext Ultra II Directional RNA kit (NEB E7760) and sequenced with 50 bp paired-end reads and 30 mio reads per sample on the Illumina HiSeq 2500. Data were analysed with CLC Genomics Workbench 12 (QIAGEN) by mapping the human reads onto the hg19 reference genome scaffold (GCA\_000001405.28). Unmapped reads not matching the human genome were subsequently mapped onto the CHIKV genome LR2006\_OPY (DQ443544.2). For HSF, infection and analysis were performed similarly, but RNA was extracted with the Direct-Zol RNA Mini-Prep Kit (Zymo Research R2051), NGS libraries were prepared with the TruSeq stranded mRNA kit (Illumina 20020594) and sequencing was performed on the Illumina NextSeq500 with 65 mio reads per sample. Biological process enrichment was analysed by Gene Ontology [25].

### Single-Cell RNA-Seq analysis

Infected cells were trypsinized, debris was removed by filtration, and the suspension was adjusted to a final amount of ~16,000 cells per lane to achieve the recovery of 10,000 cells per donor after partitioning into Gel-Beads in Emulsion (GEMs) according to the instructions for Chromium Next GEM Single Cell 3' GEM, Library & Gel Bead Kit v3.1 provided by the manufacturer (10X Genomics PN-1000121). Polyadenylated mRNAs were tagged with unique 16 bp 10X barcodes and the 10 bp Unique Molecular Identifiers (UMIs), reverse transcribed and resulting cDNAs were bulk amplified. After enzymatic fragmentation and size selection, resulting double-stranded cDNA amplicons optimized for library construction were subjected to adaptor ligation and sample index PCRs needed for Illumina bridge amplification and sequencing. Single-cell libraries were quantified using Qubit (Thermo Fisher) and quality-controlled using the Bioanalyzer System (Agilent). Sequencing was performed on a HiSeq4000 device (Illumina) aiming for 175 mln reads per library (read1: 26 nucleotides, read2: 64 nucleotides). Data were analysed using Cell Ranger v5.0 (10X Genomics) using human and CHIKV genome scaffolds as described above, and the R packages Seurat v4.0 [26] and DoRothEA v3.12 [27] were used for cell clustering, annotation, and transcription factor activity analysis. Median gene number detected per cell ranged between 2000 and 4400, with 3800–18500 median UMI counts per cell.

### Quantitative RT-PCR

RNA was extracted using the Promega Maxwell 16 with the LEV simplyRNA tissue kit (Promega AS1270), the Roche MagNAPure with the Cellular Total RNA Large Volume kit (Roche 05467535001), or the DirectZol RNA Mini kit (Zymo R2051). cDNA was prepared using dNTPs (Thermo Fisher R0181), random hexamers (Jena Bioscience PM-301) and M-MuLV reverse transcriptase (NEB M0253). For quantitative RT-PCR, specific Taqman probes and primers (Thermo Fisher 4331182) were used with TaqMan Universal PCR Master Mix (Applied Biosystems 4305719) or LightCycler® 480 Probes Master (Roche 04887301001). PCRs were performed on the Applied Biosystems ABI 7500 Fast or the Roche LightCycler 480 in technical triplicates.

### Flow cytometry, confocal and live cell imaging

For flow cytometric analysis of protein expression, OASF were fixed in 4% PFA (Carl Roth 4235.2), permeabilized in 0.1% Triton-X (Invitrogen HFH10) and immunostained with antibodies against IFIT1 (Origene TA500948, clone OTI3G8), MX1/2 (Santa

Cruz sc-47197), and IFITM3 (Abgent AP1153a) in combination with Alexa Fluor-647 conjugated antibodies against mouse- (Thermo Fisher A28181), rabbit- (Thermo Fisher A27040), or goat-IgG (Thermo Fisher A-21447). Flow cytometry was performed on a BD FACSCalibur or FACSLyric and analysed with FlowJo v10. For immunofluorescence microscopy, OASF were seeded in 8-well  $\mu$ -slides (ibidi 80826), fixed and permeabilized as described above, stained with antibodies against MXRA8 (biorbyt orb221523) with AlexaFluor647-conjugated secondary antibody (Thermo Fisher A28181), and counterstained with DAPI (Invitrogen D1306). For fluorescence microscopy and live cell imaging, cells were infected with CHIKV at an MOI of 10 and imaged with the Zeiss LSM800 Airyscan Confocal Microscope. Images were analysed and merged using Zeiss ZEN Blue 3.0.

### Immunoblotting

Cell lysates were separated on 10% acrylamide gels by SDS-PAGE and protein transferred to a 0.45  $\mu$ m PVDF membrane (GE Healthcare 15259894) using the BioRad TransBlot Turbo system. Expression was detected using primary antibodies detecting MXRA8 (biorbyt orb221523), FHL1 (R&D Systems MAB5938), IFITM3 (Abgent AP1153a), MX2 (Santa Cruz sc-47197), ISG15 (Santa Cruz sc-166755), and  $\alpha$ -Tubulin (Cell Signalling Technology 2144S) and appropriate secondary IRDye antibodies. CHIKV proteins were detected using anti-CHIKV antiserum (IBT Bioservices Cat #01-0008 Lot #1703002). Fluorescence was detected and quantified using the LI-COR Odyssey Fc system.

### Measurement of IL-6 and bioactive IFN

Anti-IL-6 ELISA (BioLegend 430504) was performed according to manufacturer's protocols. Briefly, plates were coated with capture antibodies and incubated with diluted supernatant from CHIKV- or mock-infected cell cultures. Detection antibody and substrate were added and the OD measured with the Tecan Sunrise microplate reader. Concentrations were then calculated the concentration according to a standard curve measured on the same plate. Bioactive type I IFN was quantified by incubating supernatant from CHIKV-infected cells on HL116 cells harbouring a firefly luciferase gene under the control of an IFN-sensitive promoter. After six h, cells were lysed, incubated with luciferase substrate solution (Promega E1500), and luciferase activity was quantified with the BioTek Synergy HTX microplate reader.

### Data and code availability

RNA-seq and single-cell RNA-seq datasets are available at the NCBI GEO database under the accession

number GSE152782 and GSE176361, respectively. All generated code is available at [https://github.com/GoffinetLab/CHIKV\\_scrNAseq-fibroblast](https://github.com/GoffinetLab/CHIKV_scrNAseq-fibroblast).

### Statistics

If not stated otherwise, bars and symbols show the arithmetic mean of indicated amount of repetitions. Error bars indicate S.D. from at least three or S.E.M. from the indicated amount of individual experiments. Statistical analysis was performed using CLC Workbench for RNA-seq and GraphPad Prism 8.3.0 for all other analysis. Unpaired, two-sided t-tests were applied with assumed equal standard deviation when comparing results obtained in the same cell line and Mann–Whitney–U-tests when comparing between cell lines or between cell lines and primary cells. For IC50 calculation, nonlinear fit curves with variable slopes were calculated. Differentially expressed genes in RNA-seq data were identified from raw count data, with calculation of false discovery rate correction (FDR) *p*-values for multiple comparisons. *P*-values for Gene Ontology analysis were generated after Bonferroni correction for multiple testing. For differential gene expression analysis from single-cell RNA-seq data, Wilcoxon rank sum tests with applied Bonferroni correction were applied. Cumulative distributions between groups were compared using the Kolmogorov–Smirnov (KS) test. Nonparametric Spearman tests with two-tailed *p*-values were performed to correlate gene expression. *P* values <0.05 were considered significant (\*), <0.01 very significant (\*\*), <0.001 highly significant (\*\*\*); <0.0001 extremely significant, n.s. = not significant (≥0.05).

### Study approval

The local ethic committee (Justus-Liebig-University Giessen) approved the cooperative study (ethical vote IDs 66–08 and 74–05). All patients gave written informed consent prior to inclusion in the study.

## Results

### Primary human synovial fibroblasts are susceptible and permissive to CHIKV and MAYV infection

First, we examined the ability of primary human synovial fibroblasts to support the entire CHIKV and MAYV replication cycle. Therefore, we infected synovial fibroblasts obtained from osteoarthritic patients (OASF) and from patients with a non-arthritis background (HSF) with CHIKV strain LR2006-OPY or MAYV strain TRVL7546 expressing EGFP under the control of a second subgenomic promoter. 24 h post-infection, the proportion of EGFP-positive cells

ranged between 4% and 24.5% for CHIKV and between 8.5 and 39% for MAYV and did not differ between fibroblast types (Figure 1(A)). At the same time point, supernatants of both OASF and HSF displayed CHIKV titers of  $1.6\text{--}8.8 \times 10^5$  infectious particles per ml and MAYV titers of  $0.12\text{--}2.75 \times 10^5$  infection particles per ml, with significantly higher titers produced by OASF. At 48 h post-infection, CHIKV titers produced by HSF did not further increase, whereas the titers produced by OASF reached up to  $1.5 \times 10^7$  infectious particles per ml (Figure 1(B), left panel), suggesting slightly higher virus production and/or viral spread in OASF as compared to HSF. MAYV titers did not significantly increase in OASF or HSF at 48 h post-infection (Figure 1(B), right panel).

Susceptibility of cells to CHIKV infection is enhanced by the attachment factor MXRA8 [8] and the cytosolic protein FHL-1 is essential for CHIKV genome replication [9]. We confirmed expression of these two cellular cofactors in OASF and HSF by immunoblotting and/or immunofluorescence (Figure 1(C)). We assessed the functional relevance of the MXRA8 attachment factor using a soluble MXRA8-Fc fusion protein, which blocks the binding site on the E1-E2 glycoprotein complex on the virus surface [8]. At a low MOI, MXRA8-Fc-preincubated CHIKV was 50% less infectious to synovial fibroblasts, and this inhibition was abolished when saturating amounts of infectious virus particles were used (Figure 1(D)), indicating that endogenous MXRA8 contributes, at least partially, to CHIKV entry in OASF.

Subsequently, we investigated whether IL-1 $\beta$ -mediated activation of synovial fibroblasts, a hallmark of rheumatoid arthritis [28], modulates their susceptibility to CHIKV infection. Treatment with IL-1 $\beta$  did not alter the percentage of EGFP-positive cells upon CHIKV challenge (Figure S1A), while readily inducing IL-6 secretion (Figure 1(E)). Conversely, CHIKV infection induced only low IL-6 secretion and mildly, if at all, enhanced IL-1 $\beta$ -induced IL-6 secretion (Figure 1(E)). Overall, these data suggest that IL-6 secretion is not driven by the infection in a direct manner, but may be enhanced through external stimuli.

To determine the importance of IFN-mediated antiviral immunity in this primary cell system, we analysed the secretion of type I IFN upon CHIKV and MAYV infection, which was detectable in cultures infected with CHIKV and MAYV at an MOI of 10, while detectable IFN secretion was mostly absent in cultures infected at an MOI of 1 (Figure S1B). Additionally, we monitored efficiency of CHIKV and MAYV infection in the absence or presence of the JAK/STAT inhibitor Ruxolitinib. Infection efficiency was increased 1.3–4.7-fold and 1.3–7.7-fold in infected, Ruxolitinib-treated cells at 24 and 48 h post-infection, respectively, as compared to mock-treated, infected cultures (Figure 1



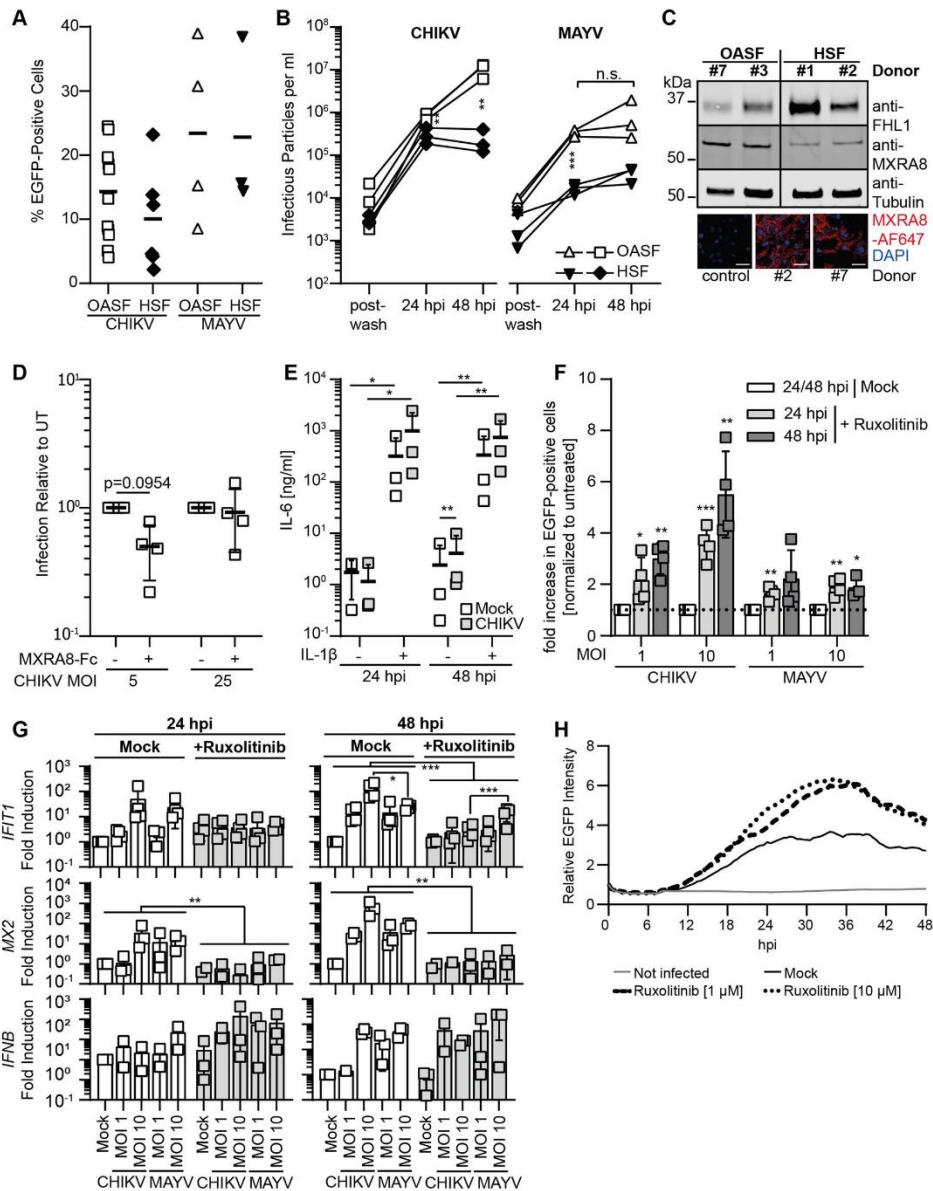


**Figure 1.** Primary human synovial fibroblasts are susceptible and permissive to CHIKV and MAYV infection. **(A)** OASF or HSF were infected with 5'EGFP-CHIKV or -MAYV (MOI 10). 24 h post-infection, the percentage of EGFP-positive cells was quantified by flow cytometry ( $n = 3-12$ ). **(B)** Supernatants of CHIKV- and MAYV-infected OASF or HSF were collected at 24 and 48 h post-infection, and titers were determined by analysing EGFP expression at 24 h post-infection of HEK293 T cells ( $n = 3$ ). **(C)** Uninfected OASF and HSF were analysed for MXRA8 and FHL1 expression by immunoblotting ( $n = 4-6$ ) and for MXRA8 expression by immunofluorescence. Scale bar = 50  $\mu\text{m}$  ( $n = 3$ , representative images shown). **(D)** OASF were infected with 5'EGFP-CHIKV at the indicated MOIs upon treatment of the virus with MXRA8-Fc recombinant protein or mock treatment. At 24 h post-infection, cells were analysed for EGFP expression ( $n = 4$ ). **(E)** OASF were stimulated with IL-1 $\beta$  at 10 ng/ml for 16 h and subsequently infected with CHIKV (MOI 10) in the presence of IL-1 $\beta$ . At 24 and 48 h post-infection supernatant was collected and analysed for IL-6 secretion by ELISA ( $n = 3$ ). **(F)** OASF were infected with 5'EGFP-CHIKV or -MAYV at the indicated MOIs in the presence or absence of 10  $\mu\text{M}$  Ruxolitinib. At 24 and 48 h post-infection, cells were analysed for EGFP expression and **(G)** for the expression of *IFIT1*, *MX2*, and *IFNB* mRNA. Raw data of EGFP expression is plotted in Fig. S1C. The dotted line in (F) indicates the relative level of EGFP-positive cells (set to 1) in mock-treated, individually infected cell cultures. **(H)** OASF were infected with 5'EGFP-CHIKV (MOI 10) in the presence or absence of 1 or 10  $\mu\text{M}$  Ruxolitinib or mock-infected. Images were analysed for EGFP intensity using ImageJ ( $n = 3$ ). Statistical analysis was performed for A, B, D, and E using two-sided, unpaired t-tests, for F and G using ratio paired t-test with assumed equal standard deviation.

(F), Figure S1C). In line with the enhanced infection efficiency, ISG expression was dampened in Ruxolitinib-treated cells, with a significant reduction of *IFIT1* expression at 48 h post-infection and a complete suppression of induction of the IFN-dependent gene *MX2* at both time points (Figure 1(G)). Interestingly, MAYV infection was only mildly enhanced by Ruxolitinib treatment (Figure 1(F)), potentially due to a higher base-line infection rate (Figure S1C) and a stronger JAK/STAT-independent induction of *IFIT1* by MAYV infection (Figure 1(G)). Using live-cell imaging, we documented the increase in EGFP-positive, CHIKV-infected cells between ten and 48 h post-infection, which progressed faster in Ruxolitinib-treated cultures, with an onset of cytopathic effects observed after 24 h in all infected cultures (Figure S1D, Suppl. Mov. 1). Analysis of the EGFP intensity in each frame over time confirmed the higher expression of EGFP in Ruxolitinib-treated cultures (Figure 1(H), Suppl. Mov. 2). Overall, these experiments establish the susceptibility and permissiveness of synovial fibroblasts to CHIKV and MAYV infection and their expression of important cellular cofactors. Furthermore, we show that the restriction of infection in this system is, to a large extent, dependent on JAK/STAT-mediated IFN signalling and secretion, and demonstrate an absence of interconnection between IL1- $\beta$  activation and susceptibility to CHIKV infection.

#### **CHIKV infection provokes a strong cell-intrinsic immune response in synovial fibroblasts**

Next, we performed RNA-seq analysis on OASF and HSF that had been infected with CHIKV in the presence or absence of the glycoprotein E2-binding, neutralizing antibody C9 [29], and on mock-infected cells. C9 pre-treatment resulted in potent inhibition of the infection by on average 16-fold (Figure 2(A)). Upon infection, expression of numerous IFN-stimulated genes (ISGs) was induced at the protein level in a C9 treatment-sensitive manner, including *IFITM3*, *ISG15*, and *MX2*. As expected, production of the viral E1-E2 and capsid proteins was detectable specifically in CHIKV-infected, but not in cells exposed to C9-pre-treated virus (Figure 2(B)). Global transcriptional profiling by RNA-seq revealed 992 (OASF) and 1221 (HSF) upregulated genes as well as 99 (OASF) and 353 (HSF) downregulated genes in CHIKV-infected cells 24 h post-infection as compared to uninfected cells (Figure 2(C)). Uninfected cells and cells exposed to C9-treated virus shared a similar profile (data not shown). A high similarity of the gene expression profile of uninfected OASF and HSF ( $R^2 = 0.9086$ ) argues against a potential transcriptional predisposition that could have exerted a rheumatoid arthritis-related gene expression profile or a broad proinflammatory activation (Figure S2A). Uninfected OASF and HSF

differed in genes involved in organ development and cellular regulatory processes, and not inflammatory or antiviral processes (Figure S2B). Additionally, the transcriptional profile in infected OASF and HSF was very similar ( $R^2 = 0.9085$ , Figure S2C-D), with an equivalently strong upregulation of a set of prototypic inflammation and arthritis-related genes which we defined for further analysis ( $R^2 = 0.8202$ , Figure 2(D)). Interestingly, the number of genes significantly up- and down-regulated upon infection was 1.23-fold and 3.57-fold higher in HSF compared to OASF, respectively, but 55.4% of upregulated genes from both groups overlapped (Figure 2(E)). Most of the prototypic antiviral and proinflammatory genes were highly upregulated in infected cultures, demonstrating a broad and strong activation of antiviral immune responses in cells from four different donors with no statistically significant deviation in the magnitude of induction (Figure 2(F), left panel). Upregulation of *IFNB* and *IFNL1*, *IFNL2*, and *IFNL3* expression was statistically significant but low in magnitude, with almost no *IFNA* mRNA detectable. Expression of arthritis-associated genes, including genes encoding immune cell chemoattractants (*CXCL5*, *IL8*, *CD13*, *RANTES/CCL5*), matrix-metalloproteases (*MMP3*, *-9*, *-14*, *ADAMTS5*) and genes commonly expressed by fibroblasts in rheumatoid arthritis (*FGF2*, *PDPN*, *NGF*, *FAP*), was not grossly altered in CHIKV-infected cells. Exceptions were a strong CHIKV-induced upregulation of *RANTES/CCL5* in both OASF and HSF and *IL8* in HSF (Figure 2(F), right panel). mRNAs for all IFN receptors were detectable and stable with exception of *IFNLR1*, whose expression was upregulated upon CHIKV infection (Figure S2E). Established host factors for CHIKV as well as fibroblast marker genes and cellular housekeeping genes were not quantitatively altered in their expression. Virtual absence of expression of monocyte/macrophage lineage-specific genes excluded the possibility of a contamination of the fibroblast culture with macrophages, which occasionally has been reported in early passages of *ex vivo*-cultured synovial fibroblasts [22] (Figure S2E). Conclusively, OASF and HSF share similar basal and CHIKV infection-induced transcriptional profiles. Overall, CHIKV-infected synovial fibroblasts react to CHIKV infection by extensive upregulation of antiviral and proinflammatory ISGs. IFN expression itself was low at 24 h post-infection, not excluding the possibility that it peaked transiently at earlier time points.

#### **The CHIKV genome replicates to a high degree with a bias towards the structural subgenome**

We noticed very little inter-donor variation regarding the distribution of identified viral reads along the viral genome. The 5' region of the genome, encoding the non-structural CHIKV proteins, replicated to a

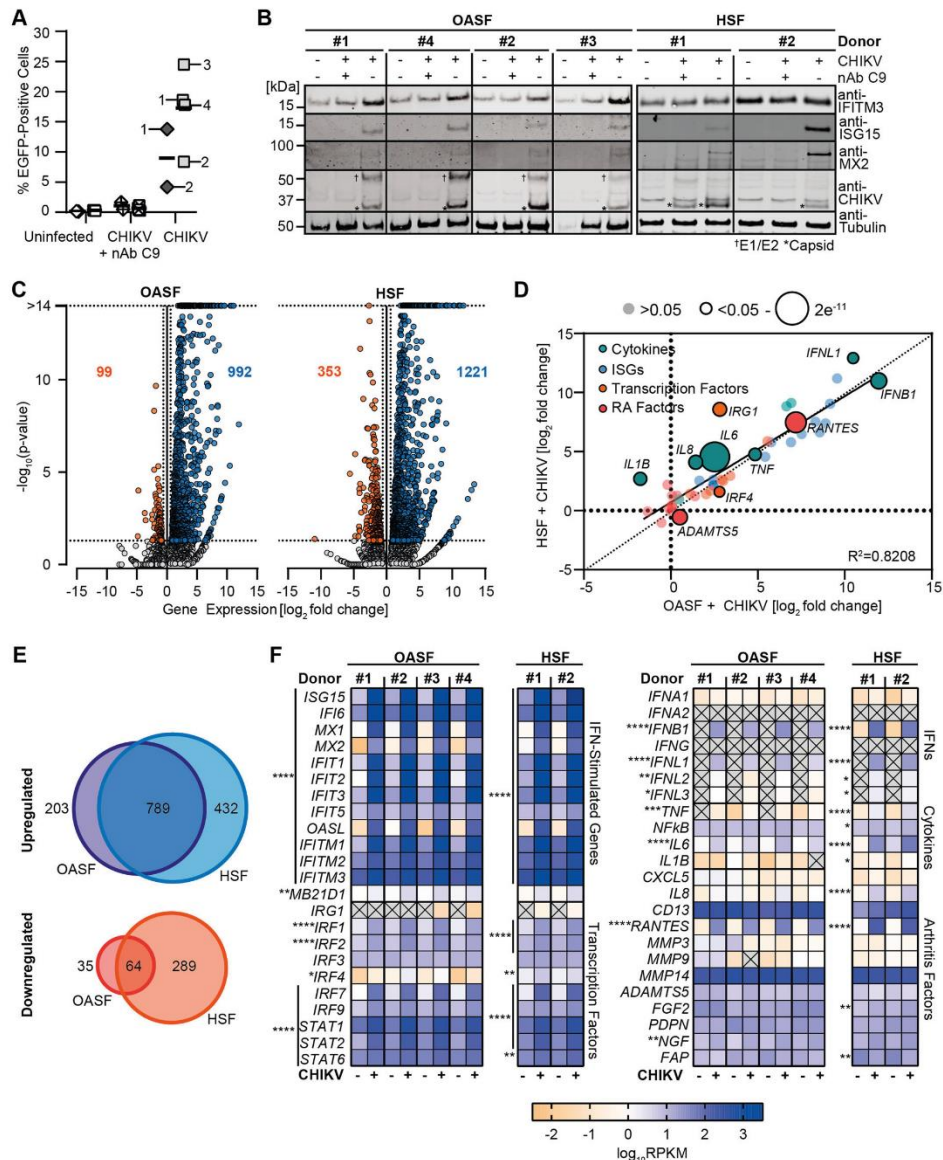


**Figure 2.** CHIKV infection provokes a strong cell-intrinsic immune response in synovial fibroblasts. **(A)** OASF were infected with 5'EGFP-CHIKV at an MOI of 10 in the presence or absence of the anti-E2 antibody C9 and the percentage of EGFP-positive cells was measured by flow cytometry (OASF: squares,  $n = 4$ ; HSF: diamonds,  $n = 2$ ). The infected samples are marked with their respective donor number. **(B)** Selected proteins of cells infected in A were analysed by immunoblotting ( $n = 4$ ). **(C-F)** RNA from cells infected in A was extracted and subjected to RNA-seq ( $n = 4$ ). Differentially expressed genes were identified by comparison of raw count data, with calculation of false-discovery rate (FDR)  $p$ -value for multiple comparisons. **(C)** Analysis of up- and downregulated genes in CHIKV-infected samples compared to mock. Dotted lines indicate cutoff for  $<1.5$  fold regulation and a  $p$ -value of  $>0.05$ . **(D)** Visualization of the fold change induction of indicated genes in CHIKV-infected OASF and HSF. Average fold change ( $\log_2$ ) values for infected OASF are plotted on the x-axis, with corresponding values from infected HSF plotted on the y-axis.  $R^2$  value and regression line for the comparison are inset, dot sizes indicate significance. **(E)** Overlap of significantly (FDR- $p < 0.05$ ) up- and downregulated genes in infected OASF and HSF. Numbers of genes up- or downregulated in either OASF or HSF only, or in both cell-types, are indicated. **(F)** Heatmaps of selected gene expression profiles related to innate immune responses (left) or to secreted proinflammatory mediators and arthritis-connected genes (right) in uninfected or CHIKV-infected cells.

lower extent than the 3', 26S subgenomic promoter-driven, structural protein-encoding genomic region. Interestingly, this differential abundance of 5' and 3' reads was also detected in cultures inoculated with C9-neutralized virus, suggesting infection of a small number of cells (Figure 3(A)). Overall, the 26S subgenomic viral RNA was 5.3-fold more abundant than nonstructural subgenomes (Figure 3(B)). 18–54% and 17–44% of the total reads in productively infected OASF and HSF, respectively, were attributed to the CHIKV genome (Figure 3(C,D)). In summary, our analysis revealed efficient replication of the CHIKV genome in infected fibroblasts with an excess of structural protein-encoding subgenomic RNA.

**Exogenous IFN administration provokes higher immune responses and leads to improved protection from infection in primary fibroblasts than in commonly used cell lines**

CHIKV and MAYV infection rates in OASF did not increase after 24 h post-infection (Figure 4(A)), and we suspected this to be the result of the strong immune activation and subsequent IFN signalling. The commonly used osteosarcoma cell line U2OS was more susceptible, while the immortalized fibroblast cell line HFF-1 displayed reduced susceptibility to alphaviral infection (Figure 4(A)). OASF exhibited strong induction of *IFIT1* and *MX2* CHIKV infection, which exceeded those mounted by U2OS and HFF-1 cells at both 24 and 48 h post-infection by 15- to 150-fold. MAYV infection-provoked ISG responses in OASF were inferior to those induced by CHIKV, despite similar percentages of infected cells (Figure 4(B)). Contrasting the cell system-specific magnitude of gene expression upon CHIKV infection, both OASF and cell lines shared similar responsiveness to 5'-triphosphate dsRNA (5'-ppp-RNA) transfection, which exclusively stimulates the RNA sensor RIG-I [30], the main sensor of CHIKV RNA in infected cells [31], and plasmid DNA transfection (Figure S3A).

Next, we tested the cells' ability to respond to exogenous type I and III IFNs, which play a crucial role in limiting virus infection and protecting the host [32,33]. We stimulated OASF individually with a range of IFN- $\alpha$ 2 and - $\lambda$  concentrations at 48 h prior to infection. At all investigated concentrations, even at the lowest dose, IFN- $\alpha$  induced a potent upregulation of *IFIT1* and *MX2* (Figure S3B), and almost completely inhibited CHIKV infection (Figure 4(C)). In contrast, IFN- $\lambda$  induced lower ISG expression levels (Figure S3B), and inhibited infection less efficiently (Figure 4(C)). Although less effective than in OASF, IFN- $\alpha$  restricted CHIKV infection both in U2OS and HFF-1 cells, while IFN- $\lambda$  pre-treatment was more potent in U2OS cells than in OASF, and ineffective in HFF-1 cells (Figure 4(C)). These antiviral activities

were largely consistent with the respective degree of ISG expression at the time point of infection (Figure S3B). IFN- $\alpha$  and - $\lambda$  induced expression of *IFIT1* and *MX2* was higher in U2OS cells than in HFF-1. We next investigated the sensitivity of CHIKV infection to IFN when applied four hours post-infection. In this set-up, IFN- $\alpha$  still displayed a clear, though less potent antiviral activity when compared to the pre-treatment setting (Figure 4(D)). In contrast, treatment of both immortalized cell lines with IFN- $\alpha$  post-infection was very ineffective (Figure 4(D)).

Interestingly, in all three cells systems, a preceding CHIKV infection did not antagonize IFN-mediated induction of ISGs, and led to expression levels of *IFIT1* and *MX2* exceeding those induced by IFN- $\alpha$  alone (Figure S3C). Overall, the data suggest a stronger sensitivity of OASF to IFN- $\alpha$ -induced immunity compared to commonly used immortalized cell lines. Most interestingly, and in striking contrast to the immortalized cell lines, OASF were unique in their ability to transform a post-infection treatment of IFN- $\alpha$  into a relatively potent antiviral programme. Collectively, these data uncover crucial differences between primary synovial fibroblasts and widely used immortalized cell lines regarding their cell-intrinsic innate response to infection and their sensitivity to exogenous IFNs.

**Strong immune activation in EGFP protein-negative and viral RNA-low cells**

Finally, we asked how the cell-intrinsic defenses correlate with the infection status within individual cells of a given infected culture by analysing virus-exposed OASF for their expression of antiviral proteins using flow cytometry. As expected, expression of *IFIT1*, *IFITM3* and *MX1/2* was enhanced in OASF upon IFN- $\alpha$  treatment (Figure 5(A)). Interestingly, these proteins were expressed at even higher levels in EGFP-negative cells of CHIKV-infected cultures, while the productively infected, EGFP-positive cells displayed markedly reduced expression levels of these factors (Figure 5(A)).

Since absence of EGFP expression does not necessarily exclude the presence of viral, potentially abortive RNA, we performed virus-inclusive single-cell RNA-seq to establish potential correlations of the quantity of viral RNA and a specific cellular transcriptional profile. To this end, we analysed OASF infected at escalating MOIs. No EGFP-positive cells were detectable at six hours post-infection by flow cytometry (Figure 5(B), left panel). In contrast, 24 h post-infection, the reporter was expressed in an MOI-dependent fashion, ranging from virtually 0% to 15% (Figure 5(B), left panel). *IFIT1* and *MX2* mRNA expression was largely proportional to EGFP expression (Figure 5(B), right panel).

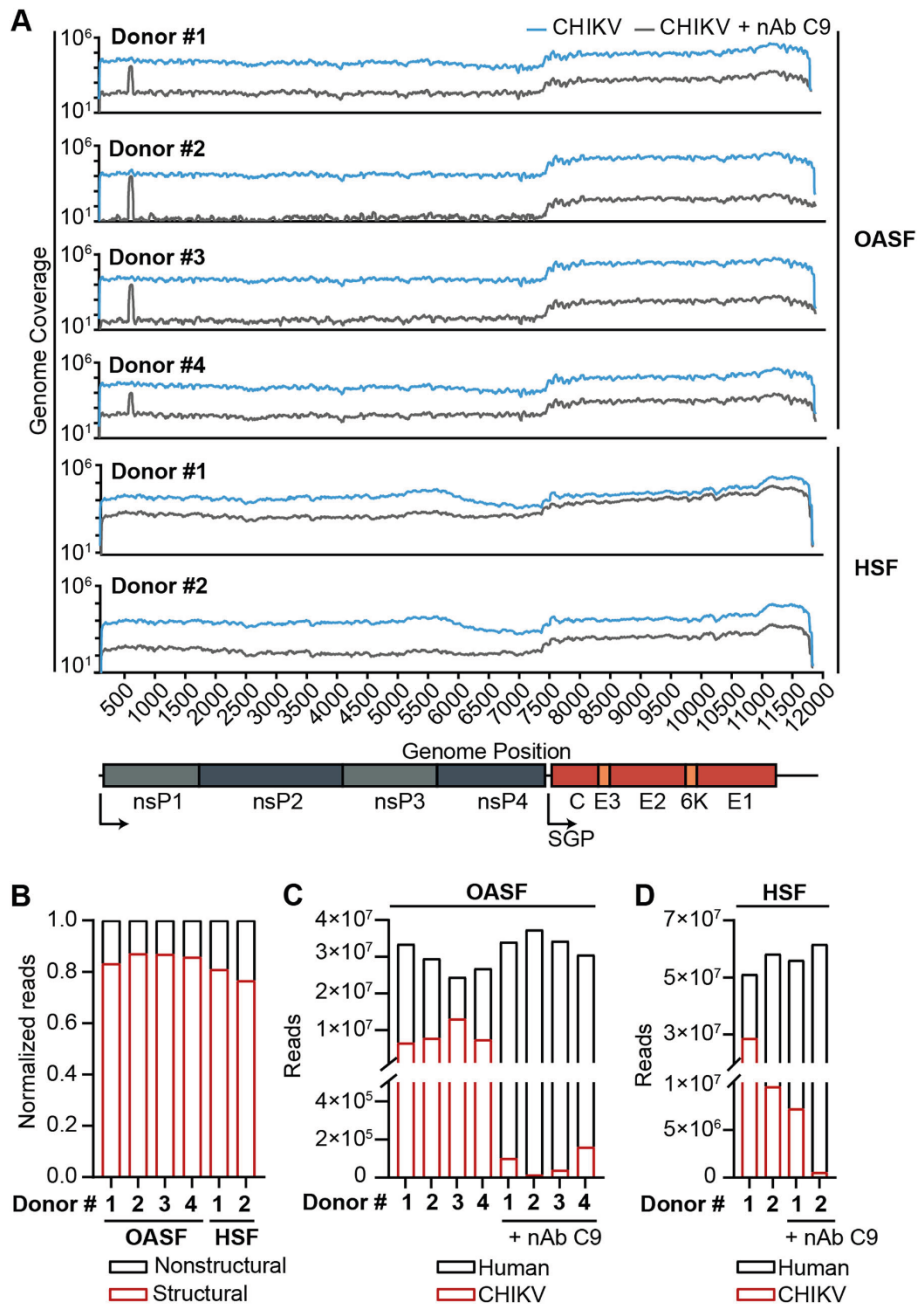


**Figure 3.** The CHIKV genome replicates to a high degree with a bias towards the structural subgenome. (A) NGS reads attributed to each individual position in the CHIKV genome plotted for synovial fibroblasts infected with CHIKV in the presence or absence of neutralizing antibody (nAb). SGP: subgenomic promoter. (B) Normalized amount of reads attributed to the structural and non-structural part of the CHIKV genome in CHIKV-infected OASF and HSF. (C) Number of NGS reads attributed to the human or CHIKV reference genome in CHIKV or neutralizing antibody-treated CHIKV infected OASF or (D) HSF ( $n = 4$ ).

Single-cell (sc) RNA-seq of the very same cells showed very little inter-donor variability, and we merged data from both donors throughout the rest

of the analysis (Figure 5(C)). In order to identify potential correlations of viral RNA abundance and the cellular transcription profile, we compared the

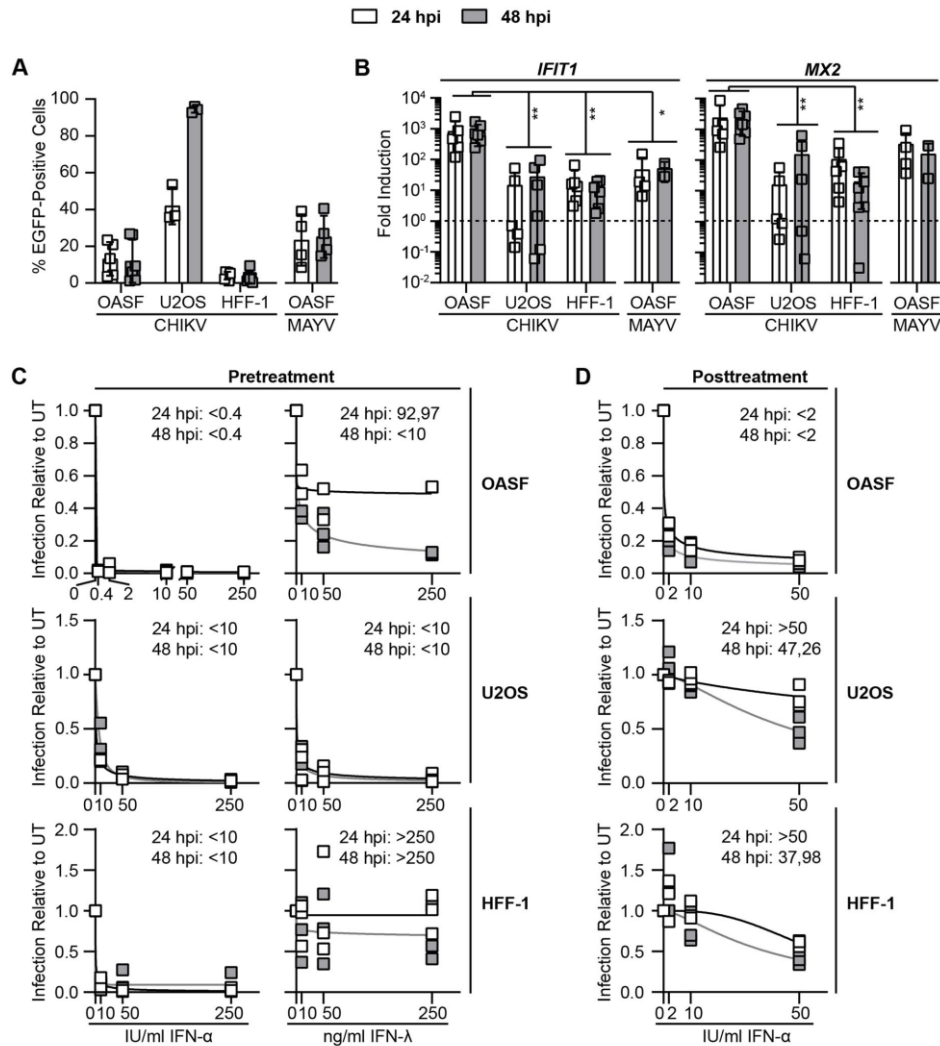


**Figure 4.** Exogenous IFN administration provokes higher immune responses and leads to improved protection from infection in primary fibroblasts than in commonly used cell lines. **(A)** OASF and HFF-1 cells were infected with 5'EGFP-CHIKV at an MOI of 10, U2OS cells were infected at an MOI of 0.5. EGFP-positive cells were quantified at 24 and 48 h post-infection by flow cytometry ( $n = 3-6$ ). **(B)** Cells infected in (A) were analysed for expression of *IFIT1* and *MX2* mRNA at 24 and 48 h post-infection by quantitative RT-PCR ( $n = 3-6$ ). Statistical analysis between samples of the same time point was performed using Mann-Whitney tests. **(C)** Cells were treated with IFN- $\alpha$  or - $\lambda$  for 48 h before infection with 5'EGFP-CHIKV (OASF and HFF-1: MOI 10; U2OS: MOI 0.5) in the continuous presence of IFN. Inset numbers indicate IC<sub>50</sub> values for each time point. **(D)** Cells were infected with 5'EGFP CHIKV (OASF and HFF-1: MOI 10; U2OS: MOI 0.5) and IFN- $\alpha$  was added four hours post-infection. 24 and 48 h post-infection, EGFP-positive cells were quantified by flow cytometry. Inset numbers indicate IC<sub>50</sub> values for each time point. UT: untreated, IU: international units ( $n = 3$  for all experiments). For C and D, nonlinear fit curves with variable slopes for IC<sub>50</sub> calculation were used.

expression of CHIKV RNA to expression of 203 IFN signalling genes listed in the REACTOME database (identifier R-HSA-913531, Table 1). For each cell, the expression of this collection of genes was summarized using Seurat's AddModuleScore function. Briefly, this summarizes the expression of a select group of genes by normalizing the aggregate expression to a randomly selected, non-overlapping

subset of genes and scores each cell based on its expression of genes in this module, creating a module score (IFN Module Score, IMS). 24 h post-infection, most identified CHIKV reads corresponded to the 3' end of the genome, along with a minor number of reads mapping to the 3' end of *EGFP*, which is expressed as a subgenomic RNA in infected cells (Figure S4A). As expected for mock-infected cells,

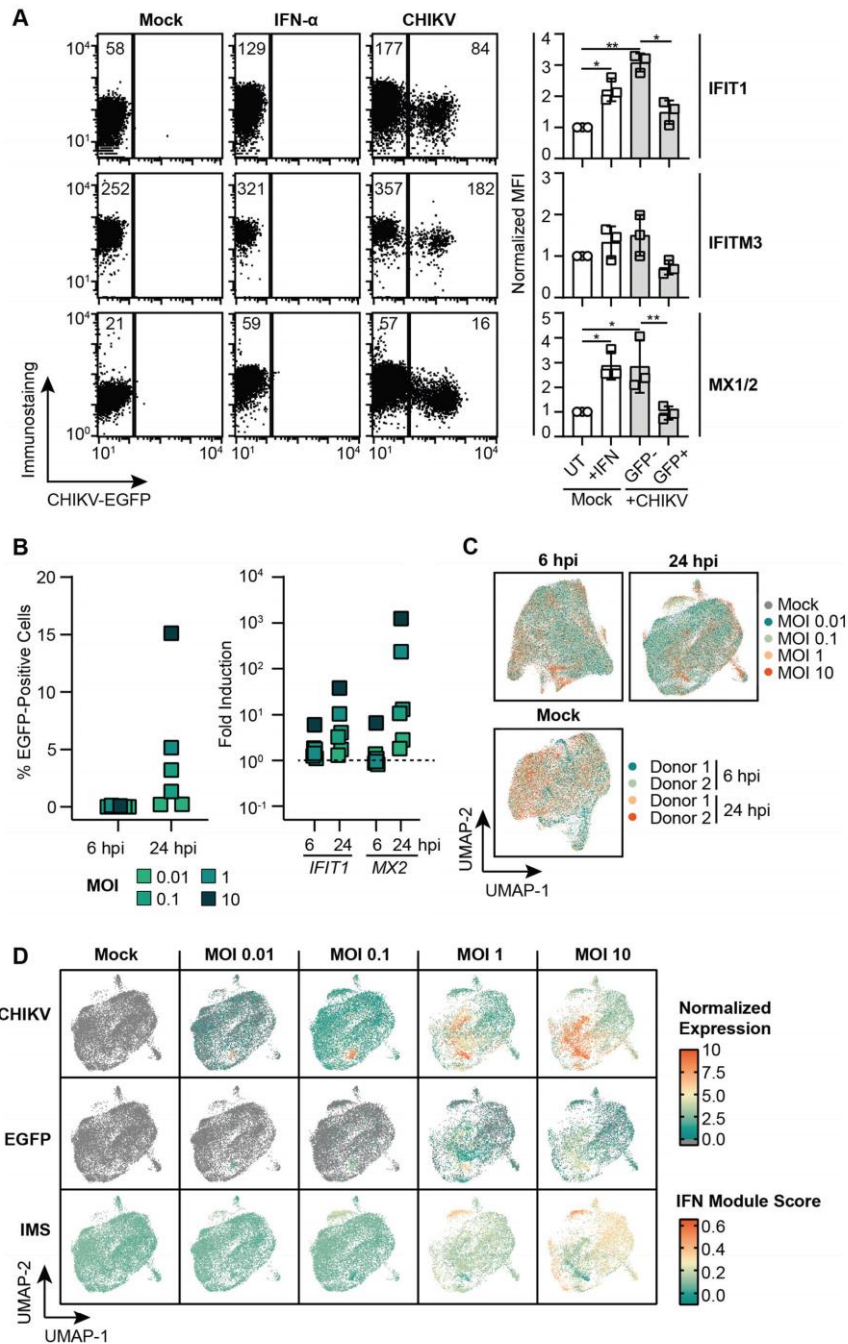


**Figure 5.** Strong immune activation in EGFP protein-negative and viral RNA-low cells. **(A)** OASF were infected with 5'EGFP-CHIKV (MOI 10) or treated with 100 IU/ml IFN- $\alpha$  and immunostained for IFIT1, IFITM3, and MX1/2 24 h post-infection. Numbers in the dot plots indicate mean fluorescence intensities (MFI) of one representative experiment, and the bar diagram shows quantification of three individual experiments with statistical analysis by two-sided unpaired t-tests with assumed equal standard deviation ( $n = 3$ ). **(B)** OASF were infected with 5'EGFP-CHIKV at indicated MOIs. Six and 24 h post-infection, EGFP-positive cells were quantified by flow cytometry (left panel), and cells were analysed for expression of *IFIT1* and *MX2* mRNA (right panel,  $n = 6$ ). **(C)** Using OASF infected with 5'EGFP-CHIKV, single-cell RNA-sequencing was conducted and UMAP visualizations for sample overlapping after integration are shown ( $n = 2$ ). **(D)** UMAP projections from infected OASF (24 h post-infection) indicate the abundance of CHIKV 3' end reads, EGFP 3' end reads, and IFN signalling gene expression as calculated by IMS ( $n = 2$ ).

CHIKV reads were undetectable, and IFN signalling genes were expressed at basal levels, as calculated by the IMS. CHIKV RNA abundance per cell increased in an MOI-dependent manner, however susceptibility to infection was unequally distributed over individual cells, and a subset of cells displayed a higher susceptibility than others, as reflected by a high percentage of reads attributed to the viral genome (Figure S4B). Strikingly, IFN signalling genes appeared to be induced predominantly in cells displaying low CHIKV gene expression. *Vice versa*, clearly CHIKV RNA-positive cells maintained basal or reduced expression of IFN signalling related genes (Figure 5(D)). Of note, six hours post-infection, CHIKV expression was low and antiviral responses as presented by the IMS were largely absent at low MOIs, while individual ISGs were induced at higher MOIs (Figure S4C-D). As opposed to the induction of IFN signalling genes, known CHIKV cofactors *MXRA8*, *FHL1*, and the fibroblast marker genes *VIM* and *COL3A1* were broadly and stably expressed under all experimental conditions. Surprisingly, *FURIN*, encoding the cellular protease considered important for viral polyprotein cleavage, was detectable only in a minority of cells (Figure S5).

#### Correlation analysis of viral and cellular gene expression reveals a switch from induction to suppression of transcription factor and ISG expression

In order to quantify expression of IFN signalling genes according to viral RNA abundance, we divided cells into three groups: cells without detectable viral RNA expression (bystander), cells displaying low amounts of viral RNA (low) and cells displaying high levels of viral RNA (high) (Figure 6(A)). Mirroring our initial observations (Figure 5), we detected a significantly lower IMS in high cells when compared to low or bystander cells of the identical culture (Figure S6A). Six hours post-infection, differential expression of non-ISGs was very modest between bystander and viral RNA-positive cells, while it was more pronounced 24 h post-infection (Figure S6B). In contrast, over 250 ISGs, including *ISG15*, *IFIT1*, *MX2*, *IFITM3*, *MX1*, and *IFI6*, were upregulated in viral RNA-positive cells as compared to bystander cells at both investigated time points. Individual comparisons of either low or high cells with bystander cells gave similar overall observations. However, at both investigated time points, no further upregulation of ISGs was detected in the high cells as compared to low cells, but rather a significant downregulation of three ISGs at 24 h post-infection and six ISGs at six hours post-infection. This suggests either a loss of cellular transcription activity or a lowered stability of cellular

**Table 1.** Interferon signalling genes identified by the REACTOME database.

<i>AAAS</i>	<i>HLA-DQA1</i>	<i>IFNGR1</i>	<i>NUP37</i>	<i>STAT1</i>
<i>ABCE1</i>	<i>HLA-DQA2</i>	<i>IFNGR2</i>	<i>NUP42</i>	<i>STAT2</i>
<i>ADAR</i>	<i>HLA-DQB1</i>	<i>IP6K2</i>	<i>NUP43</i>	<i>SUMO1</i>
<i>ARIH1</i>	<i>HLA-DQB2</i>	<i>IRF1</i>	<i>NUP50</i>	<i>TPR</i>
<i>B2M</i>	<i>HLA-DRA</i>	<i>IRF2</i>	<i>NUP54</i>	<i>TRIM10</i>
<i>BST2</i>	<i>HLA-DRB1</i>	<i>IRF3</i>	<i>NUP58</i>	<i>TRIM14</i>
<i>CAMK2A</i>	<i>HLA-DRB3</i>	<i>IRF4</i>	<i>NUP62</i>	<i>TRIM17</i>
<i>CAMK2B</i>	<i>HLA-DRB4</i>	<i>IRF5</i>	<i>NUP85</i>	<i>TRIM2</i>
<i>CAMK2D</i>	<i>HLA-DRB5</i>	<i>IRF6</i>	<i>NUP88</i>	<i>TRIM21</i>
<i>CAMK2G</i>	<i>HLA-E</i>	<i>IRF7</i>	<i>NUP93</i>	<i>TRIM22</i>
<i>CD44</i>	<i>HLA-F</i>	<i>IRF8</i>	<i>NUP98</i>	<i>TRIM25</i>
<i>CIITA</i>	<i>HLA-G</i>	<i>IRF9</i>	<i>OAS1</i>	<i>TRIM26</i>
<i>DDX58</i>	<i>HLA-H</i>	<i>ISG15</i>	<i>OAS2</i>	<i>TRIM29</i>
<i>EGR1</i>	<i>ICAM1</i>	<i>ISG20</i>	<i>OAS3</i>	<i>TRIM3</i>
<i>EIF2AK2</i>	<i>IFI27</i>	<i>JAK1</i>	<i>OASL</i>	<i>TRIM31</i>
<i>EIF4A1</i>	<i>IFI30</i>	<i>JAK2</i>	<i>PDE12</i>	<i>TRIM34</i>
<i>EIF4A2</i>	<i>IFI35</i>	<i>KPNA1</i>	<i>PIA51</i>	<i>TRIM35</i>
<i>EIF4A3</i>	<i>IFI6</i>	<i>KPNA2</i>	<i>PIN1</i>	<i>TRIM38</i>
<i>EIF4E</i>	<i>IFIT1</i>	<i>KPNA3</i>	<i>PLCG1</i>	<i>TRIM45</i>
<i>EIF4E2</i>	<i>IFIT2</i>	<i>KPNA4</i>	<i>PML</i>	<i>TRIM46</i>
<i>EIF4E3</i>	<i>IFIT3</i>	<i>KPNA5</i>	<i>POM121</i>	<i>TRIM48</i>
<i>EIF4G1</i>	<i>IFITM1</i>	<i>KPNA7</i>	<i>POM121C</i>	<i>TRIM5</i>
<i>EIF4G2</i>	<i>IFITM2</i>	<i>KPNB1</i>	<i>PPM1B</i>	<i>TRIM6</i>
<i>EIF4G3</i>	<i>IFITM3</i>	<i>MAPK3</i>	<i>PRKCD</i>	<i>TRIM62</i>
<i>FCGR1A</i>	<i>IFNA1</i>	<i>MID1</i>	<i>PSMB8</i>	<i>TRIM68</i>
<i>FCGR1B</i>	<i>IFNA10</i>	<i>MT2A</i>	<i>PTAFR</i>	<i>TRIM8</i>
<i>FLNA</i>	<i>IFNA13</i>	<i>MX1</i>	<i>PTPN1</i>	<i>TYK2</i>
<i>FLNB</i>	<i>IFNA14</i>	<i>MX2</i>	<i>PTPN11</i>	<i>UBA52</i>
<i>GBP1</i>	<i>IFNA16</i>	<i>NCAM1</i>	<i>PTPN2</i>	<i>UBA7</i>
<i>GBP2</i>	<i>IFNA17</i>	<i>NDC1</i>	<i>PTPN6</i>	<i>UBB</i>
<i>GBP3</i>	<i>IFNA2</i>	<i>NEDD4</i>	<i>RAE1</i>	<i>UBC</i>
<i>GBP4</i>	<i>IFNA21</i>	<i>NUP107</i>	<i>RANBP2</i>	<i>UBE2E1</i>
<i>GBP5</i>	<i>IFNA4</i>	<i>NUP133</i>	<i>RNASEL</i>	<i>UBE2L6</i>
<i>GBP6</i>	<i>IFNA5</i>	<i>NUP153</i>	<i>RPS27A</i>	<i>UBE2N</i>
<i>GBP7</i>	<i>IFNA6</i>	<i>NUP155</i>	<i>RSAD2</i>	<i>USP18</i>
<i>HERC5</i>	<i>IFNA7</i>	<i>NUP160</i>	<i>SAMHD1</i>	<i>USP41</i>
<i>HLA-A</i>	<i>IFNA8</i>	<i>NUP188</i>	<i>SEC13</i>	<i>VCAM1</i>
<i>HLA-B</i>	<i>IFNAR1</i>	<i>NUP205</i>	<i>SEH1L</i>	<i>XAF1</i>
<i>HLA-C</i>	<i>IFNAR2</i>	<i>NUP210</i>	<i>SOC51</i>	
<i>HLA-DPA1</i>	<i>IFNB1</i>	<i>NUP214</i>	<i>SOC53</i>	
<i>HLA-DPB1</i>	<i>IFNG</i>	<i>NUP35</i>	<i>SP100</i>	

RNA in cells containing high loads of CHIKV RNA (Figure S6B).

To increase resolution, we calculated the average CHIKV and EGFP RNA expression and the average IMS in bins of 1000 cells for a total of 36 bins, sorted by their expression level of CHIKV RNA. At both time points, while the first 7–10 bins represented cells expressing no or virtually no CHIKV RNA, the following 18–21 bins represented cells displaying (according to the cut-off defined in Figure 6 (A)) low, but gradually increasing levels of CHIKV RNA, and largely undetectable EGFP RNA. We considered the latter cells to represent unproductively infected cells due to their lack of subgenomic transcripts. The last eight bins displayed cells with overall high, starkly increasing levels of CHIKV RNA and with significant levels of EGFP mRNA. We hypothesize that these cells represent productively infected cells. Strikingly, in unproductively infected cells, IMS values increased proportionally to the abundance of viral RNA per cell, whereas in productively infected cells, an inverse proportionality was observed (Figure 6(B)). This dataset suggests that expression of IFN signalling genes is upregulated



in cells harbouring low-to-intermediate levels of viral RNA, which, however, do not or have not yet progressed to a productive infection. In contrast, cells that exceed a certain threshold of viral RNA show a prevention or downregulation of the expression of IFN signalling genes. The analysis of expression of selected genes confirmed this observation. Expression of individual ISGs, including *ISG15*, *IFI6*, *MX1*, *OASL*, *IFITs*, and *IFITMs*, and transcription factors, including *STAT1* and *IRF7*, was low in mock-infected and bystander cells, and more pronounced in representative low cells (six hours post-infection: bin 27–29, 24 h post-infection: bin 26–28) than in high cells (bins 34–36). Furthermore, expression of genes mediating arthralgia, including as *RANTES*, *IL1B*, *IL6*, and *IL8* was lower in high cells as compared to low cells (Figure 6(C)). To identify further putative targets of viral antagonism, we correlated the expression of all 203 genes of the IMS to the viral RNA expression in infected cells at 24 h post-infection. We identified 13 genes displaying a significant positive correlation ( $r > 0.3$ ) in the low CHIKV group, and a significant negative correlation ( $r < -0.3$ ) in the high CHIKV group (*IFITM3*, *IFIT3*, *OAS1*, *XAF1*, *GBP1*, *EIF4A1*, *EIF2AK2*, *STAT1*, *GBP3*, *UBC*, *PSMB8*, *UBA52*). Strikingly, the only transcription factor present in both groups, *STAT1*, was also negatively correlated at six hours post-infection in the high viral RNA group. We additionally identified transcription factors *JAK1* and *IRF7* to switch from weak correlation in the low CHIKV group to a negative correlation in the high CHIKV group at 24 h post-infection (Figure 6 (D)). We confirmed this finding using a transcription factor activity score analysis using the DoRothEa database, which scores cells based on the activity of transcription factors inferred from the expression of the associated target genes in regulons. The regulon of *STAT1* was strongly induced in bystander and low CHIKV groups at high MOIs, yet highly susceptible to viral antagonism in the high CHIKV group. The same observation was obtained for multiple other transcription factors, including IRFs and STATs as well as NF $\kappa$ B and c-JUN, at higher MOIs, indicating a strong and sensitive induction that is counteracted in high cells (Figure 6(E)). Taken together, our analyses at single-cell resolution specifically uncovered a spectrum of cellular states, displaying a range from induced to repressed cell-intrinsic immune responses depending on a threshold abundance of viral RNA per individual cell. Efficacy of mounting innate immune responses was highest in cells displaying low-to-intermediate quantities of viral RNA. Furthermore, viral antagonism manifested itself specifically in the relatively low percentage of cells presenting efficient virus replication, consistent

with expression and functionality of virally encoded IFN antagonists.

## Discussion

Given that the joints are the primarily affected body compartments and that fibroblasts are susceptible to arthritogenic alphavirus infection in general [6,34], we hypothesized that cells of the joint synovium are directly implicated in the pathophysiology of CHIKV-induced arthralgia. Cells of the synovial tissue and synovial fluid contain CHIKV RNA and protein upon CHIKV infection *in vivo* in humans [5], experimentally infected macaques and mice [7,35]. Additionally, infectious virus was recovered from the joints of infected macaques at six days post-infection, indicating the synovium as an active replication site [7]. The main cell types composing the synovium are macrophages and fibroblasts. The latter have been identified to be susceptible to CHIKV infection *ex vivo* [8]. However, the corresponding basal innate immune state of primary synovial fibroblasts and their ability to exert IFN-mediated antiviral restriction is unknown. Here, we establish that the widely available OASF and less available HSF share susceptibility and permissiveness to CHIKV infection, and describe their basal and infection-induced transcriptional programmes. We confirmed that the two cell types share a highly similar overall transcriptional profile, except in some signalling pathways unrelated to immunity. CHIKV infection provoked a striking cellular response that involves upregulation of multiple ISGs in a JAK/STAT-dependent manner, many of them exerting antiviral activity, and rheumatoid arthritis-mediating genes. Although we did not define the PAMP(s) that trigger responses in synovial macrophages, ISG induction occurred specifically in cells containing virus genome-, but not EGFP-specific reads, indicating the absence of *de novo* synthesized subgenomic RNA and therefore suggesting that these cells represent an early or unproductive infection state. Infection by alphaviruses typically raises RIG-I-mediated responses through exposure of dsRNA intermediates and provokes mitochondrial DNA leakage that is sensed via cGAS/STING [31]. Indeed, experimental ligands of both sensors were highly reactive in OASF, as was IFN- $\alpha$  treatment. Surprisingly, also IFN- $\lambda$  pre-treatment translated into an antiviral state, indicating that synovial fibroblasts may represent an exception to the notion of otherwise IFN- $\lambda$ -nonresponsive fibroblasts [36]. Finally, CHIKV infection of synovial fibroblasts was sensitive to IFN- $\alpha$  applied after inoculation with virus. These findings appear to contrast with potent virus-mediated antagonism of IFN in U2OS and HFF-1 cell lines, which has been suggested to involve counteraction of nuclear translocation of STAT1 [12]. CHIKV was unable to suppress ISG expression upon

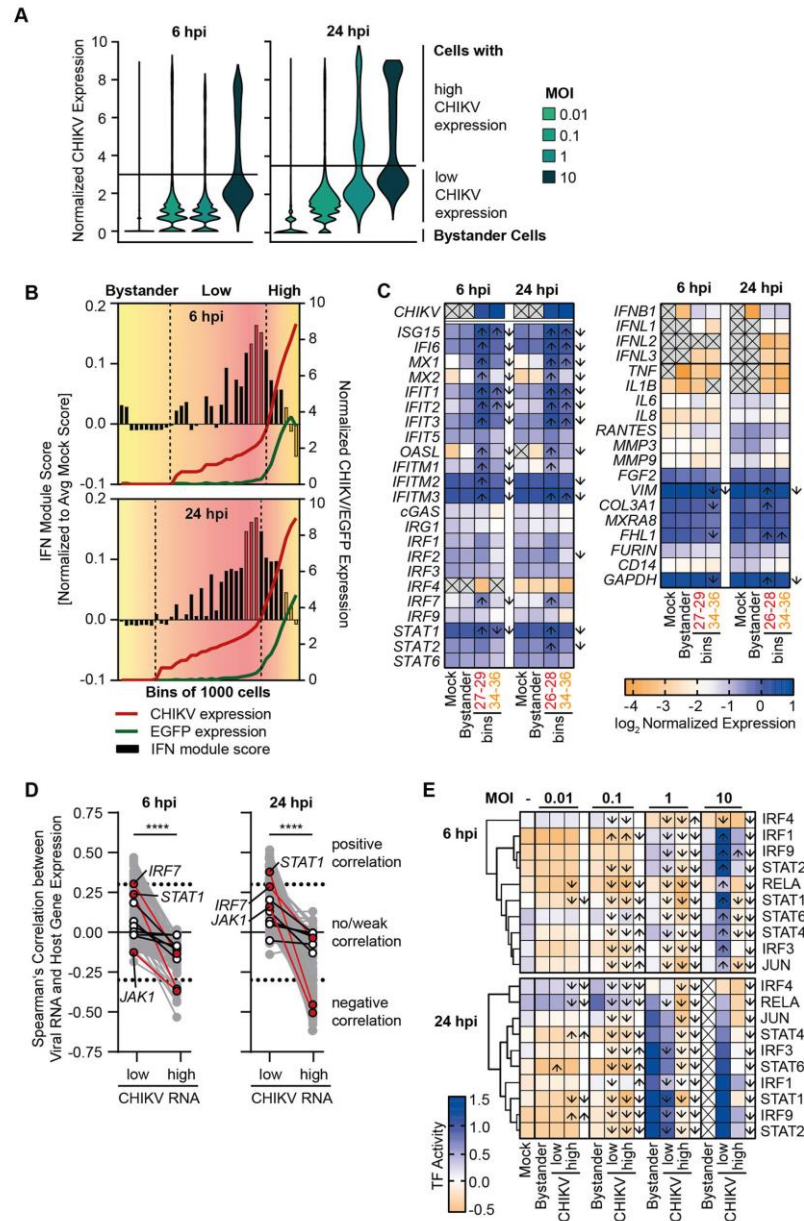


**Figure 6.** Correlation analysis of viral and cellular gene expression reveals a switch from induction to suppression of transcription factor and ISG expression. **(A)** Visualization of the viral RNA content of infected OASF from Figure 5 at six and 24 h post-infection. Line indicates the cutoff dividing cells displaying low and high content of viral RNA. Bystander cells were defined as cells with no detectable viral RNA. **(B)** Infected OASF were sorted into digital bins of 1000 cells displaying a gradual increase of the amount of viral reads per cell. Viral reads and the IMS at six and 24 h post-infection are plotted. Coloured bins indicate selected representative cells for low and high content of viral RNA. **(C)** Expression of selected genes within mock, bystander, representative low cell bins (bin 26–29) and high cell bins (bin 34–36) defined in A and B at six and 24 h post-infection. Arrows indicate a statistically significant ( $p < 0.05$ , fold change  $> 1.5$ ) up- or downregulation (depending on the arrow direction) in low or high CHIKV bins versus bystander (inside the boxes) or in high CHIKV bins versus low (next to the boxes). Differential gene expression was tested by Wilcoxon rank sum tests with applied Bonferroni correction. **(D)** Correlation of CHIKV RNA expression with expression of IFN signaling genes in high and low CHIKV RNA groups calculated by non-parametric Spearman's test. Transcription factors are plotted in white, with selected genes in red. **(E)** Activity of transcription factor regulons within groups defined in A at six and 24 h post-infection. Arrows indicate a significant up- or downregulation between bystander and low or high CHIKV groups (inside the boxes) or between low and high CHIKV groups (next to the boxes). Cumulative distributions between groups were compared using non-parametric Kolmogorov-Smirnov tests.

exogenous IFN treatment in any cell type, indicating that the proposed antagonistic functions may not be strong enough to be detectable at the bulk level. Also, unaltered levels of expression of housekeeping genes and genes encoding fibroblast markers in primary synovial fibroblasts did not generate evidence for a general virus-mediated host transcriptional shut-off that has been reported for several cell lines [13]. Overall, synovial fibroblasts appear to respond differently to CHIKV infection as commonly used cell lines. The underlying reason for this difference is unknown, but may involve a different intracellular milieu that is hyper-responsive to CHIKV infection.

While our single-cell RNA-seq approach is based on 3' end capture and does not allow to discriminate between full-length and subgenomic viral RNA, we identified a relative excess of subgenomic RNA in infected cultures by bulk RNA sequencing, in analogy to reports for Sindbis virus-infected cells [37]. Enhanced replication of the subgenomic RNA, which is mediated by the four cleaved nonstructural proteins forming a replication complex, ensures the rapid production of viral structural proteins and the formation of new virions [38]. While packaging of subgenomic RNA into virions has been described so far solely for Aura virus among alphaviruses [39], CHIKV bears a packaging signal in the nsP2-encoding region of its genome, selecting specifically full genomic RNA to be packaged into virions [40]. Therefore, we assume that the different abundance is based on *de novo* produced subgenomic RNA rather than on incoming viral RNA.

Our attempts to identify correlations of cellular gene expression with CHIKV RNA abundance in individual infected cells revealed that a certain threshold of viral RNA is required to initiate viral RNA sensing and eventually trigger ISG expression. However, expression of most ISGs is negatively regulated in the presence of a high viral RNA burden per cell. This is consistent with the idea that productive infection involves the synthesis of viral antagonists that hamper the induction and/or evade the function of ISGs, resulting in efficient virus propagation. Along these lines, West Nile virus infection also results in lowered ISG expression levels in cells harbouring high viral RNA quantities [41]. *In vivo*, actively SARS-CoV-2 infected monocytes of COVID-19 patients expressed lower levels of ISGs than non-infected bystander cells [42]. Monocytes of Ebola-infected rhesus monkeys display similar dynamics, with an additional downregulation of *STAT1* mRNA in infected cells [43]. On the contrary, cells that undergo abortive infection, or alternatively have not yet reached sufficient levels of virus replication fail to mount or repress a strong antiviral profile. Depending on the longevity of cells harbouring abortive genomic replication products and intermediates, their presence may influence the immunopathogenesis of chronic aspects of RNA-viral infection.

Owing to genetic recombination and low fidelity of the alphaviral RNA-dependent polymerase, defective alphaviral genomes (DVGs) and defective alphaviral particles arise during virus replication, but are themselves replication-incompetent [44]. Of note, our virus-inclusive sequencing approach does not have the power to distinguish between full-length viral genomes and defective or otherwise dead-end genomes. It will be interesting to test the contribution of the latter to triggering the strong cell-intrinsic innate recognition that we linked here to low intracellular viral RNA quantities in general. Strikingly, we find indication that the expression of some genes, such as proinflammatory transcription factors, may be actively targeted by CHIKV.

Particularly interesting in the context of an *a priori* acute RNA virus infection, arthritogenic alphavirus infection has been suspected to result in the generation of long-lived cellular reservoirs that may maintain low-levels of viral RNA. In mice, fibroblasts survive a CHIKV infection and joint-associated tissue can harbour viral RNA in the absence of infectious virus production for at least 16 weeks [6,45]. Prolonged shedding of infectious virus for up to 35 days from *ex vivo*-infected human synovial fibroblasts has been observed for Ross River virus (RRV), another arthritogenic alphavirus [46]. In infected macaques, infectious CHIKV particles were not shed for extended periods in the joints, but was detected in other tissues, including the liver and the spleen, at 44 days post-infection [7]. In addition to fibroblasts, other discussed cell types for long-term persistence are (synovial) macrophages and, to a lesser extent, dendritic cells. Macrophages harbour persistent viral RNA in a nonhuman primate infection model [7] and in human patients, where joint biopsies found synovial macrophages to be CHIKV RNA- and antigen-positive for as long as 18 months post-infection [5]. *In vitro*, CHIKV has been proposed to productively infect primary human macrophages [34]. Additionally, murine macrophages have been observed to periodically relapse from undetectable RRV production to spontaneous or inducible viral shedding [47]. On the other hand, persistent infection with MAYV has so far only been observed in RAG<sup>-/-</sup> mice, suggesting an efficient clearance of infection by adaptive immune responses [48]. In the absence of viral proteins antagonizing host antiviral responses, replication sites in the cytoplasm separated by single- or double membranes may shield the viral RNA from cellular detection and degradation, as has been demonstrated for flaviviruses [49] and coronaviruses [50]. Continuous sensing of viral RNA, which is not necessarily replicated to a level that would suffice for *de novo* virus production and virus spread, could thereby resonate in a state of chronic inflammation in the joints of

infected patients. It is tempting to speculate that those cell-intrinsic responses that we identified to be most pronounced in cells displaying low levels of viral RNA could be identical to those driving the pain- and inflammation-related joint immunopathology linked to chronic alphavirus infection-induced arthritis. Other suggested mechanisms for alphavirus-mediated arthralgia include, similar to Parvovirus B19- or Epstein-Barr virus-induced arthralgia [51,52], the formation of immunogenic autoantibodies through molecular mimicry [53].

Furthermore, human synovial fibroblasts secrete cytokines such as IL-6, IL1 $\beta$ , and RANTES, stimulating monocyte migration upon CHIKV infection, and drive them towards an osteoclast-like phenotype [4]. Interestingly, we identify a similar pattern in infected fibroblasts with upregulation and/or secretion of IL-6 and RANTES, but not matrix-metalloproteases (MMPs), as described before [4]. MMP expression and secretion by synovial fibroblasts can, similar to IL-6 secretion, be induced through external stimulation with IL-1 and TNF and by activated immune cells [54]. A paracrine stimulation of MMP expression by infiltrating immune cells has not been addressed in this model, but is likely to contribute to the direct induction of rheumatoid arthritis-like symptoms. Early IFN-mediated bystander cell activation and death has been reported in La Crosse virus infected cultures [55], processes which we do not observe, suggesting a limited role of bystander cell responses in this model system. On the other hand, at six hours post-infection in cultures where we expect almost all cells to have made contact with virus particles, we observe a strong activation of the RNA-negative cells. Additionally, infected synovial fibroblasts mount an immune response in the absence of JAK/STAT signalling, although low and without the induction of the strictly IFN-dependent ISG *MX2* in this model. This indicates that incoming viral RNA in the absence of a productive infection is sufficient to trigger pattern-recognition receptors such as RIG-I in an IFN-independent manner, as shown before [56], which may lead to the suppression of an active infection. Nevertheless, IFN-mediated immunity is majorly responsible for the suppression of viral spread in infected synovial fibroblasts. While paracrine and autocrine activation of expression by secreted IFN would lead to a basic level of immunity in all cells of the culture, we observed a reduced ISG activation in highly infected cells, again supporting the hypothesis that CHIKV actively counteracts JAK/STAT signalling. On the other hand, uninfected bystander cells were partially ISG-positive, which may protect them to a certain degree against infection or progression to highly infected cells. The marginal expression of *IFN* genes in most cells in the presented single-cell RNA-seq dataset indicates that at a given time, only

a small number of cells contribute to the secretion of IFN, which may explain the overall low amount of type I IFN detected here.

Finally, an interesting hypothesis foresees that pharmacological interference with the synovial fibroblast-specific hyperreactivity represents a feasible intervention approach towards the alleviation of long-term arthralgia. In rheumatoid arthritis, hyperactivated synovial fibroblasts invade the joint matrix, destroying/disrupting the cartilage and causing long-term inflammation [57,58]. This and the subsequent attraction of immune cells, including monocyte-derived macrophages to the damaged sites, may represent important events in the progression to long-term morbidity [59]. Indeed, data obtained in recent clinical studies suggests that treatment of chikungunya-induced arthritis with the immunosuppressant methotrexate may be beneficial [60]. The data presented here support the hypothesis that infected synovial fibroblasts display a phenotype that is reminiscent of those in rheumatoid arthritis, and that they are a driver of the typical symptoms in interplay with infiltrating immune cells. Key features such as the IL-1 $\beta$ -mediated IL-6 release, the aggressive proinflammatory gene expression in productively infected cells, and the strong expression of important cofactors make them likely to contribute to viral replication and disease progression *in vivo*.

## Acknowledgements

We thank the sequencing core of the Helmholtz Centre for Infection Research (HZI) in Braunschweig and the Genomics platform of the Berlin Institute of Health (BIH) for preparation of the Illumina sequencing libraries and the next generation sequencing. Additionally, we thank the sequencing facility of the Max Delbrück Center for Molecular Medicine for the next generation sequencing and bioinformatic support. We thank M. Diamond for providing the MXRA8-Fc proteins. We thank Theresia Stradal, Jens Bohne, and Sandra Pellegrini for providing the U2OS cells, HEK293T cells, and HL116 cells, respectively. We thank Thomas Pietschmann, Institute for Experimental Virology, TWINCORE, and Christian Drosten for constant support.

## Disclosure statement


No potential conflict of interest was reported by the author(s).

## Funding

This work was supported by funding from Deutsche Forschungsgemeinschaft (DFG) to CG (GO2153/3-1; GO2153/6-1), by the Impulse and Networking Fund of the Helmholtz Association through the HGFEU partnering grant PIE-008 to CG, and by funding from the Helmholtz Center for Infection Research (HZI) and Berlin Institute of Health (BIH) to CG.

## ORCID

Fabian Pott  <http://orcid.org/0000-0003-3700-1691>

Richard J. P. Brown  <http://orcid.org/0000-0002-3292-6671>

Christine Goffinet  <http://orcid.org/0000-0002-3959-004X>

## References

- [1] Matusali G, Colavita F, Bordini L, et al. Tropism of the Chikungunya virus. *Viruses*. 2019 Feb 20;11(2):175.
- [2] Diagne CT, Bengue M, Choumet V, et al. Mayaro virus pathogenesis and transmission mechanisms. *Pathogens*. 2020 Sep 8;9(9):738.
- [3] Santiago FW, Halsey ES, Siles C, et al. Long-term arthralgia after Mayaro virus infection correlates with sustained pro-inflammatory cytokine response. *PLoS Negl Trop Dis*. 2015;9(10):e0004104.
- [4] Phuklia W, Kasisith J, Modhiran N, et al. Osteoclastogenesis induced by CHIKV-infected fibroblast-like synoviocytes: a possible interplay between synoviocytes and monocytes/macrophages in CHIKV-induced arthralgia/arthritis. *Virus Res*. 2013 Nov 6;177(2):179–188.
- [5] Hoarau JJ, Jaffar Bandjee MC, Krejbich Trotot P, et al. Persistent chronic inflammation and infection by Chikungunya arthritogenic alphavirus in spite of a robust host immune response. *J Immunol*. 2010 May 15;184(10):5914–5927.
- [6] Young AR, Locke MC, Cook LE, et al. Dermal and muscle fibroblasts and skeletal myofibers survive chikungunya virus infection and harbor persistent RNA. *PLoS Pathog*. 2019 Aug;15(8):e1007993.
- [7] Labadie K, Larcher T, Joubert C, et al. Chikungunya disease in nonhuman primates involves long-term viral persistence in macrophages. *J Clin Invest*. 2010 Mar;120(3):894–906.
- [8] Zhang R, Kim AS, Fox JM, et al. Mxra8 is a receptor for multiple arthritogenic alphaviruses. *Nature*. 2018 May;557(7706):570–574.
- [9] Meertens L, Hafirassou ML, Couderc T, et al. FHL1 is a major host factor for chikungunya virus infection. *Nature*. 2019 Oct;574(7777):259–263.
- [10] Salvador B, Zhou Y, Michault A, et al. Characterization of Chikungunya pseudotyped viruses: identification of refractory cell lines and demonstration of cellular tropism differences mediated by mutations in E1 glycoprotein. *Virology*. 2009 Oct 10;393(1):33–41.
- [11] Reynaud JM, Kim DY, Atasheva S, et al. IFIT1 differentially interferes with translation and replication of alphavirus genomes and promotes induction of type I interferon. *PLoS Pathog*. 2015 Apr;11(4):e1004863.
- [12] Goertz GP, McNally KL, Robertson SJ, et al. The methyltransferase-like domain of Chikungunya virus nsP2 inhibits the interferon response by promoting the nuclear export of STAT1. *J Virol*. 2018 Aug 16;92(17):e01008–18.
- [13] Akhrymuk I, Lukash T, Frolov I, et al. Novel mutations in nsP2 abolish Chikungunya virus-induced transcriptional shutoff and make the virus less cytopathic without affecting its replication rates. *J Virol*. 2019 Feb 5;93(4):e02062–18.
- [14] Schoggins JW, MacDuff DA, Imanaka N, et al. Pan-viral specificity of IFN-induced genes reveals new roles for cGAS in innate immunity. *Nature*. 2014 Jan 30;505(7485):691–695.
- [15] Webb LG, Veloz J, Pintado-Silva J, et al. Chikungunya virus antagonizes cGAS-STING mediated type-I interferon responses by degrading cGAS. *PLoS Pathog*. 2020 Oct 15;16(10):e1008999.
- [16] Haese NN, Broeckel RM, Hawman DW, et al. Animal models of Chikungunya virus infection and disease. *J Infect Dis*. 2016 Dec 15;214(suppl 5):S482–s487.
- [17] Simarmata D, Ng DC, Kam YW, et al. Early clearance of Chikungunya virus in children is associated with a strong innate immune response. *Sci Rep*. 2016 May 16;6:26097.
- [18] Hussain KM, Lee RC, Ng MM, et al. Establishment of a novel primary human skeletal myoblast cellular model for Chikungunya virus infection and pathogenesis. *Sci Rep*. 2016 Feb 19;6:21406.
- [19] Bernard E, Hamel R, Neyret A, et al. Human keratinocytes restrict chikungunya virus replication at a post-fusion step. *Virology*. 2015 Feb;476:1–10.
- [20] Lefevre S, Meier FM, Neumann E, et al. Role of synovial fibroblasts in rheumatoid arthritis. *Curr Pharm Des*. 2015;21(2):130–141.
- [21] Uzé G, Di Marco S, Mouchel-Vielh E, et al. Domains of interaction between alpha interferon and its receptor components. *J Mol Biol*. 1994 Oct 21;243(2):245–257.
- [22] Neumann E, Riepl B, Knedla A, et al. Cell culture and passaging alters gene expression pattern and proliferation rate in rheumatoid arthritis synovial fibroblasts. *Arthritis Res Ther*. 2010;12(3):R83.
- [23] Tsetsarkin K, Higgs S, McGee CE, et al. Infectious clones of Chikungunya virus (La Reunion isolate) for vector competence studies. *Vector Borne Zoonotic Dis*. 2006 Winter;6(4):325–337.
- [24] Li X, Zhang H, Zhang Y, et al. Development of a rapid antiviral screening assay based on eGFP reporter virus of Mayaro virus. *Antiviral Res*. 2019 Aug;168:82–90.
- [25] Ashburner M, Ball CA, Blake JA, et al. Gene ontology: tool for the unification of biology. *Nat Genet*. 2000 May;25(1):25–29.
- [26] Hao Y, Hao S, Andersen-Nissen E, et al. Integrated analysis of multimodal single-cell data. *bioRxiv*. 2020:2020.10.12.335331.
- [27] Holland CH, Tanevski J, Perales-Patón J, et al. Robustness and applicability of transcription factor and pathway analysis tools on single-cell RNA-seq data. *Genome Biol*. 2020 Feb 12;21(1):36.
- [28] Georganas C, Liu H, Perlman H, et al. Regulation of IL-6 and IL-8 expression in rheumatoid arthritis synovial fibroblasts: the dominant role for NF- $\kappa$ B But Not C/EBP $\beta$  or c-Jun. *J Immunol*. 2000 Dec 15;165(12):7199–7206.
- [29] Selvarajah S, Sexton NR, Kahle KM, et al. A neutralizing monoclonal antibody targeting the acid-sensitive region in chikungunya virus E2 protects from disease. *PLoS Negl Trop Dis*. 2013;7(9):e2423.
- [30] Hornung V, Ellegast J, Kim S, et al. 5'-Triphosphate RNA is the ligand for RIG-I. *Science*. 2006 Nov 10;314(5801):994–997.
- [31] Sanchez David RY, Combredet C, Sismeiro O, et al. Comparative analysis of viral RNA signatures on different RIG-I-like receptors. *Elife*. 2016 Mar 24;5:e11275.
- [32] Schoggins JW, Wilson SJ, Panis M, et al. A diverse range of gene products are effectors of the type I interferon antiviral response. *Nature*. 2011 Apr 28;472(7344):481–485.
- [33] Zhou JH, Wang YN, Chang QY, et al. Type III interferons in viral infection and antiviral immunity. *Cell Physiol Biochem*. 2018;51(1):173–185.

- [34] Sourisseau M, Schilte C, Casartelli N, et al. Characterization of reemerging chikungunya virus. *PLoS Pathog.* 2007 Jun;3(6):e89.
- [35] Couderc T, Chrétien F, Schilte C, et al. A mouse model for Chikungunya: young age and inefficient type-I interferon signaling are risk factors for severe disease. *PLoS Pathog.* 2008 Feb 8;4(2):e29.
- [36] Sommereyns C, Paul S, Staeheli P, et al. IFN-lambda (IFN-lambda) is expressed in a tissue-dependent fashion and primarily acts on epithelial cells in vivo. *PLoS Pathog.* 2008 Mar 14;4(3):e1000017.
- [37] Lemm JA, Rümenapf T, Strauss EG, et al. Polypeptide requirements for assembly of functional Sindbis virus replication complexes: a model for the temporal regulation of minus- and plus-strand RNA synthesis. *Embo J.* 1994 Jun 15;13(12):2925–2934.
- [38] Rupp JC, Sokolowski KJ, Gebhart NN, et al. Alphavirus RNA synthesis and non-structural protein functions. *J Gen Virol.* 2015 Sep;96(9):2483–2500.
- [39] Rümenapf T, Strauss EG, Strauss JH. Subgenomic mRNA of Aura alphavirus is packaged into virions. *J Virol.* 1994 Jan;68(1):56–62.
- [40] Kim DY, Firth AE, Atasheva S, et al. Conservation of a packaging signal and the viral genome RNA packaging mechanism in alphavirus evolution. *J Virol.* 2011 Aug;85(16):8022–8036.
- [41] O'Neal JT, Upadhyay AA, Wolabaugh A, et al. West Nile virus-inclusive single-cell RNA sequencing reveals heterogeneity in the type I interferon response within single cells. *J Virol.* 2019 Mar 5;93(6):e01778–18.
- [42] Bost P, Giladi A, Liu Y, et al. Host-viral infection maps reveal signatures of severe COVID-19 patients. *Cell.* 2020 Jun 25;181(7):1475–1488.e12.
- [43] Kotliar D, Lin AE, Logue J, et al. Single-cell profiling of Ebola virus disease in vivo reveals viral and host dynamics. *Cell.* 2020 Nov 25;183(5):1383–1401.e19.
- [44] Poirier EZ, Mounce BC, Rozen-Gagnon K, et al. Low-fidelity polymerases of alphaviruses recombine at higher rates to overproduce defective interfering particles. *J Virol.* 2016;90(5):2446–2454.
- [45] Hawman DW, Stoermer KA, Montgomery SA, et al. Chronic joint disease caused by persistent Chikungunya virus infection is controlled by the adaptive immune response. *J Virol.* 2013 Dec;87(24):13878–13888.
- [46] Journeaux SF, Brown WG, Aaskov JG. Prolonged infection of human synovial cells with Ross River virus. *J Gen Virol.* 1987 Dec;68(Pt 12):3165–3169.
- [47] Way SJ, Lidbury BA, Banyer JL. Persistent Ross River virus infection of murine macrophages: an in vitro model for the study of viral relapse and immune modulation during long-term infection. *Virology.* 2002 Sep 30;301(2):281–292.
- [48] Figueiredo CM, Neris R, Gavino-Leopoldino D, et al. Mayaro virus replication restriction and induction of muscular inflammation in mice are dependent on age, type-I interferon response, and adaptive immunity. *Front Microbiol.* 2019;10:2246.
- [49] Fernandez-Garcia MD, Mazzon M, Jacobs M, et al. Pathogenesis of flavivirus infections: using and abusing the host cell. *Cell Host Microbe.* 2009 Apr 23;5(4):318–328.
- [50] Wolff G, Melia CE, Snijder EJ, et al. Double-membrane vesicles as platforms for viral replication. *Trends Microbiol.* 2020 Dec;28(12):1022–1033.
- [51] Kerr JR. The role of parvovirus B19 in the pathogenesis of autoimmunity and autoimmune disease. *J Clin Pathol.* 2016 Apr;69(4):279–291.
- [52] Houen G, Trier NH. Epstein-Barr virus and systemic autoimmune diseases. *Front Immunol.* 2020;11:587380.
- [53] Venigalla SSK, Premakumar S, Janakiraman V. A possible role for autoimmunity through molecular mimicry in alphavirus mediated arthritis. *Sci Rep.* 2020 Jan 22;10(1):938.
- [54] Fuchs S, Skwara A, Bloch M, et al. Differential induction and regulation of matrix metalloproteinases in osteoarthritic tissue and fluid synovial fibroblasts. *Osteoarthritis Cartilage.* 2004 May;12(5):409–418.
- [55] Cruz MA, Parks GD. La Crosse virus infection of human keratinocytes leads to interferon-dependent apoptosis of bystander non-infected cells in vitro. *Viruses.* 2020 Feb 25;12(3):253.
- [56] Weber M, Gawanbacht A, Habjan M, et al. Incoming RNA virus nucleocapsids containing a 5'-triphosphorylated genome activate RIG-I and antiviral signaling. *Cell Host Microbe.* 2013 Mar 13;13(3):336–346.
- [57] Neumann E, Lefevre S, Zimmermann B, et al. Rheumatoid arthritis progression mediated by activated synovial fibroblasts. *Trends Mol Med.* 2010 Oct;16(10):458–468.
- [58] Hillen J, Geyer C, Heitzmann M, et al. Structural cartilage damage attracts circulating rheumatoid arthritis synovial fibroblasts into affected joints. *Arthritis Res Ther.* 2017 Feb 28;19(1):40.
- [59] Falconer J, Murphy AN, Young SP, et al. Review: synovial cell metabolism and chronic inflammation in rheumatoid arthritis. *Arthritis Rheumatol.* 2018 Jul;70(7):984–999.
- [60] Amaral JK, Sutaria R, Schoen RT. Treatment of chronic Chikungunya arthritis with methotrexate: A systematic review. *Arthritis Care Res.* 2018 Oct;70(10):1501–1508.

1 **Single-cell analysis of arthritogenic alphavirus-infected human synovial**  
2 **fibroblasts links low abundance of viral RNA to induction of innate**  
3 **immunity and arthralgia-associated gene expression**

4

5 Fabian Pott<sup>1,2</sup>, Dylan Postmus<sup>1,2</sup>, Richard J. P. Brown<sup>3</sup>, Emanuel Wyler<sup>4</sup>, Elena Neumann<sup>5</sup>,  
6 Markus Landthaler<sup>4,6</sup>, and Christine Goffinet<sup>1,2\*</sup>

7

8 **Supplemental Material:**

9

10 **Supplemental Figures 1-6**

11 **Supplemental Movies 1-2**

12

13

14 **Supplemental Figure 1. Ruxolitinib, but not IL-1 $\beta$  treatment, changes the susceptibility**  
15 **of OASF to infection with CHIKV and MAYV.**

16 **(A)** OASF were stimulated with IL-1 $\beta$  at 10 ng/ml for 16 hours and subsequently infected  
17 with CHIKV (MOI 10) in the presence of IL-1 $\beta$ . At 24 and 48 hours post-infection, cells were  
18 analyzed for EGFP expression by flow cytometry.

19 **(B)** OASF were infected with 5'EGFP-CHIKV or -MAYV at indicated MOIs or mock-  
20 infected. 24 hours later, supernatants were incubated on HL116 reporter cells to quantify  
21 secreted bioactive type I IFN (n = 3-7). The dotted line indicates the limit of detection (LOD).

22 **(C)** OASF were infected with 5'EGFP-CHIKV or -MAYV at indicated MOIs in the presence  
23 or absence of 10  $\mu$ M Ruxolitinib or mock-infected. At 24 and 48 hours post-infection, cells  
24 were analyzed for EGFP expression.

1

25 **(D)** OASF were infected with 5'EGFP-CHIKV (MOI 10) in the presence or absence of 1 or  
26 10  $\mu$ M Ruxolitinib or mock-infected. Infection was recorded by live-cell imaging and  
27 representative images for untreated and 10  $\mu$ M Ruxolitinib-treated cells are shown. Scale bar  
28 = 100  $\mu$ m.

29

30 **Supplemental Figure 2. HSF and OASF share a similar basal and CHIKV infection-**  
31 **induced transcriptome.**

32 **(A)** Visualization of global transcriptional differences between OASF and HSF under regular  
33 culturing conditions. Average RPKM ( $\log_{10}$ ) values for all detected transcripts from OASF  
34 are plotted on the x-axis, with corresponding values from HSF plotted on the y-axis.  $R^2$  value  
35 and linear regression line for comparison are inset.

36 **(B)** Gene ontology analysis of differentially expressed genes in OASF compared to HSF. P-  
37 values were generated after Bonferroni correction for multiple testing.

38 **(C)** Visualization of global transcriptomic differences between CHIKV-infected OASF and  
39 HSF as described in A.

40 **(D)** Gene ontology analysis of the top significantly upregulated pathways in OASF, HSF, and  
41 shared by both in response to CHIKV infection. P-values were generated after Bonferroni  
42 correction for multiple testing.

43 **(E)** Heatmaps of selected gene expression profiles of IFN receptors, CHIKV host cofactors,  
44 and celltype markers. Differentially expressed genes were identified by comparison of raw  
45 count data, with calculation of false-discovery rate (FDR) p-value for multiple comparisons.

46 (n = 4 for OASF, 2 for HSF).

47



48 **Supplemental Figure 3. OASF, U2OS, and HFF-1 respond with a differently strong**  
49 **upregulation of ISGs to IFN treatment and CHIKV infection despite similar**  
50 **responsiveness to PAMPs.**

51 (A) Indicated cell cultures were transfected with 5'-triphosphate dsRNA (5-ppp-RNA, left) or  
52 plasmid DNA (right) and analyzed for the expression of *IFIT1* and *MX2* mRNA at 24 and 48  
53 hours post transfection (n = 3-4). Statistical analysis between different cell lines at the same  
54 time point was performed using Mann-Whitney tests, analysis between different time points  
55 within one cell line were performed using two-sided, unpaired t-tests with assumed equal  
56 standard deviations.

57 (B) OASF, U2OS, and HFF-1 cells were analyzed for the expression of *IFIT1* and *MX2* by  
58 quantitative RT-PCR after 48 h treatment with the indicated amounts of IFN- $\alpha$  or  $-\lambda$  (n = 3).

59 (C) OASF, U2OS, and HFF-1 cells were infected with 5'-EGFP CHIKV (MOI 10) and  
60 indicated amounts of IFN- $\alpha$  were added four hours post-infection. At 24 and 48 hours post-  
61 infection, OASF were analyzed for the expression of *IFIT1* and *MX2* mRNA by quantitative  
62 RT-PCR (n = 3).

63 For B and C, nonlinear fit curves with variable slopes for IC50 calculation were used.

64

65 **Supplemental Figure 4. Cofactor expression in OASF and mild IFN signaling gene**  
66 **expression in infected OASF.**

67 (A) NGS reads after 3' mRNA capture attributed to each individual position in the CHIKV  
68 genome plotted for cells infected with CHIKV at six and 24 hours post-infection. SGP =  
69 subgenomic promotor (n = 2).

70 (B) Infected OASF were sorted into 100 digital bins per infection condition (MOI) displaying  
71 a gradual increase of the amount of viral reads per cell. Average proportion of reads per cell  
72 attributed to CHIKV at six and 24 hours post-infection are plotted (n = 2).

3

73 (C) UMAP projections were generated for the six hours post-infection time point. Shown is  
74 the abundance of CHIKV 3' end reads and of IFN signaling genes according to IMS (n = 2).

75 (D) Expression of IFN-stimulated genes in infected OASF at six and 24 hours post-infection.  
76 UMAP visualization shows infected cells split by the MOI and mock-infected cells separately  
77 (n = 2).

78

79 **Supplemental Figure 5. IFN-stimulated gene expression in infected OASF.**

80 Expression of alphavirus infection cofactors and fibroblast marker genes in infected OASF.  
81 UMAP visualization shows infected cells split by the MOI and mock-infected cells separately  
82 (n = 2).

83

84 **Supplemental Figure 6. IFN signaling gene expression and transcriptional changes**  
85 **between infected subgroups of cells.**

86 (A) IMS in uninfected, bystander, CHIKV low and CHIKV high OASF at six and 24 hours  
87 post-infection. Statistical significance between groups was tested using non-parametric  
88 Kolmogorov-Smirnov tests (n = 2).

89 (B) Analysis of significantly up- and downregulated genes between indicated cell subgroups  
90 at six and 24 hours post-infection. Differential gene expression was tested by Wilcoxon rank  
91 sum test with applied Bonferroni correction (n = 2).

92

93 **Supplemental Movie 1. CHIKV spreads in OASF culture.**

94 OASF 5'-EGFP-CHIKV-infected OASF were monitored for EGFP expression by live-cell  
95 imaging. Scale bar = 100  $\mu$ m (n = 4, representative movie).

96

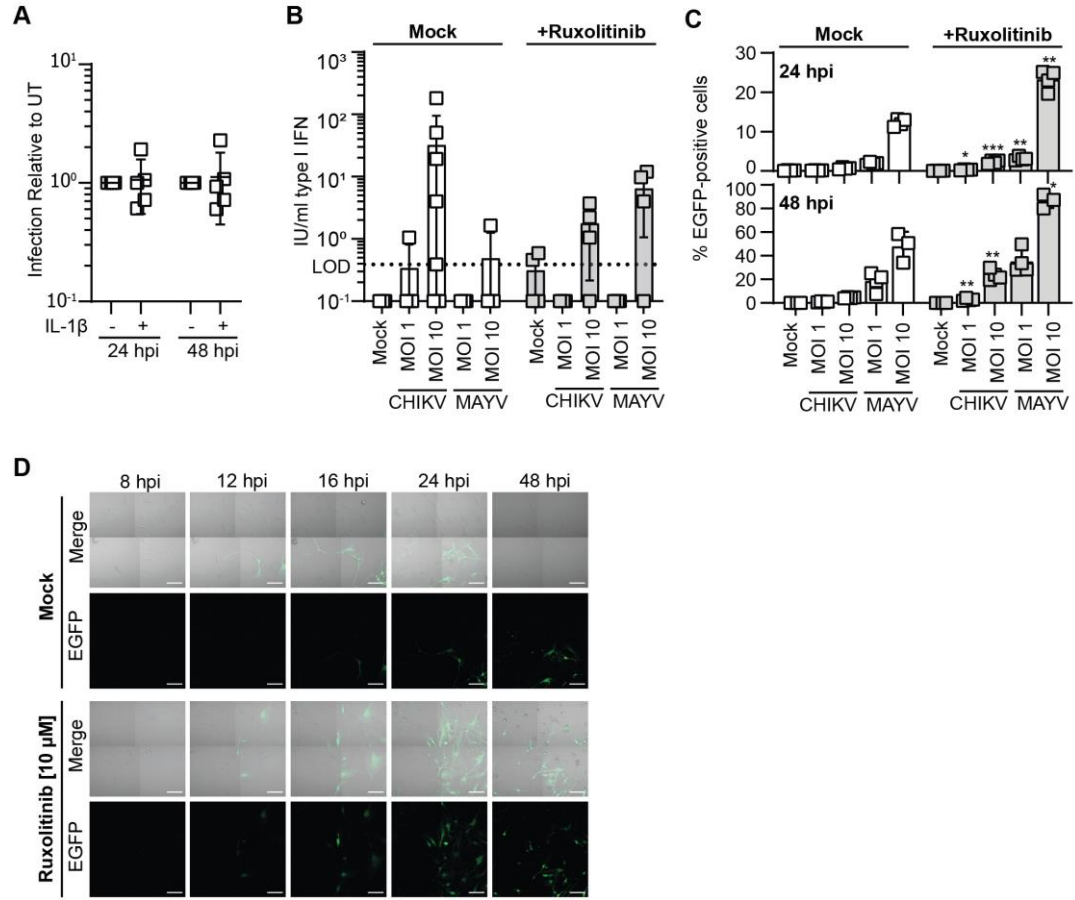
97 **Supplemental Movie 2. Ruxolitinib treatment boosts CHIKV spread.**

98 OASF were pretreated with 10  $\mu$ M Ruxolitinib for 16 hours, infected with 5'-EGFP-CHIKV  
99 in the presence of Ruxolitinib and monitored for EGFP expression by live-cell imaging. Scale  
100 bar = 100  $\mu$ m (n = 4, representative movie).

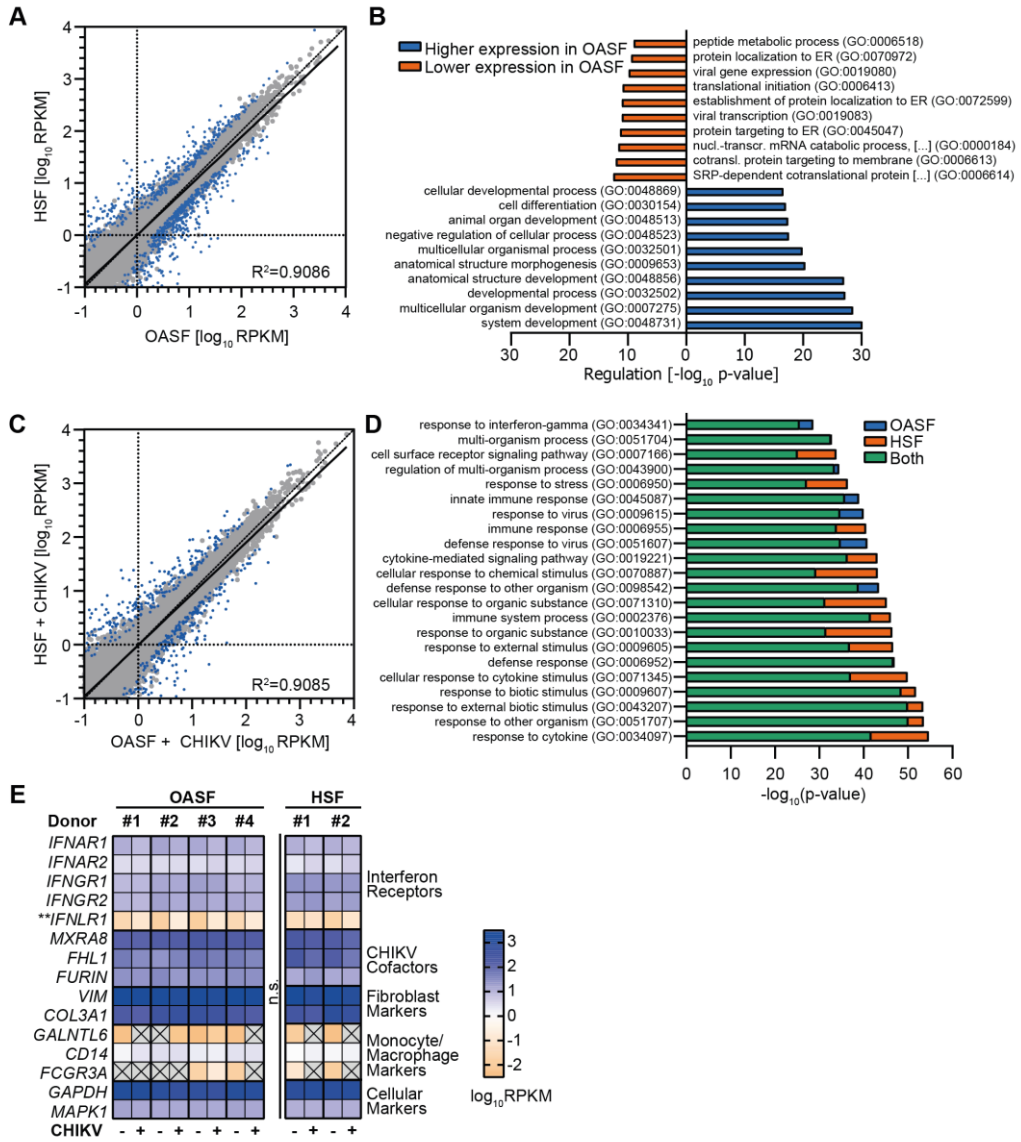
101

102

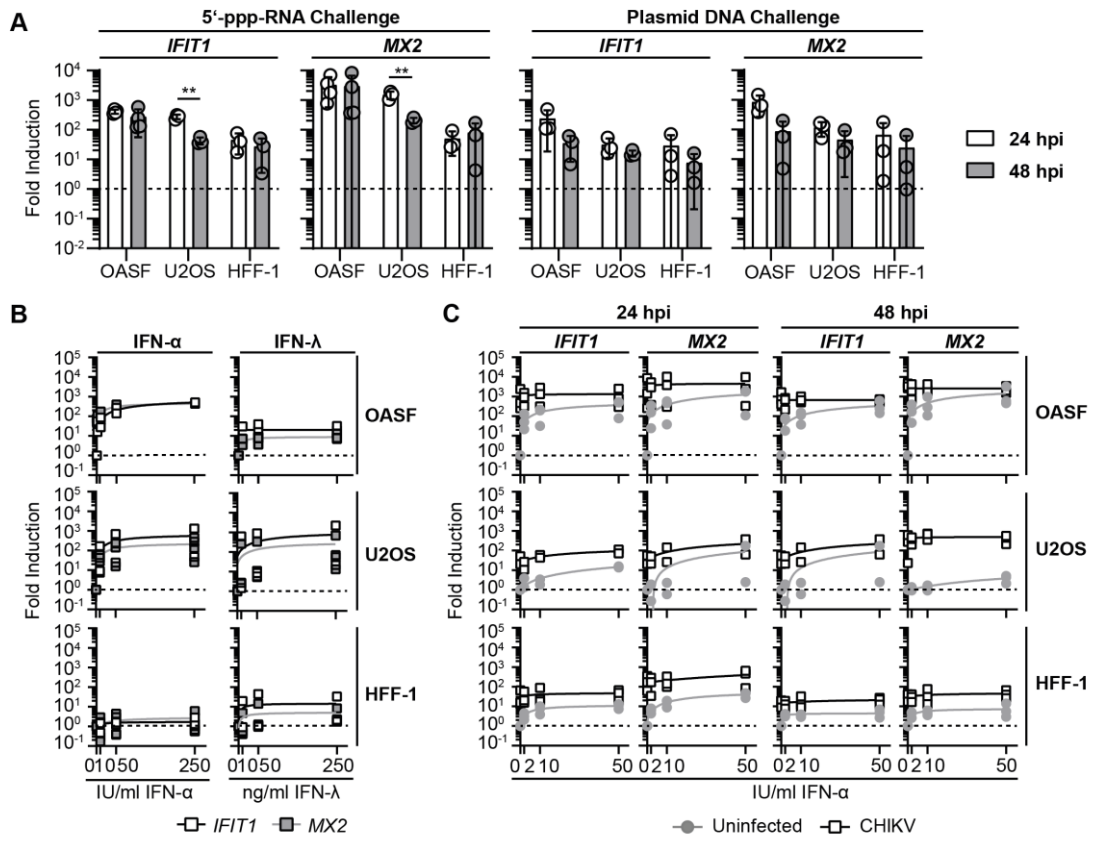
Pott *et al.*, Supplementary Figure 1



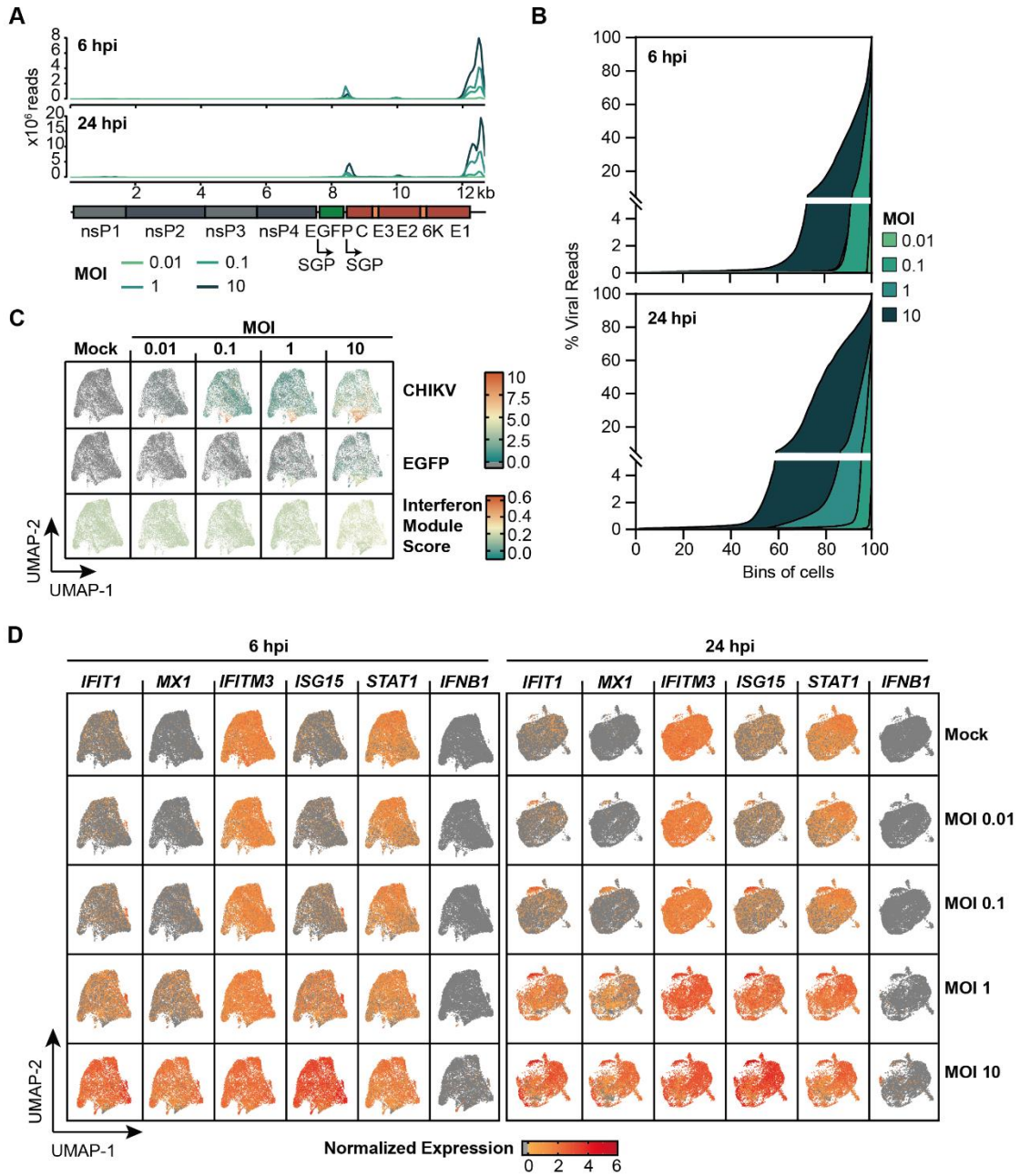
# Pott et al., Supplementary Figure 2



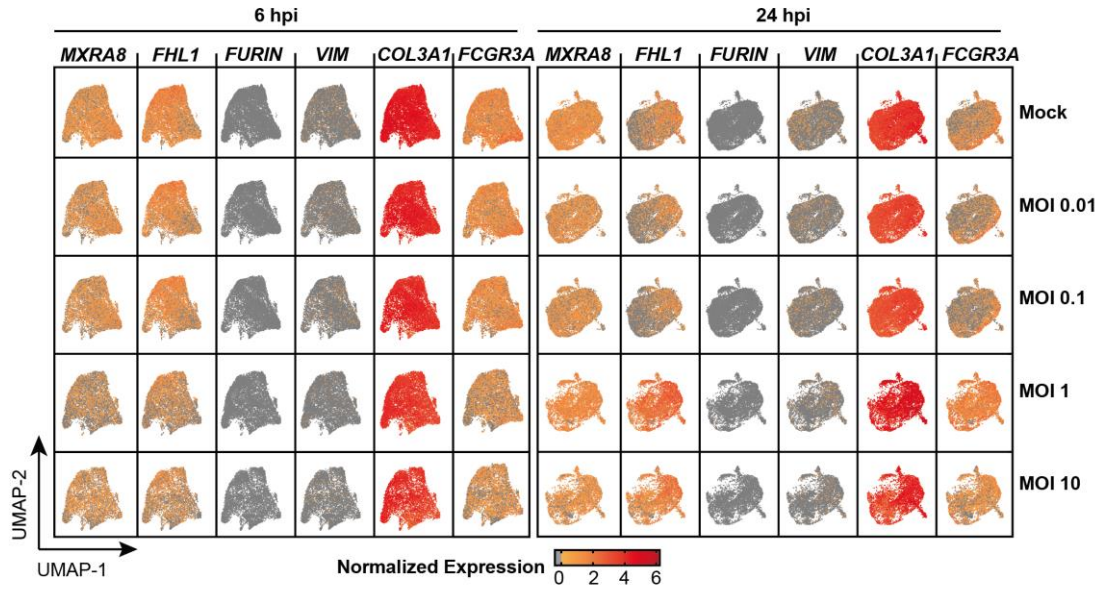
Pott *et al.*, Supplementary Figure 3



Pott *et al.*, Supplementary Figure 4

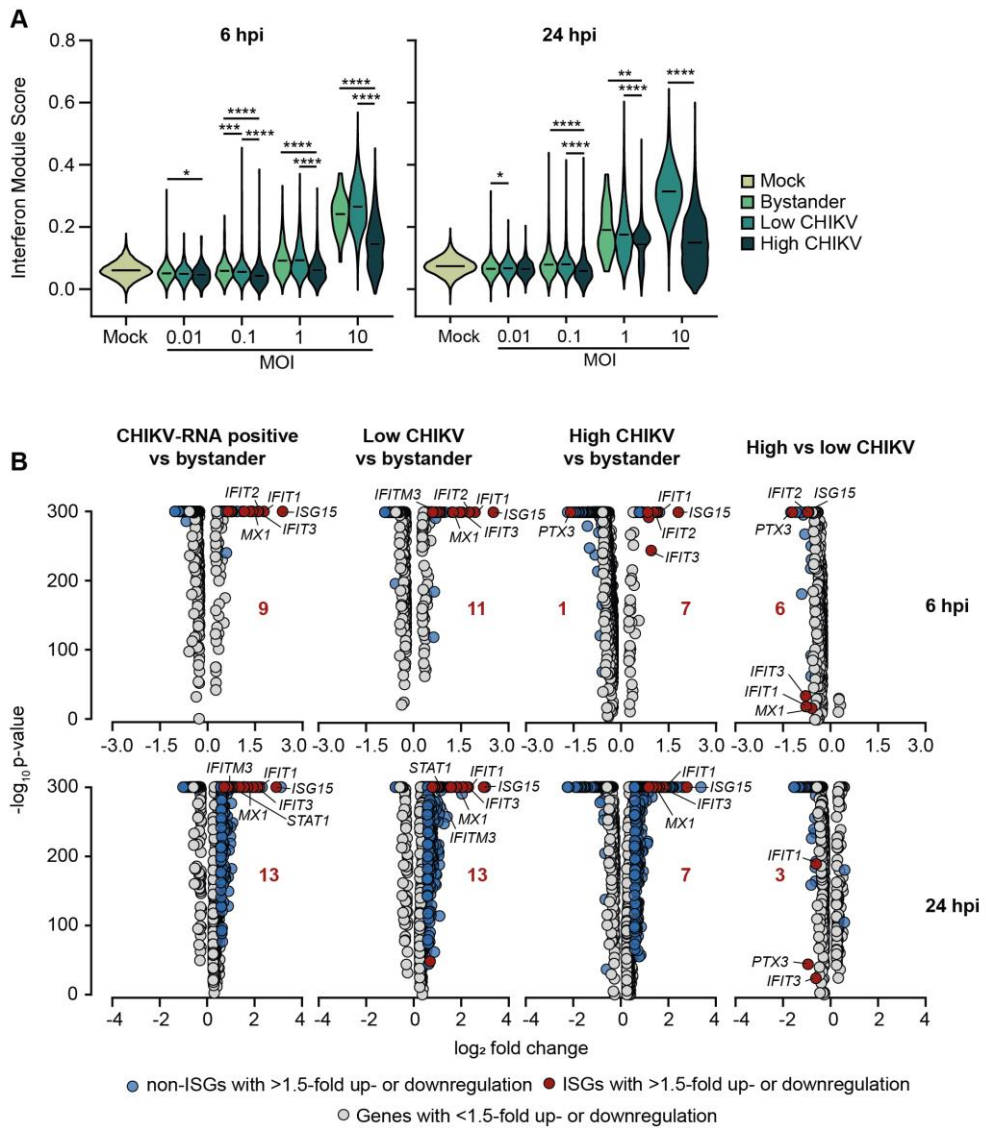


# Pott *et al.*, Supplementary Figure 5





Pott *et al.*, Supplementary Figure 6



## **Curriculum Vitae**

Mein Lebenslauf wird aus datenschutzrechtlichen Gründen in der elektronischen Version meiner Arbeit nicht veröffentlicht.

## List of Publications

**Pott F**, Postmus D, Brown RJP, Wyler E, Neumann E, Landthaler M, Goffinet C. *Single-cell analysis of arthritogenic alphavirus-infected human synovial fibroblasts links low abundance of viral RNA to induction of innate immunity and arthralgia-associated gene expression*. **Emerging Microbes & Infections**. 2021; 10(1):2151-68. DOI:10.1080/22221751.2021.2000891.

Wendisch D\*, Dietrich O\*, Mari T\*, Stillfried S\*, Ibarra IL, Mittermaier M, Mache C, Chua RL, Knoll R, Timm S, Brumhard S, Krammer T, Zauber H, Hiller AL, Pascual-Reguant A, Mothes R, Bülow RD, Schulze J, Leipold AM, Djudjaj S, Erhard F, Geffers R, **Pott F**, Kazmierski J, Radke J, Pergantis P, Baßler K, Conrad C, Aschenbrenner AC, Sawitzki B, Landthaler M, Wyler E, Horst D, Hippenstiel S, Hocke A, Heppner FL, Uhrig A, Garcia C, Machleidt F, Herold S, Elezkurtaj S, Thibeault C, Witzernath M, Cochain C, Suttorp N, Drosten C, Goffinet C, Kurth F, Schultze JL, Radbruch H, Ochs M, Eils R, Müller-Redetzky H, Hauser AE, Luecken MD, Theis FJ, Conrad C, Wolff T, Boor P, Selbach M, Saliba AE, Sander LE. *SARS-CoV-2 infection triggers profibrotic macrophage responses and lung fibrosis*. **Cell**. 2021; in press. DOI:10.1016/j.cell.2021.11.033.

Nouailles G\*, Wyler E\*, Pennitz P, Postmus D, Vladimirova D, Kazmierski J, **Pott F**, Goffinet C, Landthaler M, Trimpert J, Witzernath M: *Temporal omics analysis in Syrian hamsters unravel cellular effector responses to moderate COVID-19*. **Nature Communications**. 2021; 12(1):4869. DOI:10.1038/s41467-021-25030-7.

Franz S, **Pott F**, Zillinger T, Schüler C, Dapa S, Fischer C, Passos V, Stenzel S, Chen F, Döhner K, Hartmann G, Sodeik B, Pessler F, Simmons G, Drexler JF, Goffinet C. *Human IFITM3 restricts chikungunya virus and Mayaro virus infection and is susceptible to virus-mediated counteraction*. **Life Science Alliance**. 2021; 4(7):e202000909. DOI:10.26508/lsa.202000909.

Schroeder S, **Pott F**, Niemeyer D, Veith T, Richter A, Muth D, Goffinet C, Müller MA, Drosten C. *Interferon antagonism by SARS-CoV-2: a functional study using reverse genetics*. **Lancet Microbe**. 2021; 2(5):e210-e8. DOI:10.1016/s2666-5247(21)00027-6.

Niekamp P, Guzman G, Leier HC, Rashidfarrokhi A, Richina V, **Pott F**, Barisch C, Holthuis JCM, Tafesse FG. *Sphingomyelin Biosynthesis Is Essential for Phagocytic Signaling during Mycobacterium tuberculosis Host Cell Entry*. **mBio**. 2021; 12(1) :e03141-20. DOI:10.1128/mBio.03141-20.

Trump S\*, Lukassen S\*, Anker MS\*, Chua RL\*, Liebig J\*, Thürmann L\*, Corman VM\*, Binder M\*, Loske J, Klasa C, Krieger T, Hennig BP, Messingschlager M, **Pott F**, Kazmierski J, Twardziok S, Albrecht JP, Eils J, Hadzibegovic S, Lena A, Heidecker B, Bürgel T, Steinfeldt J, Goffinet C, Kurth F, Witzernath M, Völker MT, Müller SD, Liebert UG, Ishaque N, Kaderali L, Sander LE, Drosten C, Laudi S, Eils R, Conrad C, Landmesser U, Lehmann I. *Hypertension delays viral clearance and exacerbates airway hyperinflammation in patients with COVID-19*. **Nature Biotechnology** 2021; 39(6):705-16. DOI:10.1038/s41587-020-00796-1.

Chua RL\*, Lukassen S\*, Trump S\*, Hennig BP\*, Wendisch D\*, **Pott F**, Debnath O, Thürmann L, Kurth F, Völker MT, Kazmierski J, Timmermann B, Twardziok S, Schneider S, Machleidt F, Müller-Redetzky H, Maier M, Krannich A, Schmidt S, Balzer F, Liebig J, Loske J, Suttorp N, Eils J, Ishaque N, Liebert UG, von Kalle C, Hocke A, Witzernath M, Goffinet C, Drosten C, Laudi S, Lehmann I, Conrad C, Sander LE, Eils R. *COVID-19 severity correlates with airway epithelium-immune cell interactions identified by single-cell analysis*. **Nature Biotechnology**. 2020; 38(8):970-9. DOI:10.1038/s41587-020-0602-4.

\*These authors contributed equally

## Acknowledgements

First, I want to thank Christian Drosten for supporting my work as the director of the Institute of Virology at Charité Berlin and as my second supervisor. Additionally, I thank Thomas Pietschmann for supporting my work as the institute head at TWINCORE Hannover.

I am deeply grateful for the opportunity to work in Christine Goffinet's group and her supervision. I could not have asked for a better support during all the projects I have been working on during the last four years. Under her supervision, I have developed into a better scientist and have learned so much about critical thinking, project development, leadership, and scientific creativity. I will cherish the lessons learned in her lab throughout my future career.

I want to thank Richard Brown for his advice as my third supervisor and for always supporting me. Thanks to all other cooperation partners from the projects I have been involved in and for the outstanding results that came from these projects.

During my time in Hannover and Berlin, I have met an incredible number of wonderful people along the way. First and foremost, I want to thank all past and present members of the Goffinet Lab. Many thanks to Julia and Dylan for proofreading this dissertation and for being closely involved in many shared projects. Thanks to the former Hannover group members for the warm welcome and the great start into my PhD: Carina, Vânia, Aparna, Sergej, Angie, and Ellen. Many thanks to the fantastic current group in Berlin: Julia, Dylan, Saskia, Laure, Jenny, Bengisu, Christiane, and Baxolele. I will always happily look back to our shared lunch breaks!

In addition, I want to thank all the people in the Institute of Virology who I have met and worked with during the last three years. I am happy to have shared the best office in the institute with many outstanding people. In particular, I would like to thank (next to the people of my own group) Simon, Kirstin, Jackson, Lina, Selina, Rike, Jan, Tobi, Sabrina, Lara, Felix, Julian, and Andrea for becoming close friends and spending many days and nights out together.

Most importantly, I highly appreciate all the love and support my family gave me throughout my scientific journey. Thank you for believing in me and letting me go my way. Lastly, I deeply thank Ann-Sophie for all her love, her encouragement, and her support during the last years. I hope to spend many more with you.